UiT
THE ARCTIC UNIVERSITY OF NORWAY

Faculty of Science and Technology

Department of Geology

Geochemical investigations of northern Norwegian fjord sediments – Sources and spatial variability of marine and terrigenous components

—

Lea Philine Canzler

Master thesis in Marine Geology and Geophysics (GEO-3900)
May 2016

Abstract

Fjords represent unique coastal marine environments with high sedimentation rates. They can be used for intensive investigations focusing on geochemical, mineralogical, biological, and sedimentological processes. In this study I investigate 42 surface sediment samples from the outer and inner parts of the Vestfjord, Ofotfjord, Tysfjord and tributary fjord arms in northern Norway. Samples were analysed for their bulk elemental composition, grain size distribution, and total carbon and nitrogen contents (C_{tot}, N_{tot}). Furthermore, total organic and inorganic carbon and nitrogen concentrations (C_{org}, C_{inorg}, N_{org} and N_{inorg}) as well as the carbon and nitrogen isotopes ($\delta^{13}C$, $\delta^{15}N$) were analysed. The measurements were performed to identify geochemical proxies for the contribution of terrestrial organic matter (TOM) versus marine organic matter (MOM) into the fjords. The results indicate a sedimentary environment characterized by an overall dominant contribution of MOM compared to the relatively small input of terrestrial derived material. The extremely high supply of MOM is presented by C_{org}/N_{org} ratios ranging between 6 and 10, stable carbon isotope values ($\delta^{13}C_{org}$) between -24‰ and -21‰, and stable organic nitrogen ($\delta^{15}N_{org}$) signatures that vary between 4.7‰ and 6.9‰. The terrigenous material content is in general extraordinary low, and TOM increases from the outer part of the Vestfjord towards the innermost fjord parts of the Ofotfjord and Tysfjord. A correlation between $\delta^{13}C_{org}$ and $\delta^{15}N_{org}$ and the C_{org}/N_{org} ratios indicates high influences of marine derived OM. In addition, marine primary productivity is found to be the main contributor of calcium carbonate ($CaCO_3$). $CaCO_3$ increases towards the outer fjord parts and can be used to identify carbonate aquatic productivity by marine organisms and potentially trace the variable and relatively strong inflow of Atlantic water masses. Numerous proxies as those described above can be used to develop a better understanding of environmental processes since fjord sediments provide important reservoirs for the study of past and present environmental and climatic changes.

Contents

List of figures

Acknowledgement

I would like to thank all people who supported me during the last two years of my master studies. First and foremost, I would like to thank my supervisors Dr. Johan Faust, Dr. Jochen Knies and Dr. Matthias Forwick for their help and support. A special thanks goes to Dr. Johan Faust for his great guidance and endless endurance during the whole course of this thesis.

I would like to express my gratitude to Sebastian Worm and Lisbeth Jensen for their friendship, which grew strongly during our stay in Tromsø. Furthermore, I would like to thank Mats Amundsen, Eira Enguidanos and Katrin Kraut, for not just sharing an office but also for our adventurous ski trips and social get-togethers. Likewise, my thanks goes to all my friends left behind in Germany, especially Verena, Svenja, Mandy, and Stefanie.

Last but not least, I would like to thank my supportive family: My sister Felia, my mother and stepfather, Astrid and Michael Kretschmann, my father and stepmother, Ralf and Rita Canzler, as well as my grandparents and our dogs for their support and encouragement during my entire stay in Tromsø.

Thanks!

Tromsø, May 2016

Lea Philine Canzler

1 Introduction

In the following I describe the goals of my Master thesis and provide background information focusing on previous scientific studies that concern similar topics. Basic information about fjord environments and an introduction into carbon and nitrogen biogeochemistry including stable carbon and nitrogen isotopes are presented as well.

1.1 Objectives

This Master thesis was performed at the University of Tromsø, The Arctic University of Norway, in cooperation with the Geological Survey of Norway (NGU) in Trondheim. It is part of the project "Basement fracturing and weathering on- and offshore Norway – Genesis, age, and landscape development (BASE)" which is a joined program of the NGU and the SINTEF Petroleum Research in Trondheim.

The Master project comprises a geochemical, mineralogical, biological, and sedimentological study of 42 surface sediment samples from the Vestfjord (68° 3′ 0″ N, 14° 46′ 0″ E), Ofotfjord (68° 25′ 0″ N, 17° 1′ 0″ E), Tysfjord (68° 5′ 38″ N, 16° 21′ 12″ E) and their tributary fjords in northern Norway. The sediment samples were taken during a scientific cruise with the "FF Seisma", owned by the NGU, in June 2014.

The purpose of this study is to characterize the predominant sedimentary environment and environmental mechanisms influencing the terrigenous and marine inorganic and organic sediment supply and their distribution in the fjords. Different analyses are performed with numerous measuring instruments by different scientific institutes and in this thesis I concentrate on investigating the samples for their:

- Bulk mineral and elemental composition, and grain size distribution
- Total carbon (C_{tot}) and total nitrogen (N_{tot}) contents
- Total organic and inorganic carbon (C_{org}, C_{inorg}) and nitrogen (N_{org} and N_{inorg}) concentrations
- Stable carbon ($\delta^{13}C$) and nitrogen ($\delta^{15}N$) isotopes
- C_{org}/N_{tot} and C_{org}/N_{org} ratios.

In addition, the aim is to identify the relative contributions of marine organic matter (MOM) versus terrigenous organic matter (TOM) into the sediments of the study area. C_{org}/N_{org} ratios

are used as proxies for quantifying the autochthonous (marine) OM that is preferentially produced by marine primary producers, from allochthonous (terrestrial) OM, which originates from the hinterland vegetation and is transported by rivers into the ocean. Characteristics of the drainage area and the predominant oceanography are important parameters influencing the bulk sediment supply.

Furthermore, this study may be used as a base for future work focusing on past environmental processes and climate changes as well as on a better comprehension of the global carbon and nitrogen cycles. All results are compared to and discussed with previous published studies from different fjord systems in Norway and on a global scale.

1.2 State of the art

The identification of marine (autochthonous) versus terrigenous (allochthonous) sediment sources from the oceans´ continental shelves and different fjord systems has been performed by several studies from numerous locations focusing either on the contribution of organic material (Goñi et al, 1997; Stein and McDonald, 2004; Winkelmann and Knies, 2005; Knies and Martinez, 2009) or on the concentrations of the bulk elemental composition in sediments (Hayes, 1993; Calvert et al, 1993; Cho et al., 1999; Karageorgis et al., 2005; Govin et al., 2012). Fjords are important coastal environments with high inorganic and organic sedimentation rates providing high-resolution sedimentary records (e.g. Skei, 1983). Due to their high sedimentation rates, fjords are assumed to be important coastal sites for the burial of carbon and the sequestration of carbon dioxide (CO_2) (Syvitski et al., 1987; Hedges et al., 1997; Knies, 2005; Sepúlveda et al., 2011). However, only a few studies have been performed by using surface sediment samples instead of long sediment cores as data source to investigate environmental processes and sources that influence the organic and inorganic geochemistry of fjord sediments (Winkelmann and Knies, 2005; Smith et al., 2010; Sepúlveda et al., 2011; Silva et al., 2011; Bertrand et al., 2012; Faust et al., 2014a/b).

Sepúlveda et al. (2011), Silva et al. (2011), and Bertrand et al. (2012) investigated numerous fjords in northern Patagonia, Chile. They analysed surface sediment samples to identify the provenance of inorganic and organic material. By focusing on the grain size distribution, the content of the total organic carbon and nitrogen, and $\delta^{13}C$ and $\delta^{15}N$, they found a strong influence of seasonal freshwater supply and hydrodynamic mineralogical sorting controlling the sediments´ geochemical composition. The authors present a decreasing gradient of

terrestrial derived organic and inorganic matter from the inner part of the fjords towards the open ocean, and estimated marine and terrestrial endmember values for $\delta^{13}C_{org}$ and C/N. Furthermore, carbon accumulation calculations characterize fjords as potentially important settings for the global burial of C_{org} and the sequestration of atmospheric CO_2.

Similar distribution patterns for the terrestrial derived material with a decreasing proximal to distal trend from the inner part of the fjords towards the outer part are found in fjords of New Zealand (Smith et al., 2010) and Svalbard (Winkelmann and Knies, 2005). Winkelmann and Knies (2005) show that sedimentation is mainly controlled by river and meltwater discharges, as well as by coastal erosion due to sea ice and glaciers. In addition, the fjords in Svalbard are characterized by predominantly high accumulation rates of organic material in comparison to the open ocean.

Geochemical, mineralogical and sedimentological investigation of surface sediment samples from the Trondheimsfjord in northern Norway were performed by Faust et al. (2014a/b). They also observed a decreasing gradient of marine-derived OM from the entrance to the inner parts of the Trondheimsfjord. Furthermore, they found a linkage between the terrigenous sediment supply and climate variabilities as well as between calcium carbonate and carbonate aquatic productivity.

As fjords are concerned as enclosed mini-oceans (Skei, 1983) each individual fjord provides different sedimentological and mineralogical characteristics which are influenced by several environmental processes and source-to-sink mechanisms. Sediments accumulating in fjords offer unique opportunities to study both local and regional land-ocean interactions as they provide high-resolution records of past environmental changes (Skei, 1983). For understanding local and regional past environmental conditions, it is important to perform various analyses by using different proxies and parameters concerning the bulk sedimentary environment. In Norway, only two studies focused on surface sediment samples with respect to the contribution of marine versus terrigenous material: Trondheimsfjord (Faust et al., 2014) and the fjords of Svalbard (Winkelmann and Knies, 2005).

1.3 Basic information about fjords

Fjords are relatively deep, high-latitude coastal inlets excavated by glacial ice-streams (Syvitski et al., 1987). They formed during intense glaciations and originated by glacier advance and retreat at geological weakness zones in the continental crust. Fjords occur in high-latitude regions north of 43° and south of 42° in Scotland, Norway, Chile, Iceland, Canada, Greenland, Russia, Alaska, Antarctica, and New Zealand (Syvitski et al., 1987). More than 25% of all fjords are under the influence of tidewater glaciers or floating glaciers (Syvitski, 1989).

Generally, fjords are long and narrow, U-shaped, often curved or branching, and have steep sides (Holtedahl, 1975). Fjord lengths range between a few kilometres up to a several of hundred kilometres (e.g. Syvitski et al., 1987) and they can be up to thousand meters deep like for example the 1308 m deep Sognefjord in mid-Norway. The outer part of a fjord near the seaward opening is defined as the fjord entrance, the inland termination is defined as the end of a fjord. Fjords can be classified by their climate regime (Domack and McClennen, 1996) or based on their glacier regime (Hambrey, 1994). Based on climate, they can be divided into polar fjords, which are permanently covered by sea ice as in Antarctica, sub-polar fjords where sea ice is present but breaks up normally completely each year like in Svalbard or Greenland, and temperate fjords where sea ice is absent most of the year like in South-East (SE) Alaska, or Norway (Fig. 1). Based on the glacier regime, five different regimes can be characterized: The Alaskan, Svalbard, Greenland, Antarctic maritime, and Antarctic arid regime. They differ due to their dynamics including glacier flow, sedimentation rates, the receiving amounts of meltwater, and ambient temperatures (Hambrey, 1994).

Typically one or more submarine ridges (sills) are present at fjord entrances and between different fjord basins (Fig. 2). These sills normally consist of glaciofluvial, morainal, or rocky material and have been deposited as terminal moraines due to the advance and retreat of previous glaciers (e.g. Fløistad et al., 2009). Sills influence the water circulation by hindering free exchange between the fjord basins and the open ocean (e.g. Skei, 1983; Jacobson, 1983).

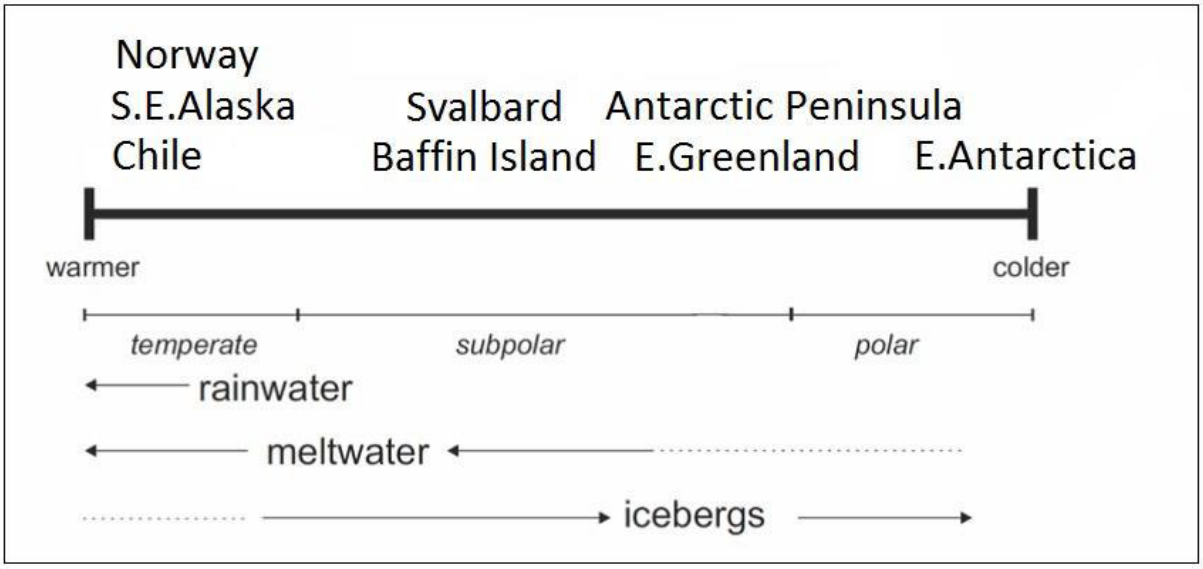

Figure 1: Classification of fjords based on climate. The arrows are indicating the increase of rainwater and meltwater towards temperate fjords with warmer temperatures, and the increase of icebergs towards polar fjords with colder conditions. Modified after Dowdeswell et al., 1998.

1.3.1 Water circulation

The water circulation in fjords is characterized by a typical estuarine circulation pattern with three water layers: a surface layer, an intermediate layer, and a deep water layer (Fig. 2) (Jacobson, 1983). The overall water circulation depends on different features acting on the water masses like the bathymetry, the shape of coastlines, and seasonal variations of freshwater supply from rivers and glaciers (Svendsen et al., 2002). The circulation is characterized by inward flowing marine currents and outward flowing brackish water masses above it (Fig. 2). The intensity of stratification depends on seasonality of freshwater supply, tidal mixing, brine formation, and wind acting on the upper surface layer (Syvitski, 1989). The surface water layer is influenced by seasonal river discharge, by the amount of meltwater mostly discharging in spring and summer, precipitation and evaporation, and by external forces as for example local wind patterns that act on the water surface (e.g. Jacobson, 1983; Syvitski et al., 1987; Syvitski, 1989). The intermediate water layer is affected by incoming oceanic water masses. Those water masses have higher salinities than the surface water above and thus are denser (e.g. Jacobson, 1983). The intermediate layer is controlled by the tides acting in the fjord restricted down to the height of the sill top (e.g. Jacobson, 1983). The deep-water layer is normally the most saline layer and occurs beneath the sill height. In fjords with shallow sills or no sills, this layer might be absent.

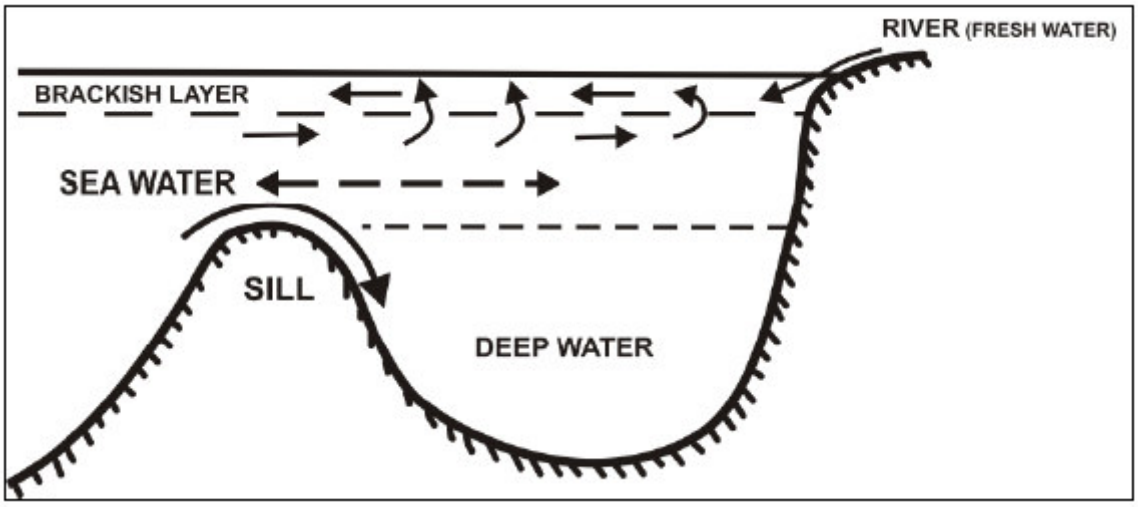

Figure 2: Classification of water masses in a typical Norwegian west coast fjord showing the three water layers: the brackish water layer, intermediate layer and deep water layer. The arrows indicate current flow directions. Modified after Jacobson, 1983.

Interaction between the Coriolis force, wind and water masses causes Ekman transport. Ekman transport is the net movement of surface waters approx. 90 degrees to the right to the wind direction in the northern hemisphere (Price et al., 1987). Thereby, coastal upwelling describes the movement of surface water masses flowing away from the coast and get replaced by deeper water masses moving upwards (Fig. 3a). Downwelling is characterized as the Ekman transport of surface water towards the coast causing water masses to pile up and subsequently sink (Fig. 3b). Upwelling and downwelling influence the sea-surface water temperatures and the biological productivity in fjords as cold nutrient-rich, high-salinity water masses are temporally replacing warm surface water during coastal upwelling or nutrient-depleted surface waters being pushed downwards during downwelling processes (Svendsen et al., 2002).

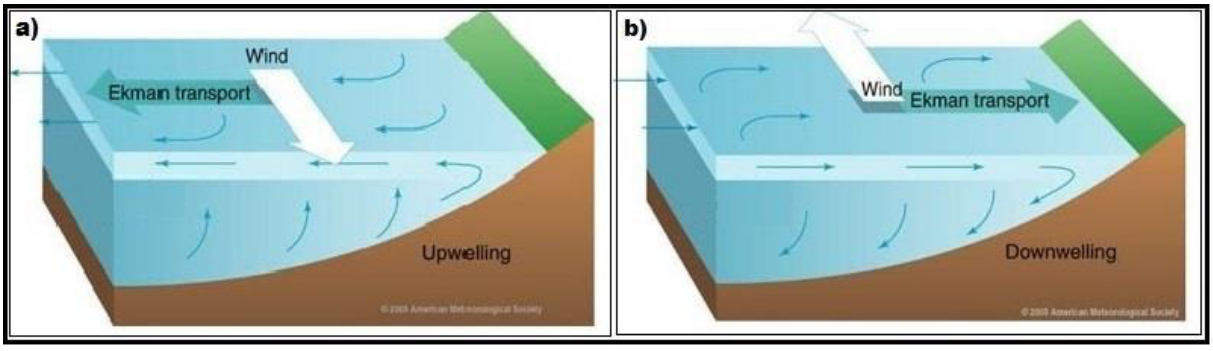

Figure 3: Examples for Upwelling (a) and Downwelling (b) processes in the northern hemisphere. The white arrow indicates predominant wind direction, thin blue arrows indicate water flow direction. Modified after American Meteorological Society, 2005.

1.3.2 Sedimentary processes

Sediments are transported to fjords by river runoff and meltwater discharge. Coarse-grained material is mostly deposited close to river mouths entering the fjords (Hoskin et al., 1978), whereas fine material is capable to be transported over long distances, possibly even to the continental shelf (Hoskin et al., 1978). The fine material is suspended in a brackish surface plume above the halocline in freshwater masses and overflows the more saline water layers beneath (Hoskin et al., 1978). Particle volume, density and radius, the acceleration of gravity, and the velocity and density of the fluid are main factors controlling the settling rate of sediments in the water column. Terrigenous sediments consist usually of freshly weathered material of local origin like for example bedrock material as well as they consist of the hinterland vegetation (e.g. Syvitski et al., 1987). Marine sediments originate from material produced by marine organisms. Fjords are controlled by several parameters and processes as illustrated in Figure 4. Terrestrial influences refer for example to pollution, agriculture, mass movement, or river and meltwater discharges, whereby marine influences are caused by the inflow and outflow of seawater, mixing of water layers, and primary productivity (Fig. 4) (Howe et al., 2010 and references therein).

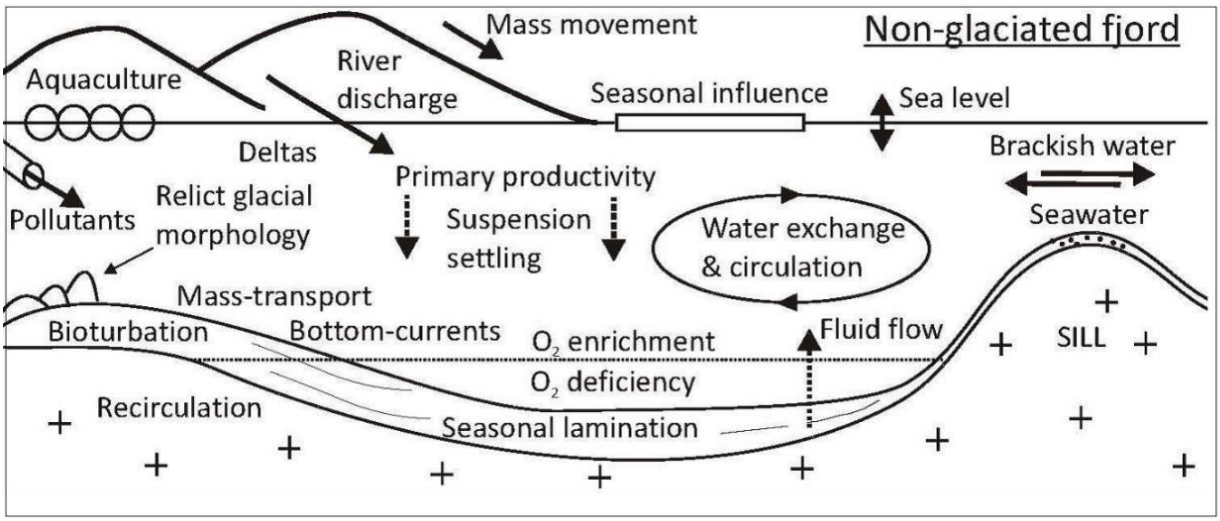

Figure 4: Sedimentary sources and processes in non-glaciated fjords. After Howe et al., 2010.

In addition, fjords have relatively high sedimentation rates and high OM production rates compared to the open ocean (Skei, 1983). Sedimentation rates may provide high-resolution sedimentary records which reflect local sediment patterns (Skei, 1983) and can be suitable for investigating past climate changes as sediment sources like marine productivity and hinterland vegetation are vulnerable to climatic variations (e.g. Svendsen et al., 2002).

1.3.3 Origin of organic matter

Organic matter (OM) consists of organic compounds that remain from organisms like plants and animals (Bordovskiy, 1965). It can be classified into terrestrial organic matter (TOM) and marine organic matter (MOM) (Bordovskiy, 1965). TOM sources include terrestrial soils, hinterland vegetation, and continental sediments, whereas sources for MOM are mainly primary production of marine organisms like zooplankton and phytoplankton (Bordovskiy, 1965). OM in coastal settings is typically a mixture of marine, terrigenous and anthropogenic material (e.g. Meyers, 1994) and is unevenly distributed in marine basins like fjords (Bordovskiy, 1965). The flux of the material is controlled by primary productivity, heterotrophic degradation by organisms using C_{org} for growth, water column depth, and advective transport (e.g. Wakeham and Lee, 1993). The majority of OM in continental margin sediments derives from phytoplankton blooms followed by the fluvial supply of land plant detritus (Meyers, 1997). OM concentrations decrease from this uppermost photic zone, which is the predominant site for primary production, towards the sediment. During sinking processes through the water column, OM is remineralized and degraded by bacteria and fungi (e.g. Altabet and François, 1994; Freudenthal et al., 2001). The water depth, sinking velocity, and oxygen availability within the water column influence the degree of remineralization processes (Meyers, 1997). OM occurs either in true solution (particle sizes < 1 nm), colloidal solution (1-1000 nm) or suspension (>1000 nm) within the water column (Bordovskiy, 1965).

1.3.4 Primary productivity in fjords

Primary productivity is defined as the rate at which energy is converted from atmospheric or aqueous CO_2 to organic substances by utilizing photosynthetic processes and using the sunlight (Fisher, 1939). It takes place in the photic zone in well-mixed water layers of a water body. Photosynthesis is the most common process that uses sunlight as energy source (Fisher, 1939). Microscopic and free-drifting organisms (phytoplankton), which are responsible for primary productivity are defined as primary producers or autotrophs. They form the base of the global marine food chain (Fisher, 1939). In marine environments phytoplankton are the main producers of OM. Main producers among phytoplankton organisms are diatoms. Within certain limits, the rate of primary production is proportional to light intensity and plankton abundance depends on temperature, salinity and the availability of nutrients. As investigated by Eilertsen (1993) and Wassmann et al. (1995), three plankton blooms occur within one year taking place in March and April, in May during the early stages of increased freshwater run-off, and in June

caused by high amounts of nutrient-rich fresh-water inputs. During the rest of the year, variations in plankton dynamics are small throughout the fjords in northern Norway (Eilertsen, 1993). Typically, the strongest phytoplankton bloom occurs in late March to April developing in cold, weakly stratified to non-stratified surface waters (Eilertsen and Taasen, 1984). Greatest influence on these annual spring blooms that support cell growth of the phytoplankton are light penetration, wind-driven vertical mixing, and sporadic freshwater supply to the water body, as well as the increasing solar radiation and the seasonal development of the pycnocline within the water column (Sverdrup, 1953). Phytoplankton is consumed by phytophagous zooplankton which itself is consumed by large crustaceans, fish, whales, and other animals (Eilertsen, 1993). The distribution of phytoplankton and zooplankton is directly related to each other as the amount of zooplankton is high in regions with high abundances of phytoplankton (Eilertsen, 1993).

1.4 Carbon and nitrogen

1.4.1 Stable isotopes

Atoms consist of protons, neutrons and electrons. An isotope of a specific element differs by the number of neutrons in its nucleus while the number of protons remains the same. Both stable and unstable (radioactive) isotopes occur naturally. Stable isotopes are measured with the isotopic signature δ in ‰ as the ratio of $(R_{sample} - R_{standard}) / R_{standard}$. R_{sample} is the isotopic ratio of the sample given for example as $^{13}C/^{12}C$, $^{18}O/^{16}O$, or $^{15}N/^{14}N$. $R_{standard}$ is the corresponding rate in a standard. International defined standards are the PDB Pee Dee Belemnite for measuring $^{13}C/^{12}C$ and $^{18}O/^{16}O$ ratios (e.g. Craig, 1957), and N_2 (atmospheric) air nitrogen for $^{15}N/^{14}N$ (Mariotti, 1983). Using these ratios, stable isotope geochemistry can be used for understanding the ocean´s changing environment and processes. Several physical and chemical reactions as for example the mobilization of light isotopes cause isotopic fractionation. Isotope fractionation describes processes that affect relative abundances of for example carbon and nitrogen isotopes. Within these processes, mass differences due to the ratio between protons and neutrons play an important role as light isotopes are more mobile and thus more affected by fractionation than heavy isotopes (e.g. Wada and Hattori, 1991).

1.4.2 Carbon isotopes and fractionation processes

On Earth, carbon (C) occurs in a wide variety of compounds including two natural stable isotopes, ^{12}C and ^{13}C, and one instable isotope ^{14}C (e.g. Rundel et al., 1989). Stable carbon isotope signatures of $\delta^{13}C$ can be used as tracers for reconstructing past temperatures and salinities, circulation patterns or productivity rates and gas exchange rates within the ocean-atmosphere system (e.g. Hoefs, 2009). The organic stable carbon isotope signature ($\delta^{13}C_{org}$) reflects the isotopic composition of carbon sources and fractionation processes between ^{12}C and ^{13}C during photosynthesis (Hayes, 1993). Fractionation intensity decreases with decreasing CO_2 availability. By using $\delta^{13}C_{org}$, it is possible to distinguish between TOM and MOM sources in sediments and to identify OM from different land plants (Sacket, 1964). Typical carbon stable isotope signatures are presented in Figure 5 and illustrate several settings on a continental margin close to the Congo fan as an example. The $\delta^{13}C_{org}$ demonstrates pathways from different biological systems to mixed data within the sediments.

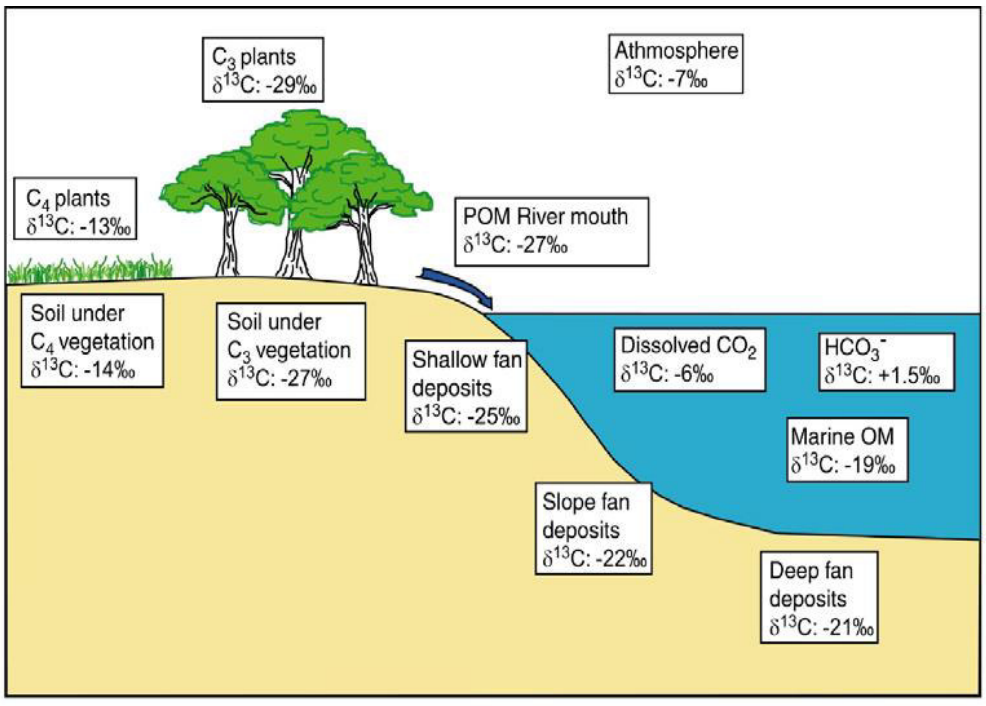

Figure 5: Different carbon stable isotope values are presented in different settings on the continental margin with the Congo Fan as an example. Data of biota and sediments are taken from measurements at the Congo Fan and the Congo River catchment area (Mariotti et al., 1991; Muzuka 1999; Schwartz et al., 1986).

The $\delta^{13}C$ signature of seawater is mainly controlled by differences in carbon sources used for biochemical fractionation processes by marine organisms. In addition, $\delta^{13}C$ is controlled by physical fractionation due to gas exchange at the seawater-air boundary) and species characteristics, light intensity, or the growth rate of the phytoplankton which utilizes fractionation (e.g. Broecker and Maier-Reimer, 1992. Fractionation processes are affected by

the formation and decay of both TOM and MOM. Marine phytoplankton uses in seawater dissolved CO_2, whereas terrestrial plants utilize atmospheric CO_2. Generally lower $\delta^{13}C$ values in the terrestrial fraction are effected by initial $\delta^{13}C$ of -7‰ of atmospheric CO_2 (Hayes, 1993). Carbon sources for marine organisms are isotopically enriched in ^{13}C with $\delta^{13}C$ endmember values of -20 to -22 ‰, compared to the source for land plants which mainly consists of atmospheric CO_2 and is indicated by endmember values of approx. -27 ‰ (Schubert and Calvert, 2001; Meyers, 1994). Modern $\delta^{13}C$ values of surface seawaters are close to 0 ‰ and vary only within a small range (Hoefs, 2009). Within the water column nearly all OM produced by photosynthesis subsequently is re-mineralized by different processes and organisms. Remineralisation causes deeper water masses to have lower $\delta^{13}C$ values than upper water layers.

Photosynthesis is characterized by two pathways commonly used for carbon fixation. These pathways highly influence $\delta^{13}C$ values and are defined either by the Calvin C_3 for both terrestrial and marine plants or the Hatch-Slack C_4 incorporation for terrestrial plants (Collins and Jones, 1986). Marine plants like phytoplankton and terrestrial plants like trees or shrubs fix atmospheric CO_2 into their biomass using the Calvin (C_3) pathway. Plants which take up this pathway, are light-dependent and exist where sunlight intensity and temperatures are moderate like in higher latitudes (Collins and Jones, 1986; Still et al., 2003). The incorporation of carbon using the C_3 pathway produces a shift in $\delta^{13}C$ values of about -20‰. Contrary, some plants like subtropical grasses use the Hatch-Slack (C4) carbon fixation which is more effective in hot or dry areas and in lower latitudes leading to an isotopic shift of about -7‰. C_4 plant types are negligible in higher latitudes (Collins and Jones, 1985).

1.4.3 The global organic carbon cycle

Carbon fixation is part of the global organic carbon (C_{org}) cycle (e.g. Tissot and Welte, 1984) which is divided into the biological and the geological cycle (Fig. 6). Photosynthesis is part of the biological carbon cycle as plants and bacteria transform CO_2 to C_{org} (Fig. 6) by using atmospheric CO_2 or bicarbonate and CO_2 of aquatic surface waters. Due to plant consumption and decay processes, C_{org} can enter the oceans as dissolved organic carbon and might be stored in recent sediments and soils (Tissot and Welte, 1984). Chemical or metabolic oxidation of decayed biomass takes place in the water column and the sediments. CO_2 is released to the atmosphere and to waters. The C_{org} reservoir which is stored in recent soils and sediments has an extent of approx. $6.4x10^5$t carbon. This is several orders of magnitude lower than the

geological carbon reservoir with $3x10^{12}$t carbon (Tissot and Welte, 1984). The geological organic carbon cycle contains the incorporation of biogenic OM into sediments or soils (Fig. 6). Deposition and burial of OM indicates the overlap between both cycles. Within the geological cycle carbon leads to the formation of petroleum, natural gases and coal or to metamorphic forms of carbon like graphite (Tissot and Welte, 1984). Graphite may re-oxidize to CO_2 as a result of sedimentary erosion or due to combustion processes of fossil fuels. The transformation of organic to fossil material starts immediately after the decay of living organisms while sinking in the water column, during alteration processes at sediment surfaces, or within the uppermost sediment layers (Fig. 6) (Tissot and Welte, 1984).

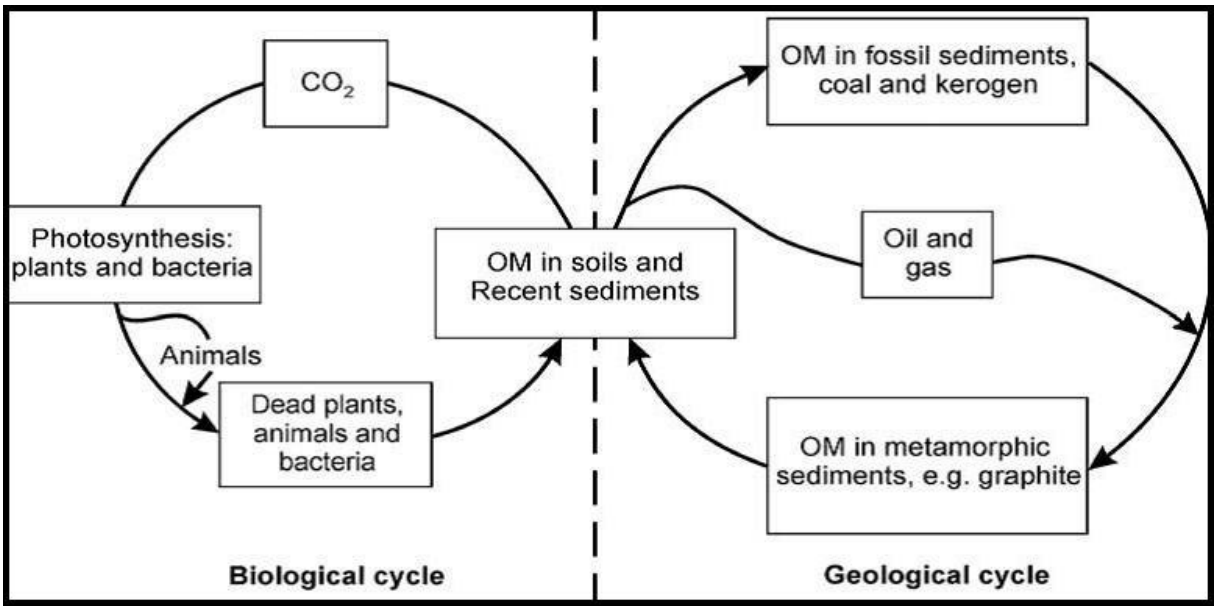

Figure 6: The two major parts of the organic carbon cycle on Earth with the biological cycle on the left side and the geological one on the right side. OM = organic matter. After Tissot and Welte, 1984.

1.4.4 Nitrogen isotopes and fractionation processes

More than 99% of the Earth´s nitrogen (N_2) occur as atmospheric nitrogen (N_{atm}) or dissolved nitrogen in water bodies. The largest nitrogen pool is represented by the atmosphere. Nitrogen has two stable isotopes: ^{14}N with 99.63% of all natural occurrences and ^{15}N (e.g. Rundel et al., 1989). N_{atm} is converted to organic nitrogen (N_{org}) by several species of bacteria and algae. Those microorganisms are responsible for fractionation processes within the biological nitrogen cycle (e.g. Rundel et al., 1989). Figure 7 shows the marine nitrogen cycle, which is part of the global biological nitrogen cycle. Fractionation processes are characterized by nitrogen fixation which occurs in plant roots both on land and in aquatic environments (Fig. 7), nitrification which presents the production of nitrate due to oxydation (Fig. 7), and denitrification

representing nitrate production from N_2 (Fig. 7). Denitrification is presented in stratified anaerobic water bodies (Fig. 7) and in poorly aerated soils (Hoefs, 2009).

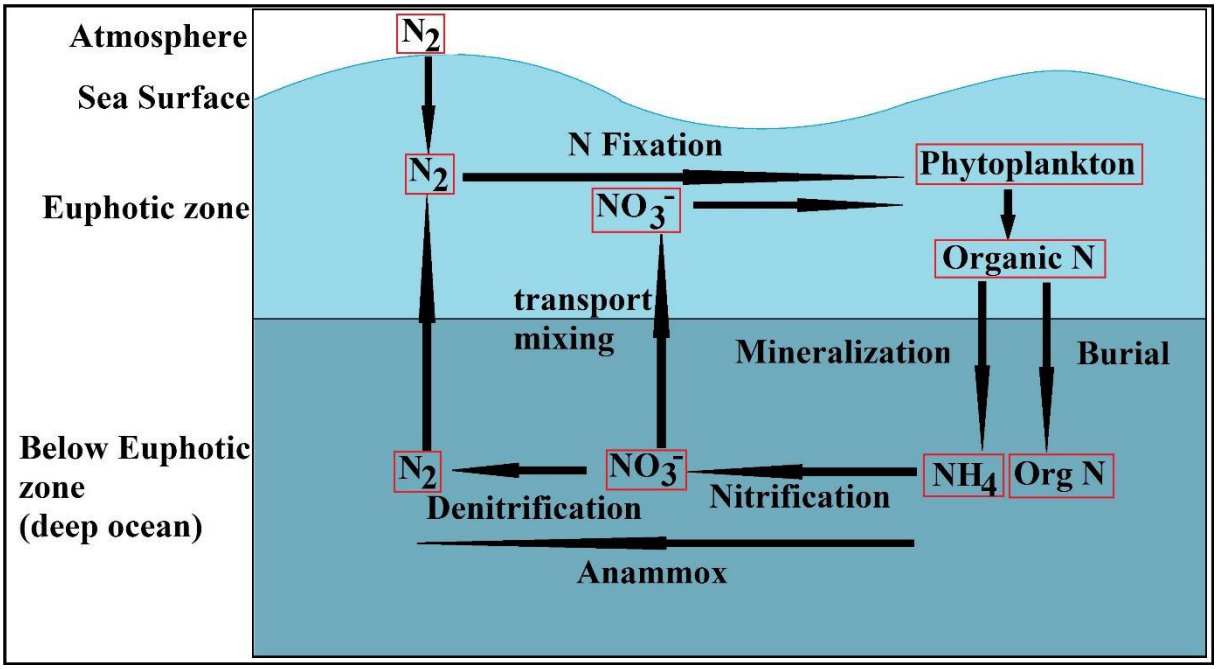

Figure 7: Schematic figure of the major processes in the marine nitrogen cycle: Presenting the production of OM by assimilation of inorganic nitrogen and N_2 fixation by phytoplankton in surface waters following in the mineralization and/or the burial of organic material and the release of ammonium. Below the euphotic zone, the oxidation of NH_4 (nitrification) leads to the production of nitrate and further to denitrification to N_2. Anaerobic ammonium oxidation (Anammox) is presented as well.

Nitrogen stable isotopes ($\delta^{15}N$) are part of the global nitrogen cycle as well and involved in the utilization of dissolved inorganic nitrogen (N_{inorg}) by phytoplankton, the consumption of phytoplankton by grazers and the remineralisation of organic compounds by animals and bacteria (Hoefs, 2009). Total $\delta^{15}N$ contents can be controlled and decreased by the atmospheric nitrogen, which has a value of approx. $\delta^{15}N = 0‰$, and which is fixed by both land plants and soil OM and by marine organisms (Wada et al., 1987b). Low $\delta^{15}N$ concentrations and hence the low shift of the atmospheric isotopic signature usually occur in terrestrial derived material that is defined by values of approx. 0.4‰ as fractionation by land plants is low or even absent (e.g. Peters et al., 1978). High $\delta^{15}N$ concentrations are effected by marine organisms that cause fractionation processes leading to a shift of approx. 7‰, and thus usually have values between 4‰ and 8‰ (Peters et al., 1978). Therefore, high $\delta^{15}N$ concentrations indicate strong influences of marine fractionation, whereas lower values are indicators for terrigenous derived material (e.g. Peters et al., 1978).

This leads to the use of $\delta^{15}N$ as another proxy for distinguishing between marine and terrestrial derived OM (e.g. Sepúlveda et al., 2011; Schubert and Calvert, 2001) and to track the relative

nutrient utilization in nitrate depleted environments (e.g. Calvert et al., 1992; Altabet and François, 1994; Schubert and Calvert, 2001). Furthermore, $\delta^{15}N$ is used for tracking changes in denitrification (e.g. Altabet et al., 1995) and N_2-fixation processes (e.g. Haug et al., 1998). Thereby, $\delta^{15}N_{inorg}$ and $\delta^{15}N_{org}$ values can be separated due to the fact that $\delta^{15}N_{inorg}$ strongly depends on the terrestrial fraction of ammonium (NH_4^+) bound between the lattice structures of terrestrial clay minerals like illite (Schubert and Calvert, 2001), whereby $\delta^{15}N_{org}$ is not influenced by the NH_4^+. Therefore, $\delta^{15}N_{org}$ signatures are more reliable compared to $\delta^{15}N_{inorg}$ when identifying variations in nutrient utilization and fractionation processes by phytoplankton in an aquatic environment (e.g. Wada and Hattori, 1991; Calvert et al., 1992; Altabet and François, 1994; Schubert and Calvert, 2001; Knies et al., 2007). Changes in $\delta^{15}N$ contents reveal variations in productivity and nutrient levels in the water column (e.g. Ostrom et al., 1997). In addition, $\delta^{15}N_{org}$ signatures can indicate diagenetic processes in a sediment column caused by the degradation of organic compounds and hence by isotope fractionation during those degradation processes (e.g Lange et al., 1994). Due to fractionation processes in marine environments and the low or even absence of fractionation on land, nitrogen and thus nitrogen isotopes can be used for recording changes in nutrient dynamics both on land and within the water column over time.

To sum up, both $\delta^{13}C_{org}$ and $\delta^{15}N$ are widely used as proxies for the identification of biogeochemical processes in marine sediments and for tracing the contribution of TOM versus MOM into marine sediments (Sacket, 1964). Thereby, $\delta^{15}N$ is more affected by biogeochemical processes than $\delta^{13}C_{org}$ signatures (Sacket, 1964). Processes are related to nutrient utilization, denitrification, the formation and accumulation of TOM and MOM, dilution effects of detrital material, and the preservation and mineralization in sediments (Hedges and Keil, 1995).

2 Study area

The temperate Ofotfjord, Vestfjord, Tysfjord, and their tributary fjords are located around 200 km above the Arctic Cycle close to the Lofoten Islands and the Norwegian mainland (Fig. 8). The three fjords are separated by submarine sills. Main cities in the study area are Bodø in the south of the Vestfjord, Svolvær on the Lofoten Islands and Narvik in the east (Fig. 8).

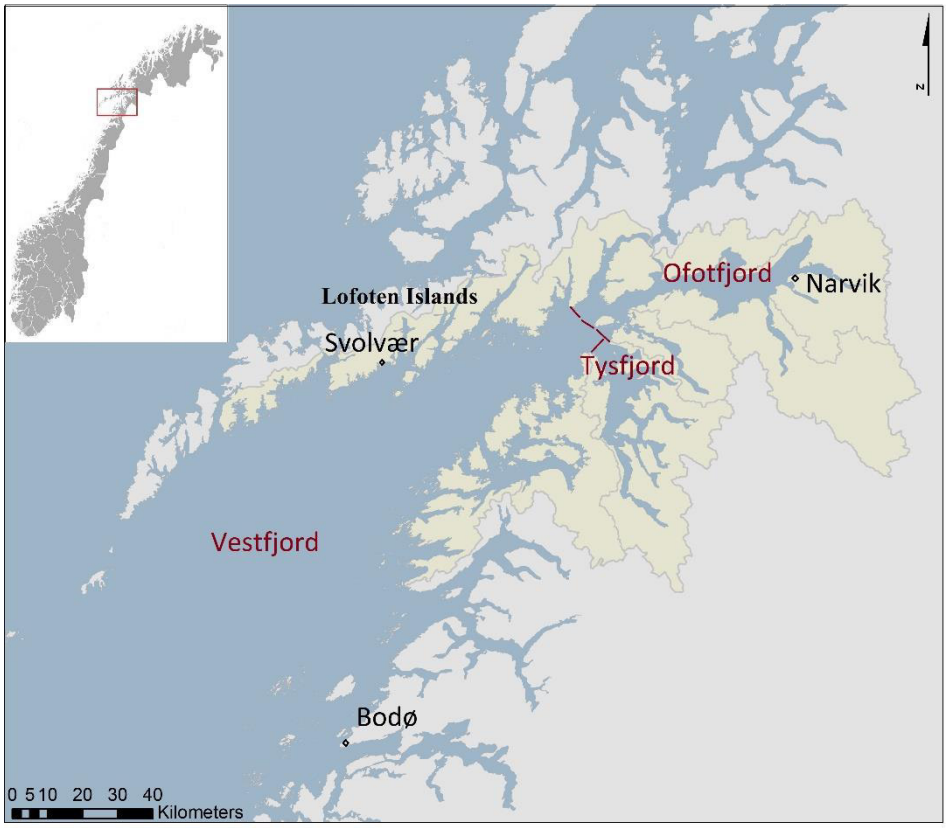

Figure 8: Location of the study area indicated by the red square in the upper left inlet. The dotted lines between the Vestfjord, Ofotfjord, and Tysfjord mark the presence of sills. The fjord boundaries are defined by these sills. The yellowish border around the fjords indicates the drainage area.

The Vestfjord (68° 3′ 0″ N, 14° 46′ 0″ E) is an atypical fjord with a shape more like a coastal bay. It has a length of approx. 200 km and terminates where the basin coincides with the Trænadjupet cross-shelf trough (Fig. 13) (e.g.Ottesen et al., 2005). The fjord has a width of 80 km and a water depth of 350-400 m at the widest part between Bodø and the Lofoten Islands (Fig. 8) and narrows gradually towards the north-east (NE) where the water depth decreases to 200-300 m. In the inner part of the Vestfjord, the water depth increases again up to 600 m (Fig. 9). The narrowest part of the Vestfjord (20 km wide) is located at the entrances of the Ofotfjord and Tysfjord.

Two across-fjord ridges are located at the merging of the fjords (Fig. 8) (e.g. Fløistad et al., 2009). These submarine ridges are defined as the Ofotfjord sill and the Tysfjord sill. The Ofotfjord sill can be followed across the Ofotfjord for more than 5 km in length and 2 km in width. Close to the sill, the water depth is more than 500 m deep; the depth at the ridge itself rises 200 m above the adjacent sea floor (Fløistad et al., 2009). The Tysfjord sill is also an across-fjord ridge and water depth at the sill ranges between 140 and 350 m, which is more than 350 m above the adjacent seafloor which can exceed 700 m water depth (e.g. Fløistad et al., 2009). Both sills are characterized by well-developed subglacial bedforms like crag and tail formations, drumlins, and glacial lineations on top of the ridges (Fløistad et al., 2009). All bedforms are generated by the retreat of one of the large paleo-ice streams of the Fennoscandian Ice Sheet (see chapter 2.4) (Ottesen et al., 2005). The lineations indicate ice-flow coming from NNE (Fløistad et al., 2009).

The Vestfjord comprises a Mesozoic and Cenozoic sedimentary basin (Rokoengen and Sættem, 1983), whereas older crystalline rocks occur on land and along the coastline. The seafloor is characterized by features formed due to glacial erosion like mega-scale glacial lineations parallel to the fjord axes, megaflutes, longitudinal ridges and transverse morainal ridges (Fig. 9) (e.g. Ottesen et al., 2005a,b; Laberg et al., 2007; Knies et al., 2007). Submarine ridges between 200 to 500 m wide and up to 10 m high are present in the inner part of the Vestfjord. Elongated troughs parallel to the axis of the Vestfjord in the inner part of the fjord can be found in 600 m water depth. They are up to 75 km long and 10 km wide, and have been partly eroded into bedrock, partly into Quaternary sediments (Fløistad et al., 2009). Several moraine ridges are present and located perpendicular to the inferred ice-flow direction (Ottesen et al., 2005; Laberg et al., 2007).

The Ofotfjord (68° 25′ 0″ N, 17° 1′ 0″ E) is an open E-W trending embayment and acts like an extension of the Vestfjord. It is located between the Vesterålen Islands to the north and the Norwegian mainland to the south. The fjord has a length of 78 km and a maximum water depth of 553 m. Several small fjord branches extend from the main fjord. Where the Ofotfjord and Tysfjord merge, the outer part of the Ofotfjord narrows to 5 to 10 km. The middle basin has an average depth of 500 m (Fig. 9).

The Tysfjord (68° 5′ 38″ N, 16° 21′ 12″ E) is a 59 km long branch of the Vestfjord and has a north-south extension with a maximum water depth of 725 m. The outer parts are located at the merging with the Ofotfjord and the inner part of the Vestfjord. Five tributary fjord arms discharge into the Tysfjord.

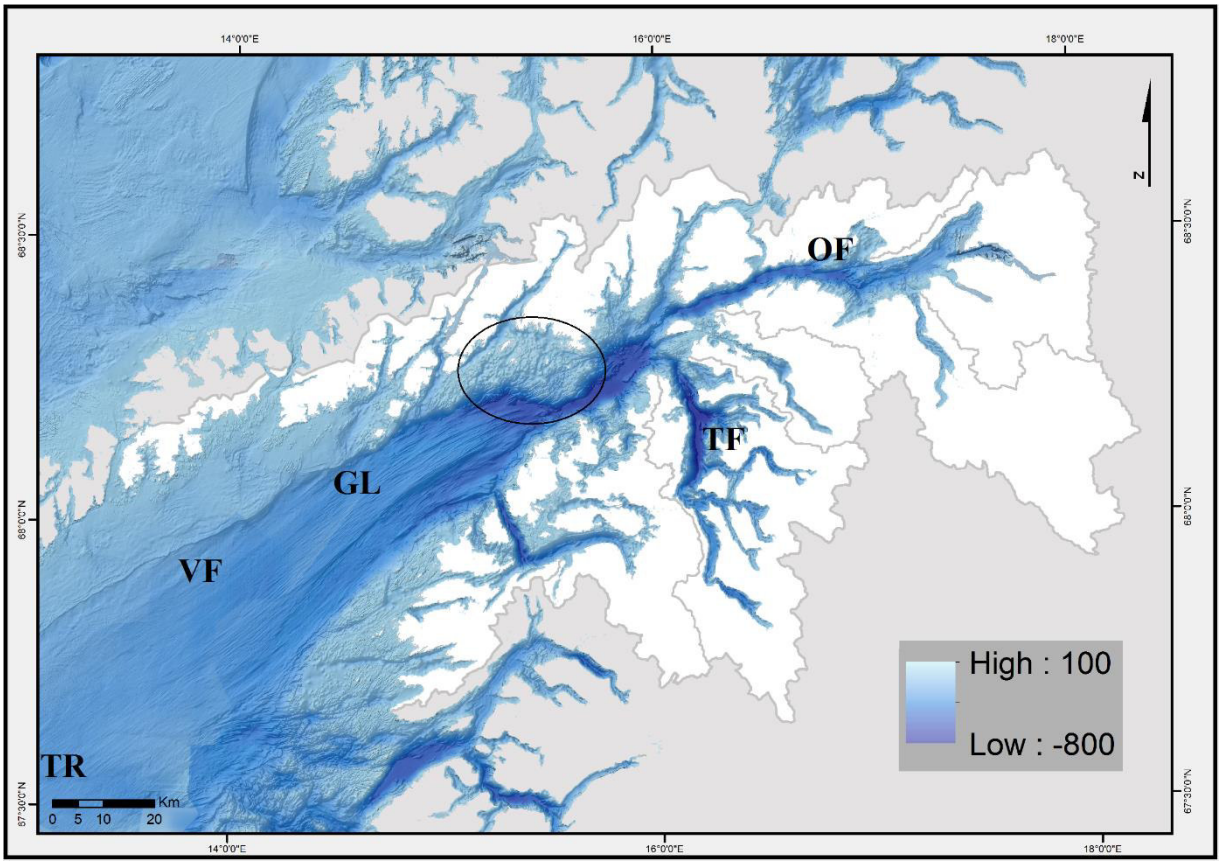

Figure 9: Bathymetry of the study area illustrating the Vestfjord (VF), Ofotfjord (OF) and Tysfjord (TF). Glacial lineations (GL) are shown in the middle parts of Vestfjord as well as the slightly illustrated Tennholmen Ridge (TR). The black cycle illustrates the dominant upwelling area of the Vestfjord. The drainage area for the study area is defined by the white shape around the several fjords.

2.1 Regional climate

The fjords of the study area are located in a typically oceanic and semi-continental climate. Annual mean temperatures with mean summer and winter temperatures as well as total annual precipitation are presented in Table 1 for the cities of Bodø, Narvik and Svolvær in the years 1961-1990 (Norwegian Meteorological Institute, 2015).

Table 1: Mean annual, summer and winter temperatures and the total annual precipitation for Bodø, Narvik and Svolvær (Norwegian Meteorological Institute, 2015).

	Bodø	**Narvik**	**Svolvær**
Annual mean temperature (°C)	4.5	3.6	4.6
Mean summer temperature (°C)	11.7	11.9	11.4
Mean winter temperature (°C)	-1.8	-3.5	-0.9
Total annual precipitation (mm/year)	1020	855	1500

The outer parts of the Lofoten Islands are climatically different compared to the narrow fjords of the mainland. The outer parts are characterized by relatively warm and mild winters as well as summers with moderate rainfall. Inner parts proximal to the mainland are more influenced by continental climatic conditions (Norwegian Meteorological Institute, 2015). Precipitation is high during the whole year in areas close to the mountains due to orographic enhancement (Furnes and Sundby, 1981) and total precipitation in all fjords is heaviest in autumn (Norwegian Meteorological Institute, 2015). Increased precipitation is demonstrated for Svolvær compared to Bodø and Narvik (Table 1). In winter, the snow covers parts of the land-facing side permanently, whereas snow-cover at the coast is more infrequently (e.g. Mitchelson-Jacob and Sundby, 2001).

Two wind directions are predominant in the Vestfjord fjord system: south-west (SW) and NE, respectively (Furnes and Sundby, 1981). SW winds are dominant during autumn (September to November) and winter (December to February) with wind intensities reaching 38 km/h (Jones et al., 1997). During summer (June to August), the predominant wind direction is NE with an average velocity of approx. 20 km/h.

2.2 Drainage area

The drainage area of the Vestfjord, Ofotfjord, Tysfjord and their tributary fjords is presented in Fig. 8. It has a total extend of 13 489 km^2. The total fjord surface area is 6 371 km^2 and 7 118 km^2 are land area. Larger rivers do not exist, as river lengths are restricted by the mountainous character of the entire drainage area. Due to snow-melt in the mountains, runoff during summer is much higher than during winter (Sundby, 1982). The snow-melt starts in May and highest runoff rates occur from June to August. In those months, two thirds of the annual runoff enter the Vestfjord (Sundby, 1982). Three larger glaciers are located in the drainage area (Fig. 10). With an extensive ice cap area of 28.44 km^2 the Kitjejekna is the largest glacier located in the mountains south of Tysfjord close to the Swedish border (Fig. 10, no. 1). The Storsteinsfjellbreen is another large icefield with an area of 12 km^2. It is located in the SE of Narvik (Fig. 10, no. 3). The Frostisen glacier covers an area of 27 km^2 and is located south of Narvik (Fig. 10, no. 2).

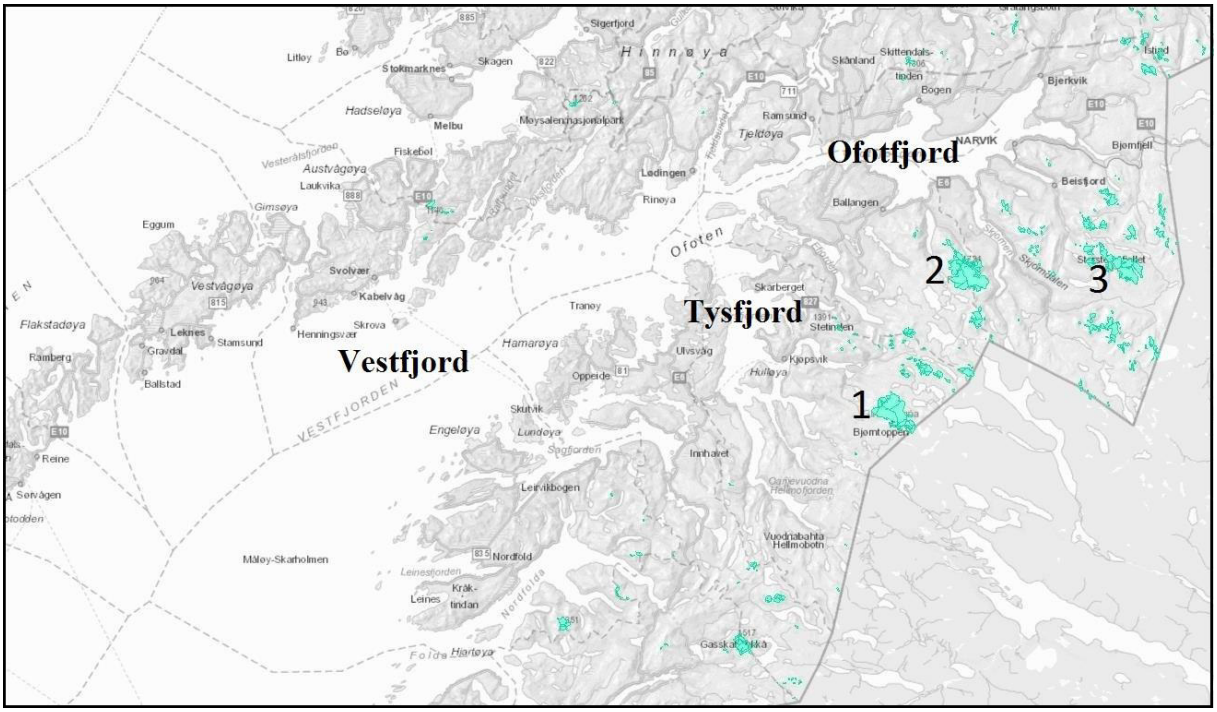

Figure 10: Location of the largest glaciers in the region by blue colours. The largest one, Kitjejekna, indicated by number 1, is located south of Tysfjord. Number 2 shows the location of Frostisen glacier, whereas number 3 illustrates the location of the Storsteinsfjell glacier located close to Narvik. (atlas.nve.no).

2.3 Bedrock geology

The drainage area of the three fjords is characterized by high mountains reaching more than 1000 m a.s.l. The highest one, Storsteinfjellet close Narvik reaches 1894 m a.s.l. Most of the mountains consist of Precambrian basement rocks, which are part of a NNE trending basement height (Ramberg et al., 2008). They form tectonic windows in the overlying younger Caledonian nappe pile. The basement rocks were uplifted and locally deformed during crustal extension after the Caledonian orogeny 490 – 390 Ma ago (Ramberg et al., 2008) (Fig. 11). Precambrian rocks of sedimentary and volcanic origin are found on the island of Langøya, tonalitic gneisses and small greenstone belts of over 2500 Ma old ages (e.g. Gullesfjorden Granite) are found on the island of Hinnøya. Early Proterozoic metasedimentary rocks (ca. 2100 Ma old) are scattered around the Lofoten Islands. They consist of quartzo-feldspathic gneisses, minor banded-iron formations (BIF), graphitic schists, and marble (Ramberg et al., 2008). Calcitic and dolomitic marble of the Caledonian nappe complex are highly presented in the Ofotfjord region (Melezhik et al., 2002). Precambrian rocks are transected by younger plutonic rocks like granites with up to 1870 Ma. Charnockite (granite carrying orthopyroxene) and mangerite (orthopyroxene-bearing monozonite) are the most common plutnic rock types. All

local plutonic rocks form one single group called the anorthosite-magnerite-charnockite-granite suite which is typical for the Proterozoicum (Ramberg et al., 2008). Furthermore, the SE side of the Vestfjord is characterized by the boundary to crystalline bedrock and by a steep, up to 300 m high escarpment (Ottesen et al., 2005) which might be the result of enhanced glacial erosion of the Vestfjord Basin (Rokoengen and Sættem, 1983).

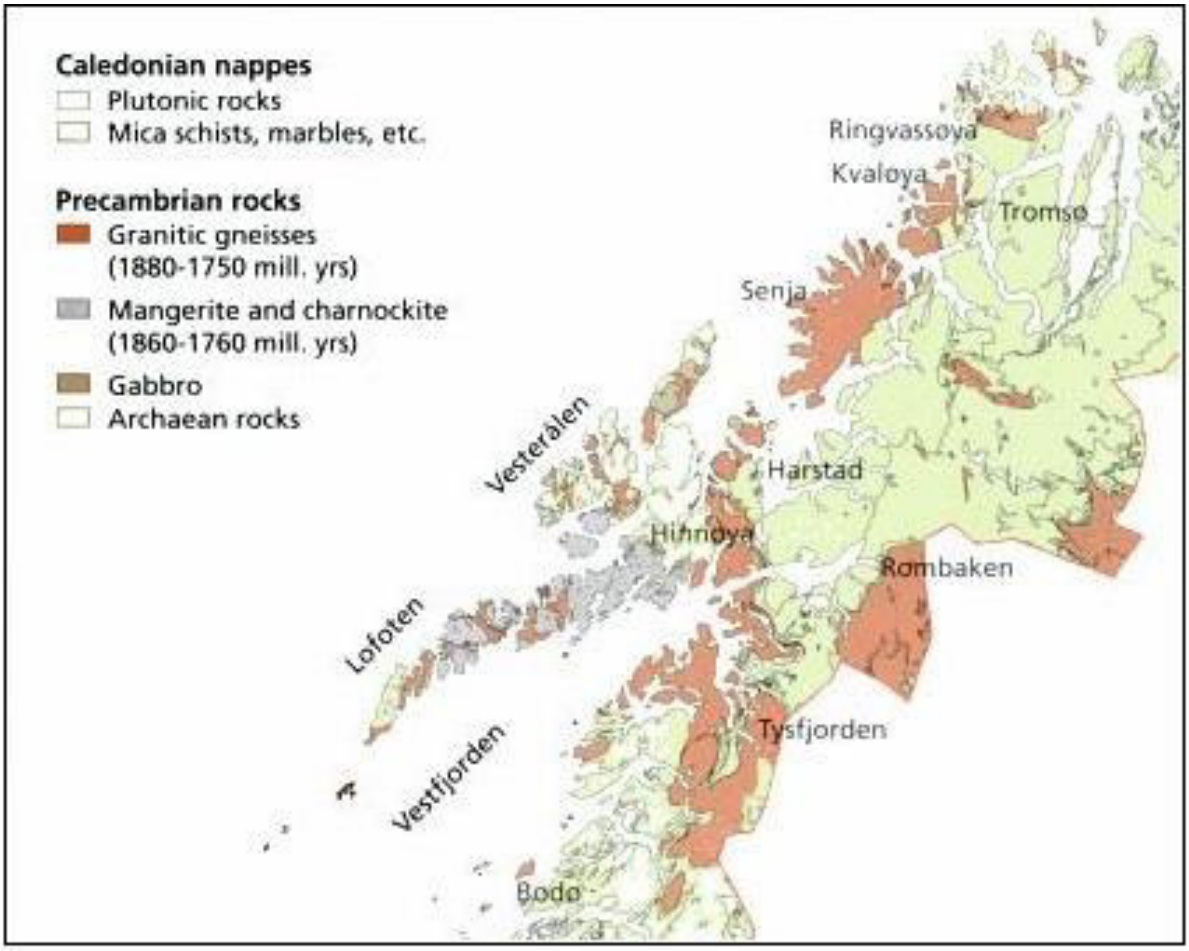

Figure 11: Regional geology of northern Norway. Modified after Ramberg et al., 2008.

2.4 Glacial history

The Fennoscandian Ice Shield was subject to a complex glacial history in the Cenozoic (66 Ma to present day). Glaciation and deglaciation periods occurred during the entire Quaternary from 2.58 Ma to present day (Appendix Fig. 2). Corresponding ice sheet advance and retreat from the mainland towards the continental shelf in Norway were included in these periods. The main Weichselian Fennoscandian Ice Sheet developed at approx. 70 ka and was initially concentrated over southern Norway (Kleman et al., 1997) before the ice masses grew slowly towards the NE during the period from 65-22 ka (Kleman et al., 1997). During the Late Weichselian (approx.

24 ka to the beginning of the Holocene 11.7 ka) the western and north-western (NW) parts of Fennoscandia were covered by ice as well as the Norwegian continental shelf, where grounded ice accumulated with the ice front near the shelf break (e.g. Vorren, 2003). The fjords of the study area were also exposed to intense glaciation (e.g Sejrup et al., 1994; Dahlgren and Vorren, 2003; Ottesen et al., 2005; Laberg et al., 2007; Knies et al., 2007; Laberg et al., 2009) with a glacial maximum when the Fennoscandian Ice Sheet reached the shelf break off Norway as illustrated in Figure 12 (Vorren and Plassen, 2002). The re-advance of the ice masses occurred rapidly at 15 ka ^{14}C BP (radiocarbon years before present) (Vorren and Plassen, 2002; Dahlgren and Vorren, 2003).

Along the Norwegian continental shelf and the western and northern Barents Sea slopes in the western part of the FIS, ice drainage was concentrated in intensive fast-flowing ice streams expanding across the shelf towards the shelf edge (e.g. Laberg et al., 2002a; Sejrup et al., 2003; Ottesen et al., 2005a). The ice streams usually consisted of more than 2 km thick ice masses and delivered large proportions of glacial debris to the marine realm of the shelf edge and the deep sea (Kleman et al., 1997; Ottesen et al., 2005b). One of those major paleo-ice streams along the NW part of the Fennoscandian Ice Sheet during the Late Weichselian was confined by the Ofotfjord-Vestfjord-Trænadjupet troughs and formed the glacial landforms of the present fjords of the study area (Fig. 9, 12) (Ottesen et al., 2005a). The ice-stream was fed by confluent ice flow through the Ofotfjord, Tysfjord and tributary fjords to the south (Bennet, 2003) and flowed towards SW in the Vestfjord before it merged with other ice masses in the eastern part of the Trænadjupet (Fig. 12) and supplementary moved towards NW (Laberg et al., 2002a; Ottesen et al., 2005b). The Trænadjupet-Vestfjorden-Ofotfjorden system was entirely glaciated at 23.7 ka ^{14}C BP (Dahlgren and Vorren, 2003) and after the Last Glacial Maximum (LGM) break-up, the ice retreated rapidly from the shelf edge to the Vestfjord (Dahlgren and Vorren, 2003; Ottesen et al., 2005b). The inner part of the Vestfjord have been deglaciated supplementary at approx. 12.5 ^{14}C ka BP. The deglaciation in the area is consistent with late Weichselian ice sheet dynamics along the entire western Norwegian continental shelf and in the Barents Sea (e.g. Knies et al., 2007).

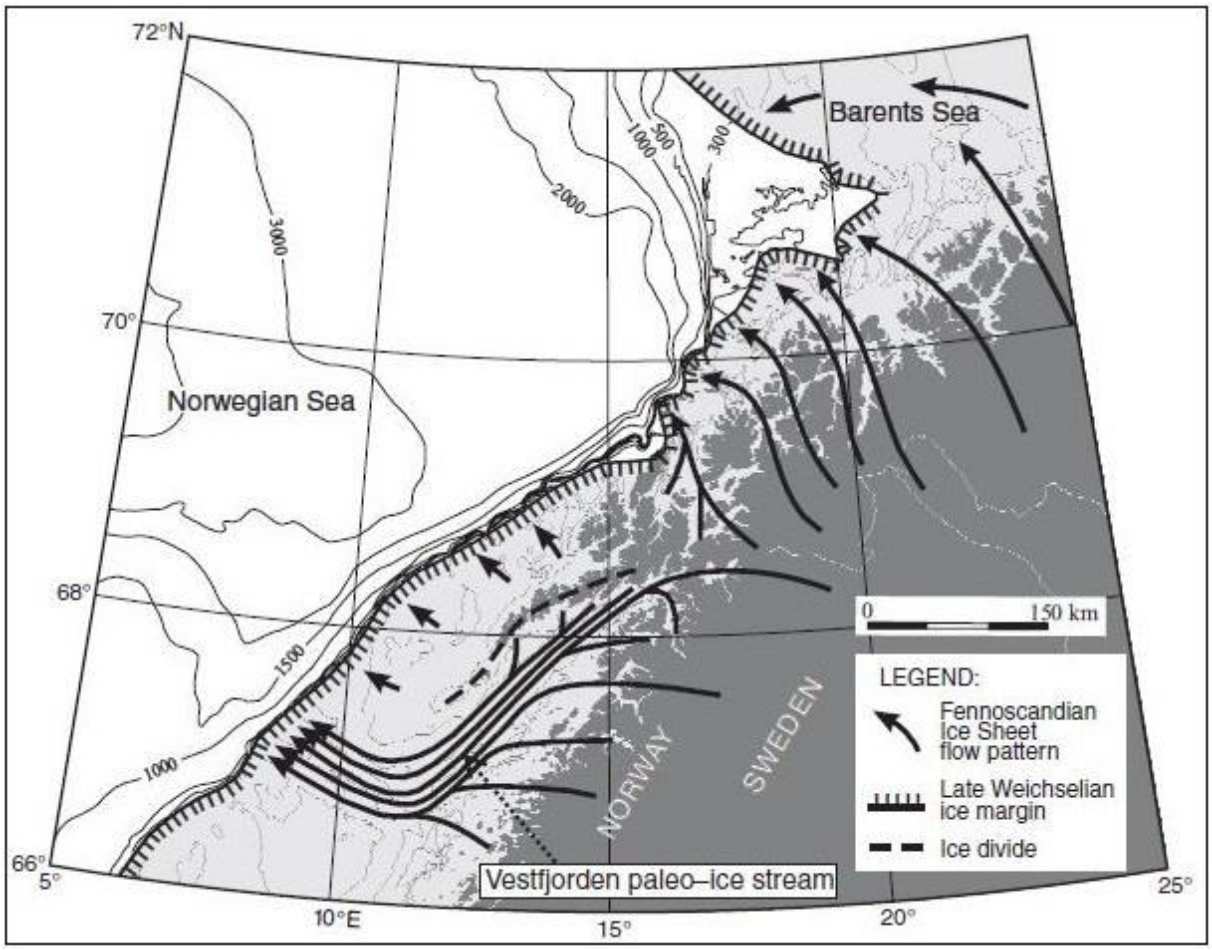

Figure 12: Reconstruction of the NW part of the Fennoscandian Ice Sheet during the Last Glacial Maximum (LGM) inclunding the Vestfjord paleo-ice stream. The flow pattern is modified from Laberg et al. (2002b), Vorren (2003), and Ottesen et al. (2005a). The locations of the ice margin is taken from Vorren and Laberg (1996). After Laberg et al. (2009).

The paleo-ice stream had a length of approx. 400 km and covered an area of approx. 20,000 km^2 with a drainage area of 150,000 km^2 within the Fennoscandian Ice Sheet during the LGM (Ottesen et al., 2005). The average flow velocity has been calculated as approx. 750 m/yr (Ottesen et al., 2005a). The paleo-ice stream eroded extensively into Mesozoic and Cenozoic sedimentary rocks and Quaternary sediments (e.g. Rokoengen and Sættem 1983), but its presence and location prevented large ice masses from reaching and eroding the mountains of the Lofoten Islands and Vesterålen (Ottesen et al., 2005). The average sedimentation rate in the paleo-ice stream drainage area during between 35-11 ka has been calculated by presumably 2.6 m/ka which estimates an average sediment discharge of 35 x 10^6 t/year and an erosion rate of approx. 1.7 mm/year (Laberg et al., 2009). The outermost part of the Vestfjord close to the Tennholmen Ridge (Fig. 9) is characterized by low sedimentation rates between 2 and 4 cm/ka in a period of 13-3 ^{14}C ka BP, whereas central parts of the Vestfjord reveal sedimentation rates between 7 and 61 cm/ka with highest values (61 cm/ka) during the initial phase 13-12 ^{14}C ka BP of the deglaciation (Knies et al., 2007).

Today, the Vestfjord and the Trænadjupet generally are covered by sediments from the deglaciation and the Holocene and are characterized by well-developed subglacial sedimentary bedforms like glacially eroded troughs, extensive glacial lineations (Fig. 9), longitudinal ridges, and transverse moraine ridges (Ottesen et al., 2005; Laberg et al., 2007; Knies et al., 2007).

2.5 Oceanography

Surface water temperatures in the Vestfjord are 4°-5°C in January and 10°-11°C in July (Norwegian Institute of Marine Research, 2015). In 150 m water depth, temperatures are around 7°C in winter, and 6.4°C in summer. Salinity seasonally varies between 32 and 34 in the surface layer, and 34 to 35 in the intermediate water layer. Salinity in water depths <300m is 35 all year long (Norwegian Institute of Marine Research, 2015). The inflow of relatively warm and saline Atlantic water keeps most of the fjords ice-free during winter times (Mitchelson-Jacob and Sundby, 2001).

The Norwegian Atlantic Current (NAC) and the Norwegian Coastal Current (NCC) enter the Vestfjord, Ofotfjord, Tysfjord, and tributary fjords (Fig. 13) (Geddes and Scott, 1994). The general circulation pattern in the Vestfjord and Ofotfjord is described by inflowing water masses along the eastern side along the inner parts of the fjords, and outflowing water along the western side flowing along the Lofoten Islands (Eggvin, 1931). The NAC flows from low to high latitudes and follows the steep Norwegian continental shelf break northwards (Fig. 13). It has relatively high salinity contents (>35) and relatively warm temperatures (>6°C even in winter) compared to the NCC which is a lower-salinity current (<34.8) due to high amounts of river runoff along the Norwegian coastline. The NCC originates in the Baltic Sea and flows to the north. It bifurcates due to the morphology of the Lofoten Islands and continues into the Vestfjord with approx. 10% of its total volume (Sundby, 1978). The remaining water masses flow towards the west over the Træna Trough (Trænadjupet), and continue northwards along the west side of the Lofoten Islands as shown in Figure 13 (Sundby, 1978; Geddes and Scott, 1994).

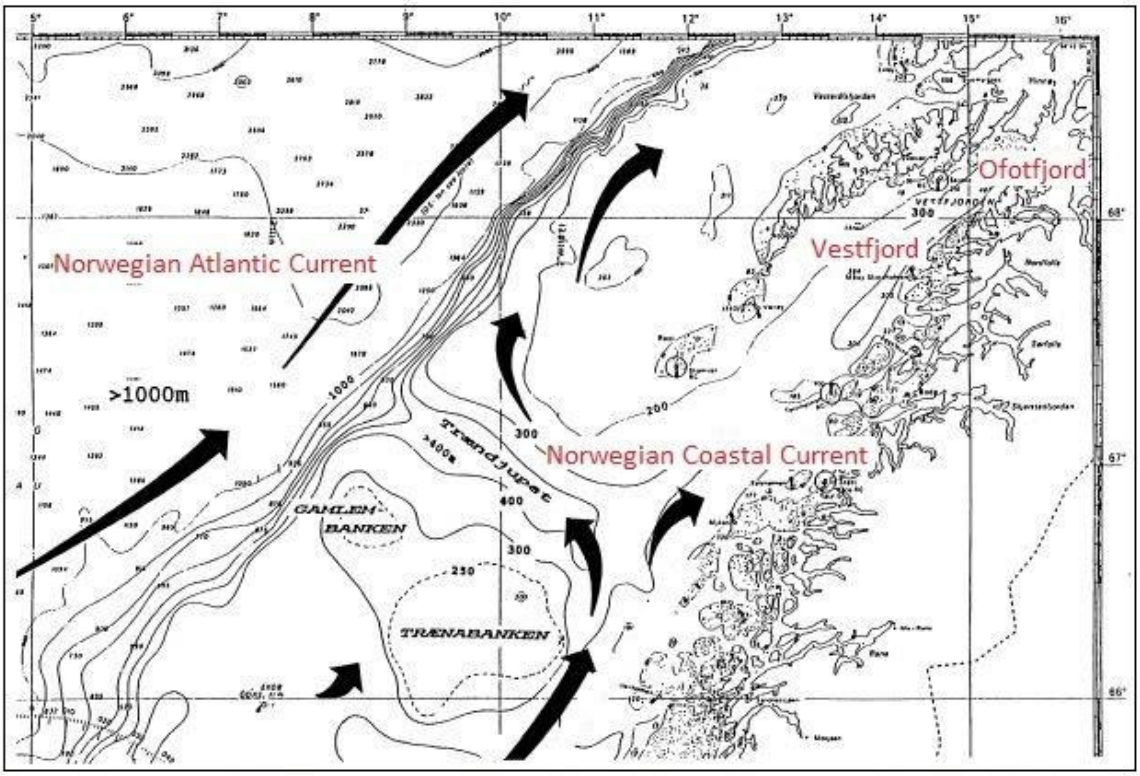

Figure 13: The Norwegian Atlantic Current and the Norwegian Coastal Current along the Norwegian coast entering Vestfjord and Ofotfjord. Modified after Geddes and Scott, 1994.

During autumn and winter months, the NCC entering the Vestfjord and Ofotfjord on the eastern side, is cooled by heat loss at the water surface and leaves the fjords on the west side with cooler water masses (Sundby, 1978). In the inner part of the Vestfjord a homogenous surface layer is formed in winter months due to the lack of fresh water supply and strong convection caused by surface cooling (Mitchelson-Jacob and Sundby, 2001). The depth of the layer varies between 50 m to 200 m in extreme dry and cold winters.

Dominant wind directions alter the uppermost water mass circulation in the fjords. During SW winds, water masses are pushed towards the inner fjord with outflowing water masses on the SE side of the Vestfjord (Fig. 14a), and cause upwelling close to the Lofoten Islands (Furnes and Sundby, 1981). During dominant winds from the NE (Fig. 14b), upper water layers are pushed outside the fjord resulting in downwelling of water masses (Furnes and Sundby, 1981). NE wind patterns are usually weaker than winds from the SW, but more constant over time, and create cyclonic circulation patterns (Furnes and Sundby, 1981).

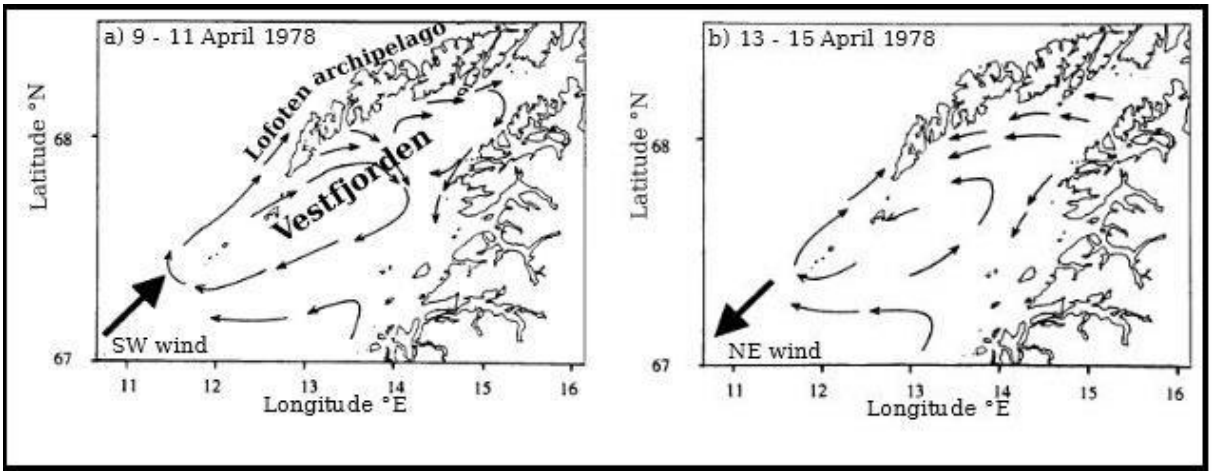

Figure 14: Circulation of the upper water layer in Vestfjord from oceanographic observations in April 1978 during a) winds from the SW, and b) winds from the NE. Modified after Furnes and Sundby (1981).

In addition, the topography plays an important role for water circulation patterns. McClimans and Johannessen (1994) found out that eddies are generated also by tidal jets through the sounds between the Lofoten Islands. Eddies remain during calm and stable wind conditions and break down later in summer when circulation becomes stronger again due to freshwater supply and mixing of stratified water layers (Mitchelson-Jacob and Sundby, 2001). The location and diameter of eddies vary from year to year and their sizes depend on the width of the fjord (Mitchelson-Jacob and Sundby, 2001). In the inner part of the Vestfjord and in the Ofotfjord, eddies have smaller diameters (<50 km) than in the outer part of the Vestfjord (50-60 km) (Mitchelson-Jacob and Sundby, 2001). In addition, a dominant upwelling area is presented in the central part of the Vestfjord (Fig. 9). This area is influenced by cold and nutrient-rich Atlantic deep water masses that are piled up replacing the relatively warm, less saline surface water masses (Furnes and Sundby, 1981).

Due to the inflow of tidal currents, there is a difference in water height between the outer part of the Lofoten Islands and the inner part close to the Norwegian mainland. This difference causes a strong sea level gradient of up to 25 cm (Gjevik et al., 1997) and results in strong tidal currents with flow velocities up to 3 m/s through the sounds between the Lofoten Islands. For example, one of the strongest tidal currents in the world, the Moskenesstraumen is located between Moskenesøy and Mosken in the southern parts of the Lofoten Islands (Gjevik et al., 1997).

3 Material and methods

3.1 Sediment sampling

In June 2014, 42 surface sediment samples were collected on board the research vessel "FF Seisma" owned by the Geological Survey of Norway (NGU). Using a multi-corer (Fig. 16a), the samples were obtained across the entire Ofotfjord, inner parts of the Vestfjord and in the Tysfjord at water depths between 73 m and 634 m (Fig. 15 and Appendix Table 1). The samples are labelled 1 to 44, whereby sample stations 9 and 11 were not used for further investigations due to extremely high concentrations of calcium carbonate. The uppermost 2 cm of the multi-cores with a diameter of 5.5 cm were sampled and subsequently stored on board the vessel at -18°C. For further laboratory work, all samples except the ones taken for grain size measurements, were freeze-dried and homogenised using a Fritsch Micro Mill PULVERISETTE 7 with agate grinding bowls and balls at a speed of 250 rotations per min for 1-2 minutes each.

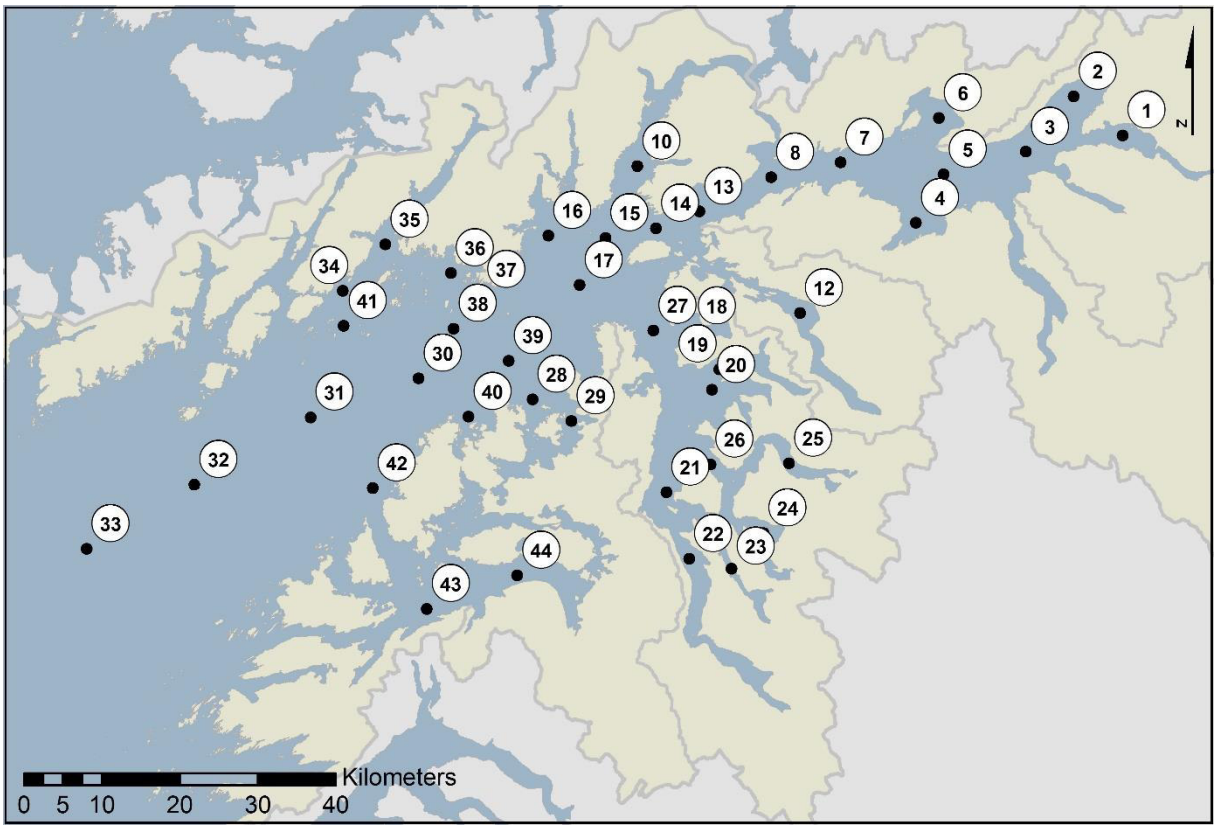

Figure 15: Location of the surface sediment samples.

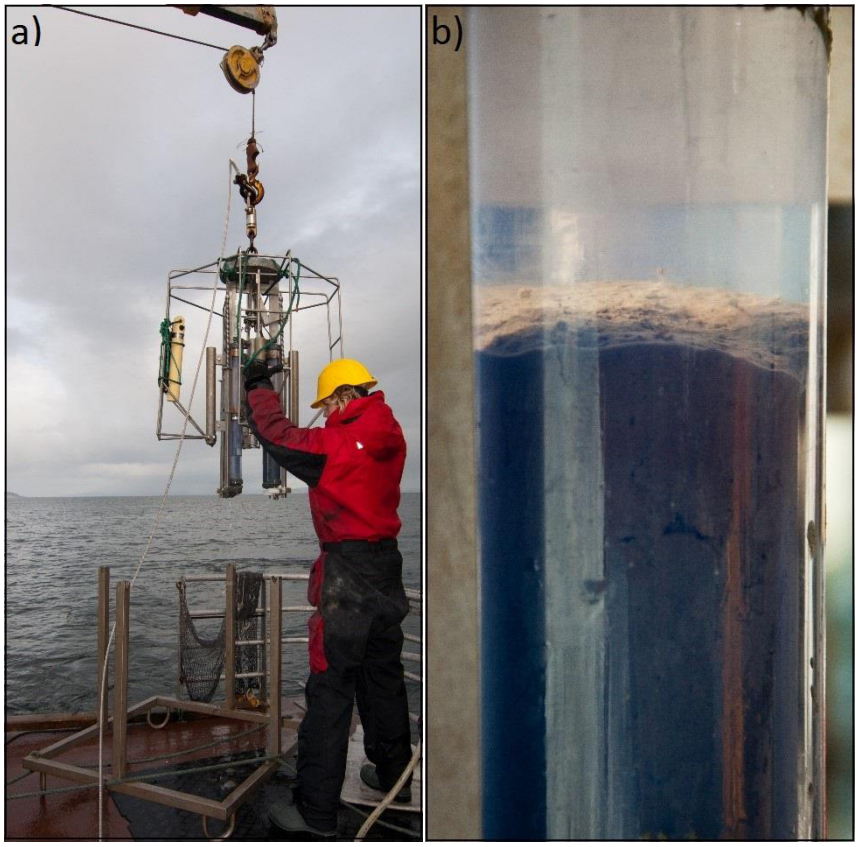

Figure 16: Image illustrating the multi-corer which takes up sediment cores in a fjord (a) and a sediment core with the undisturbed surface (b). Photos taken by Dr. Johan Faust.

3.2 Carbon and sulphur measurements

Total carbon (C_{tot}) and total organic carbon (C_{org}) were measured at the laboratories of the NGU in Trondheim using a LECO SC-444. Results are given in weigh percentages (wt-%). To analyse the proportions of C_{tot} and C_{org} the samples were split into two aliquots of 200 mg and measured separately: one including calcium carbonate ($CaCO_3$), the other one without $CaCO_3$. For analysing C_{org}, the aliquots were transferred into carbon-free pervious ceramic combustion boats and subsequently placed in an oven which has an oxygen-rich atmosphere and temperatures up to 1375°C. To get rid of the $CaCO_3$, the combustion boats were placed on a heating plate with 50°C and treated with 10% volume hydrochloric acid (HCl). Subsequently, the samples were washed 10 times with distilled water to remove the HCl. For measuring the C_{tot}, samples including the $CaCO_3$ were burned, oxidation took place and CO_2 was released. The resulting gases were detected with an infrared gas detector. Certified reference material LECO 501-034, blanks and sample replicates were included for every subsample. To calculate the $CaCO_3$ content, the following equation was used: $CaCO_3 = (C_{org} - C_{org}) \times 8.33$.

3.3 Grain size analyses

Grain sizes were measured with a Coulter LS 200 which is a multifunctional particle characterization tool using laser diffraction. It is based on light scattering. The material was analysed within a particle diameter range of 0.4 – 2000 µm and the results are presented on the basis of volume, as cumulative volume percentage. Laser diffraction measures particle size distributions by applying a narrow beam of monochromatic light from a helium-neon laser. It measures the angular variation in intensity of light as the laser beam is passing through a dispersion of particles and transmitted to the sample. The angle of diffraction increases as particle size decreases. Each particle size has a specific pattern shown on the detector. Thus a stream of particles passing through the beam generate a stable diffraction pattern with the intensity depending on the amount of particles. The diffraction pattern does not vary with particle movement. Prior to the grain size analyses, sediment samples were de-carbonated using 10% (vol.) and to prevent the particles to become charged and agglomerated, samples were treated with 5% sodium pyrophosphate $Na_4P_4O_7$ x 10 H_2O and placed in an ultrasonic bath for 5 – 6 min. At least one duplicate with the same net weight was analysed for each sample.

3.4 Total nitrogen and carbon isotopes analyses

The total nitrogen content was analysed on freeze-dried and homogenized sub-sediment samples. Total nitrogen (N_{tot} in wt-%) and the inorganic nitrogen (N_{inorg} in wt-%) were determined by the Analysator LECO FP-628. One aliquot of each sample was measured for N_{tot}. Another one was treated with a 20 mg KOBr-KOH solution aiming to remove the organic nitrogen content (N_{org}). The measuring instrument works similar to the one described above for the C_{org}. Organic nitrogen was calculated by subtracting the N_{inorg} fraction from the N_{tot}.

Stable carbon isotope ($\delta^{13}C_{org}$) and stable nitrogen isotope ($\delta^{15}N$) signatures were measured by the elemental analyser isotope ratio mass spectrometry (EA-IRMS). Mass spectrometry is ionizing chemical compounds by transmitting electrons to generate charged molecules or molecule fragments and to measure their mass-to-charge ratios. For this analysis, samples were placed in an oven with oxygen atmosphere. Prior measuring, they were determined on de-carbonated subsamples using 10% HCl. While measuring, the samples were combusted using the elemental analyser. Subsequently, the evolved gases were introduced followed by the ionization of the gas molecules. The presented ions were separated and detected in the mass

spectrometer according to their mass-to-charge ratio, typically by accelerating them and subjecting them to an electric or magnetic field. Ions of the same ratio underwent the same amount of deflection. In the last part, raw data could be evaluated. Values are notated in per million versus Vienna-PDB and $\delta^{15}N_{org}$ were calculated from the measured amounts of N_{inorg} applying a simple isotope mass balance (Schubert and Calvert, 2001).

3.5 Bulk mineral assemblage analyses

Bulk mineral assemblages were measured with a X-ray diffraction XRD (X-Ray Diffraction) using a Philips X´Pert Pro MD, Cu-radiation (k(alpha) 1.541,45kV, 40mA) and X`Celerator detector system at the NGU. Prior to analysing, the material was pulverized before transferred to the sample specimen holder. When having insufficient sample material, the back side of the specimen holder was provided with a special plate filling up the material. The XRD reflects monochromatic x-rays which are irradiating a crystal plain. X-rays depend on the lattice structure and are transmitted with different angles of incidences. Using a diffractogram, the reflection is registered due to the corresponding emergent angle. Furthermore, the mean position of the atoms, their chemical bonds, their disorder and other information can be distinguished. Every mineral shows its own unique lattice pattern and is connected to further existing patterns recorded in a database.

3.6 Bulk elemental composition analyses

SiO_2, Al_2O_3, Fe_2O_4, MgO, TiO_2, CaO, K_2O, Na_2O, MnO, and P_2O_5 were measured at the NGU using a PANalytical Axios 4kW X-Ray Fluorescence Spectroscopy (XRF). For measuring the main elements, samples were placed in melting tablets with a diameter of 20 – 50 mm after they were diluted with Lithium-Tetraborate ($Li_2B_4O_7$). The samples were pressed into flat disks because x-rays from lighter elements often only emit from the top few micro-meters of a sample surface. For measuring, x-rays with high energy were bombarding the sample in a specific angle of incidence. When material is exposed to x-rays, ionization within the element takes place. This ionization is responsible for emitting energy. For the XRF, different elements emit fluorescending radiation with characteristic patterns each for the angle of refraction. Fluorescence hereby means that the emission of radiation results in the re-emission of the same radiation with a different energy. A detector is registering the angles of refraction.

4 Results

4.1 Bulk mineral assemblages

On average, the bulk mineral composition of the surface sediment samples mostly consists of phyllosilicates (22.7%; n = 40), plagioclase (21.7%; n = 40), quartz (14.3%; n = 40), calcite (12.9%; n = 40), and illite/mica (12.6%; n = 40) (Appendix Table 4). Other minerals are represented with lower average concentrations like for example aragonite (2.6%). Different minerals show variable spatial distributions in the study area. The distribution for phyllosilicates, for example, illustrates no distinct pattern (Fig. 17). Concentrations are ranging between 7.1% (station 36) and 49.8% (station 30) as shown in Appendix Table 4. Plagioclase shows highest values in the inner parts of the Ofotfjord and Tysfjord (Fig. 18), whereas lowest values can be found in the upwelling areas of the Vestfjord. Plagioclase concentrations range between 2.3% (station 41) and 35.9% (station 19) (Appendix Table 4). The distribution of the calcite shows highest values in the central and outer part of the Vestfjord with strong gradients towards the innermost parts of the Ofotfjord and Tysfjord (Fig. 19). The concentrations range from 0.9% (station 2) to 51% (station 41). Illite/mica are distributed unevenly (Fig. 20), highest amounts are present in the inner parts of the Tysfjord and Ofotfjord with values varying between 2.6% (station 40) and 24.6% (station 21) as illustrated in Appendix Table 4. Aragonite is strongly available in the upwelling areas close the northern rim of the Vestfjord (Fig. 21) with highest values of 16% at station 34 (Appendix Table 4).

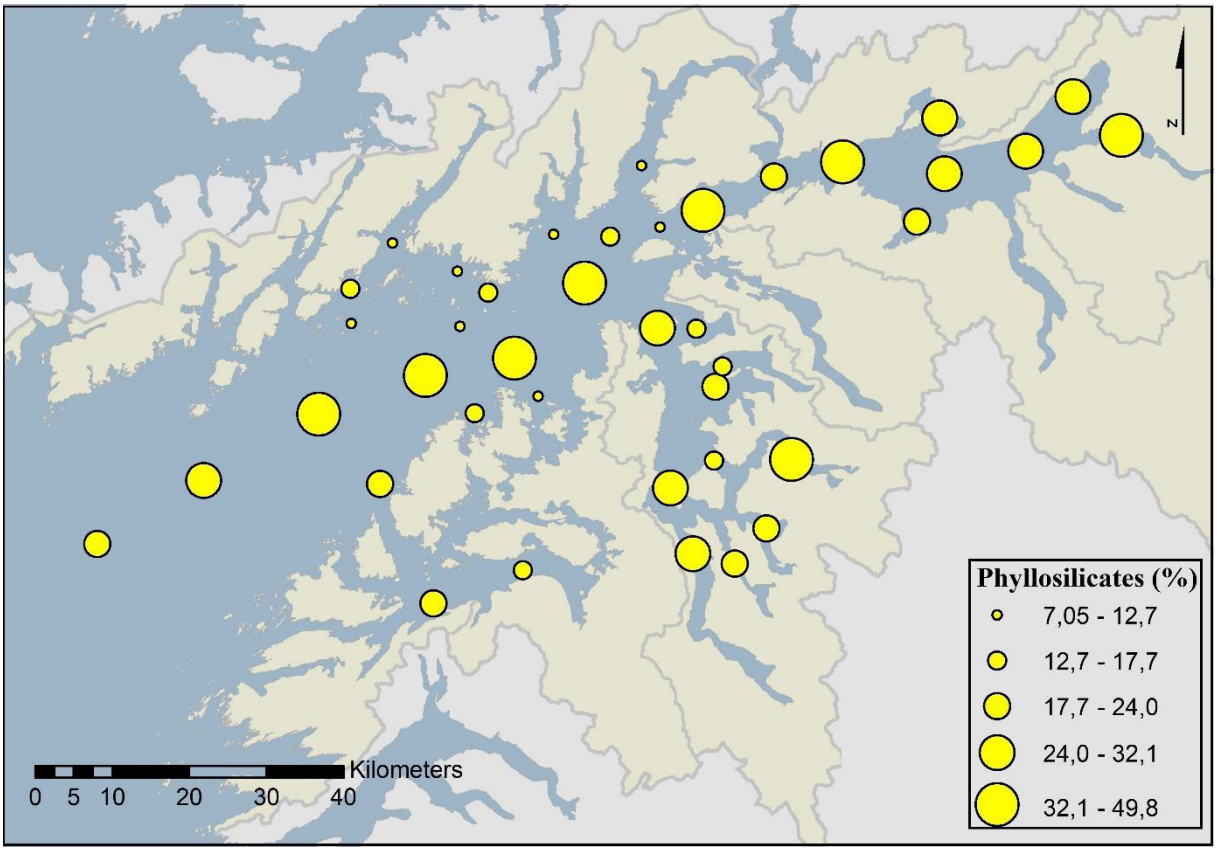

Figure 17: Distribution of phyllosilicates.

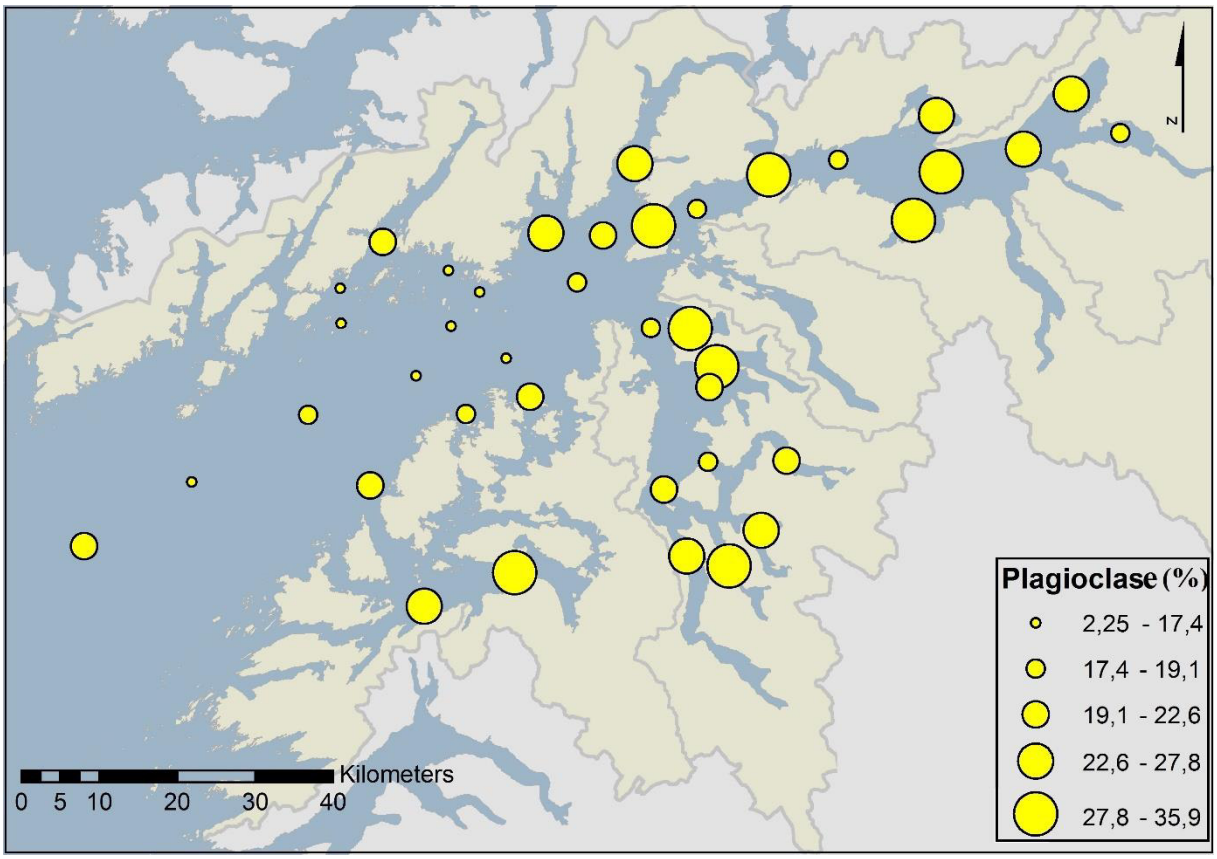

Figure 18: Distribution of plagioclase.

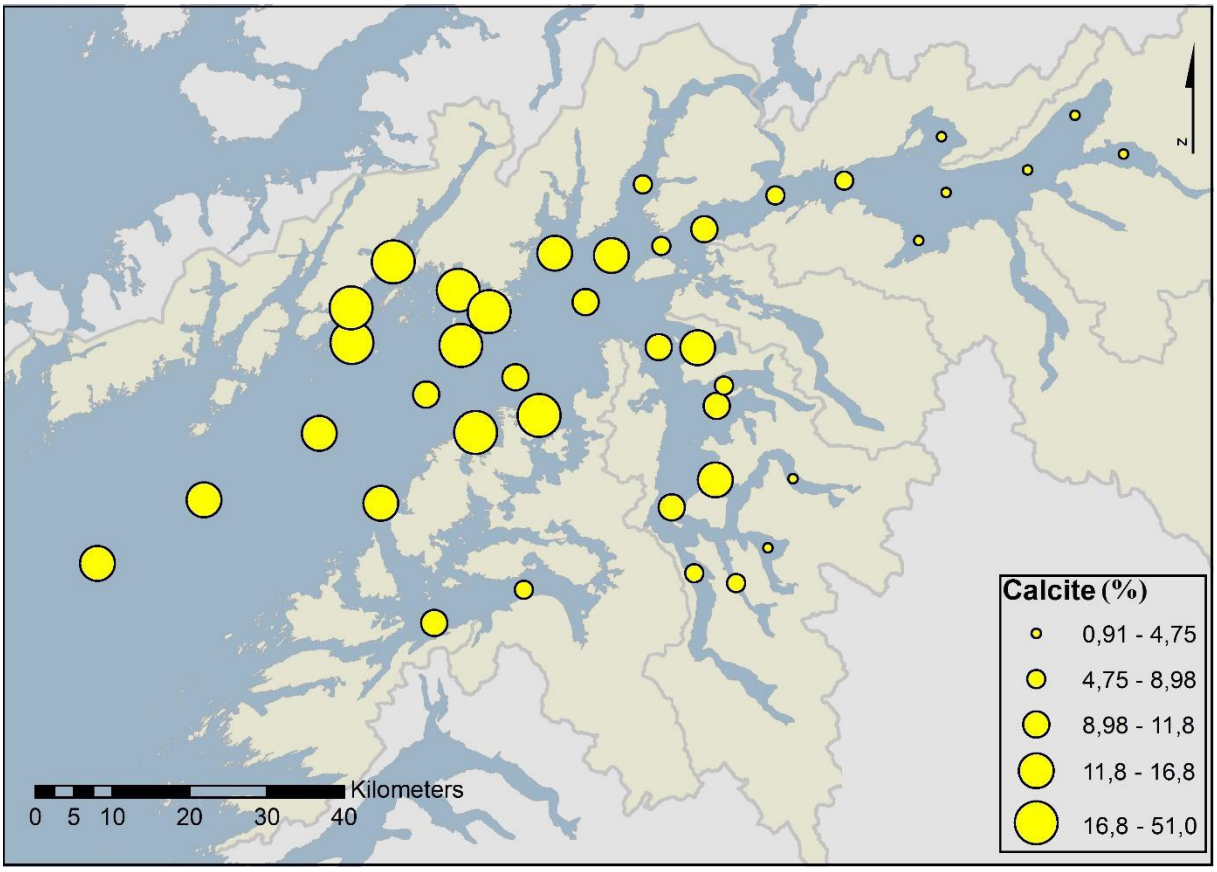

Figure 19: Distribution of calcite.

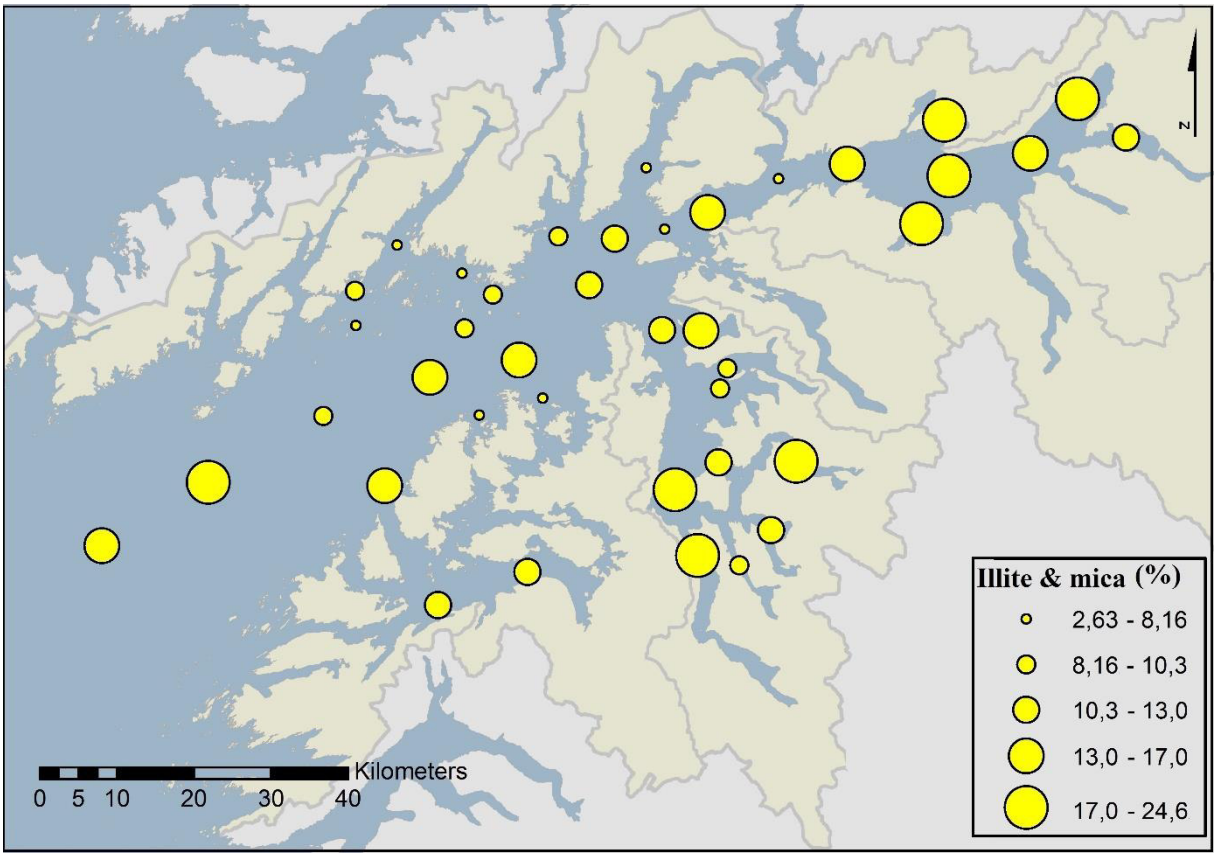

Figure 20: Distribution of illite / mica.

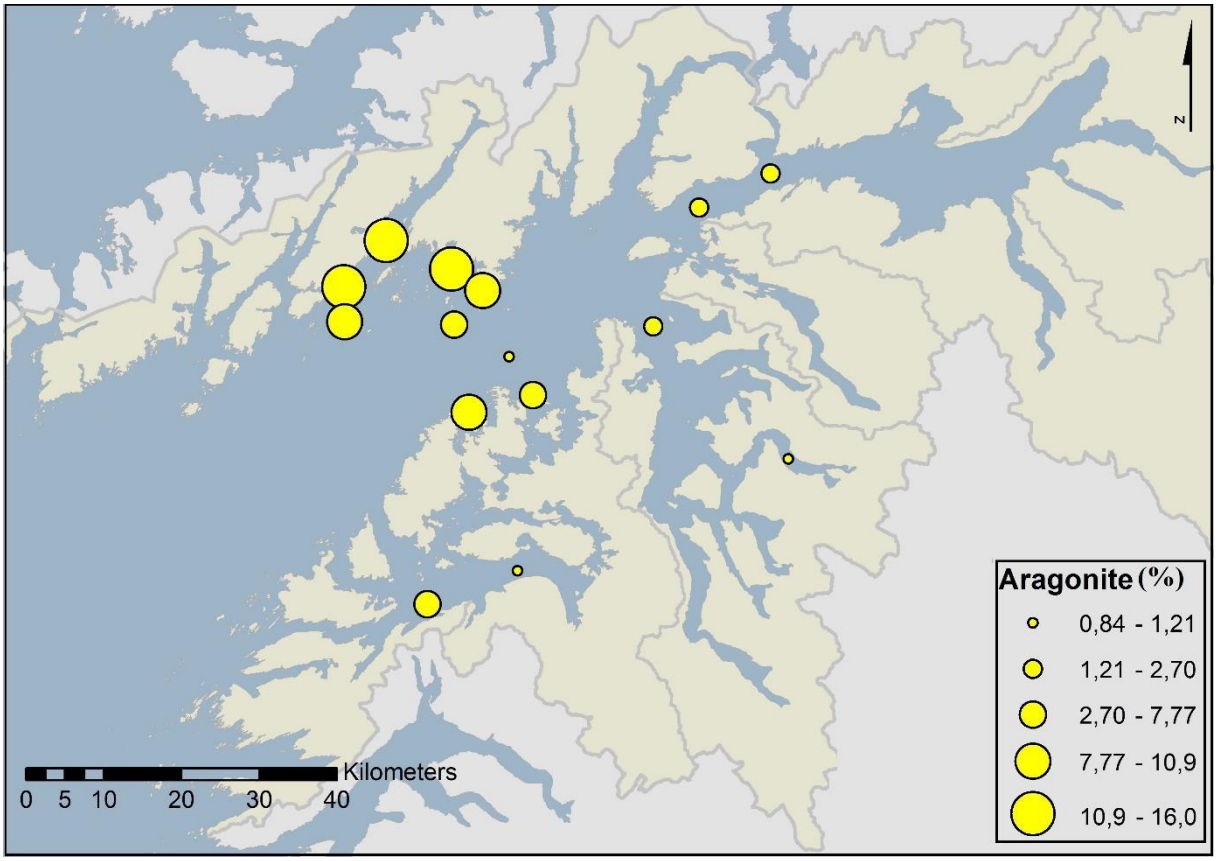

Figure 21: Distribution of aragonite.

4.2 Grain sizes

Grain size fractions are highly variable in the study area. Concentrations for the clay fraction (<2 µm) range between 10% (station 28) and 1% (station 22) with an average value of 5% (Appendix Table 1). The content is lowest near the shore in the Tysfjord (average 3.9%) and Ofotfjord (average 4.3%) and increase towards the outer parts of the fjords (Fig. 22) with highest values in the Vestfjord (average 6.1%). In the outermost part of the Vestfjord, concentrations are low again. The silt fraction (2-63 µm) shows a maximum value of 93.3% (station 5) and a minimum of 27.3% (station 34), and an average of 74% (Appendix Table 1). As illustrated in Figure 23 the values are spread indistinctly with lowest concentrations close to the merging of the fjords, in the inner part of the Tysfjord, and near-shore in the Vestfjord. Values of the very fine sand fraction (63-125 µm) vary between 1% (station 28) and 39.6% (station 21) with an average of 15%. The distribution pattern illustrates a gradient between lowest values in the deepest parts of the Vestfjord and Ofotfjord and highest concentrations located near-shore in shallow water depths (Fig. 24). The fine sand fraction (125-250 µm) ranges between 0% and 32.9% (station 34) with an average of 4.8% (Appendix Table 1). The distribution has no pattern (Fig. 25). Medium to very coarse sand (>250 µm) is represented by

generally small concentrations. Average values range between 0.9% (medium sand, 250-500 µm) and 0.3% (coarse and very coarse sand, >500 µm). Highest values can be found near-shore in the Vestfjord and Tysfjord (Fig. 26 and 27). In general, numerous samples do not consist of any grain sizes <250 µm or >500 µm (Appendix Table 1)

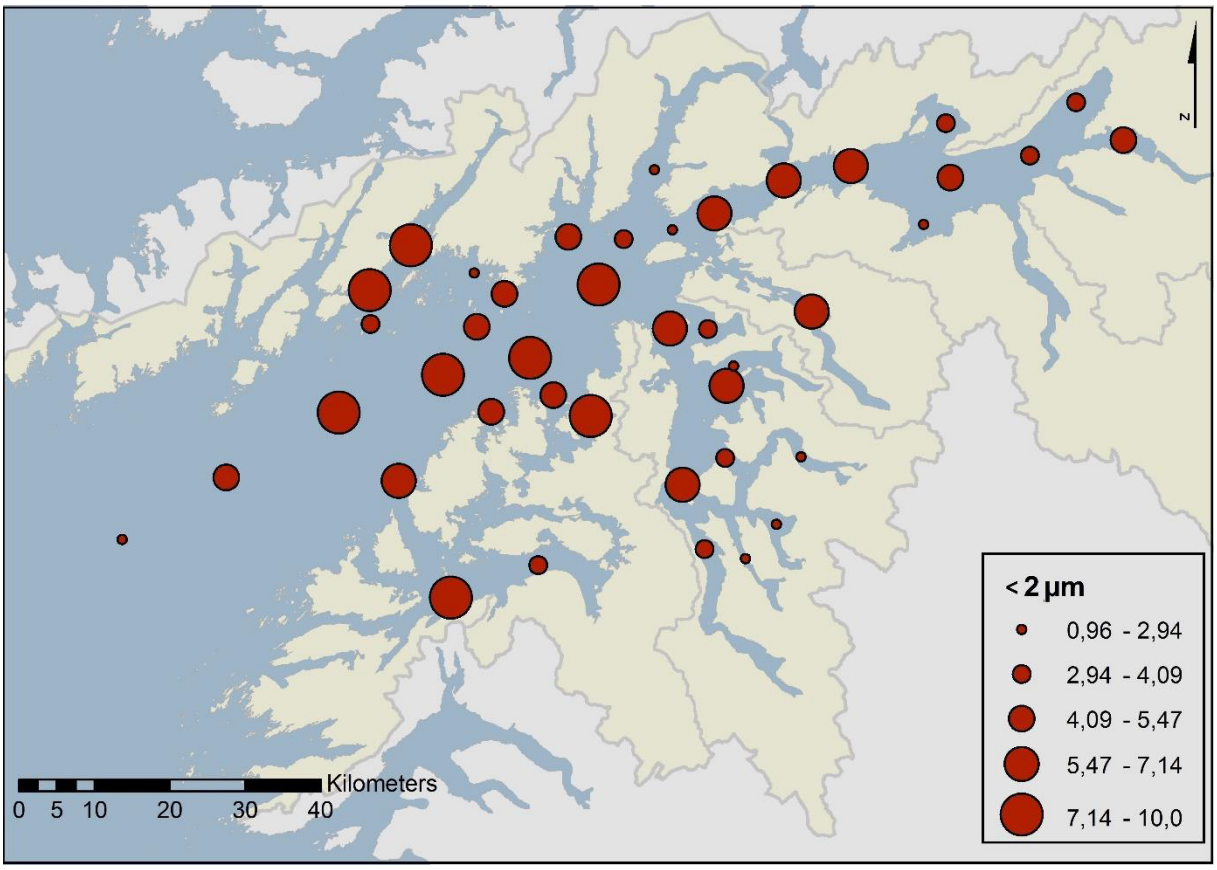

Figure 22: Distribution of the grain size fraction <2 µm.

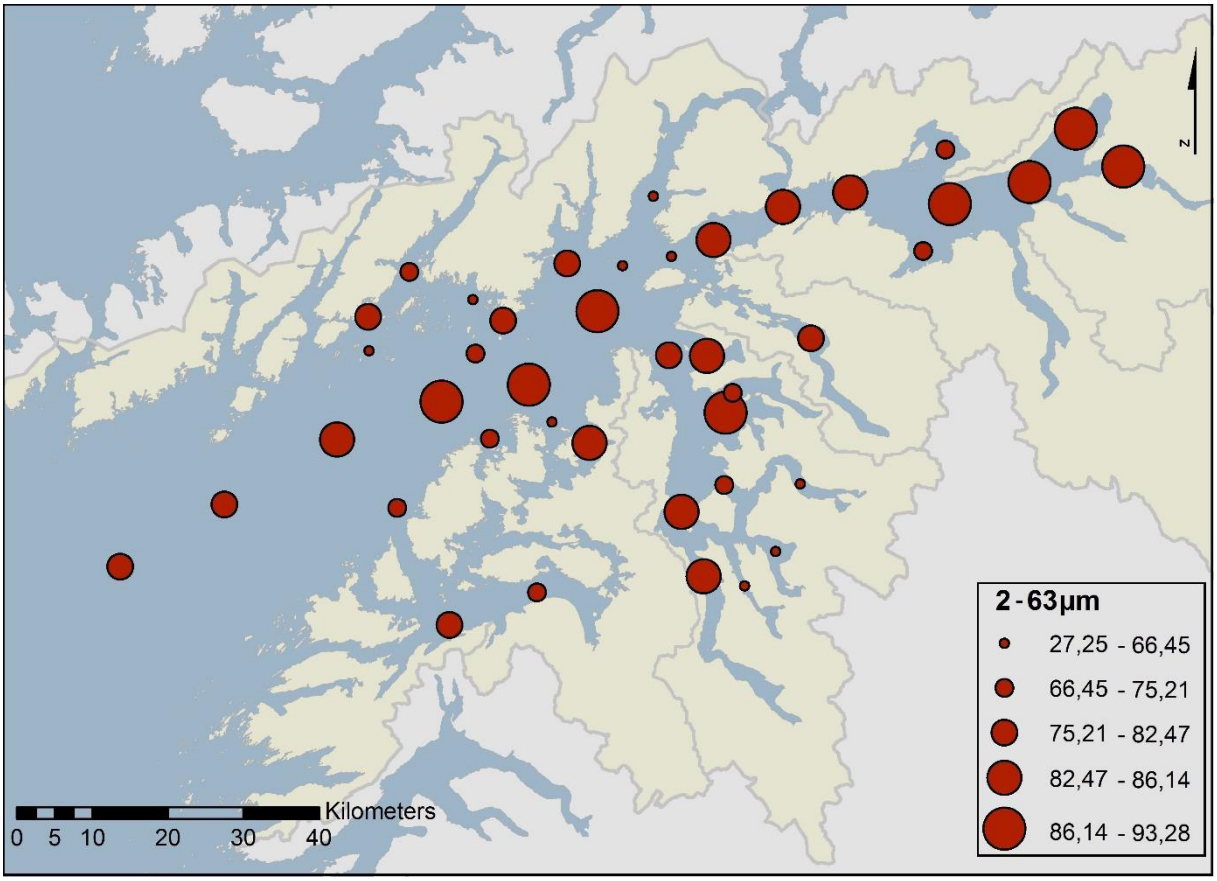

Figure 23: Distribution of the grain size fraction 2-63 µm.

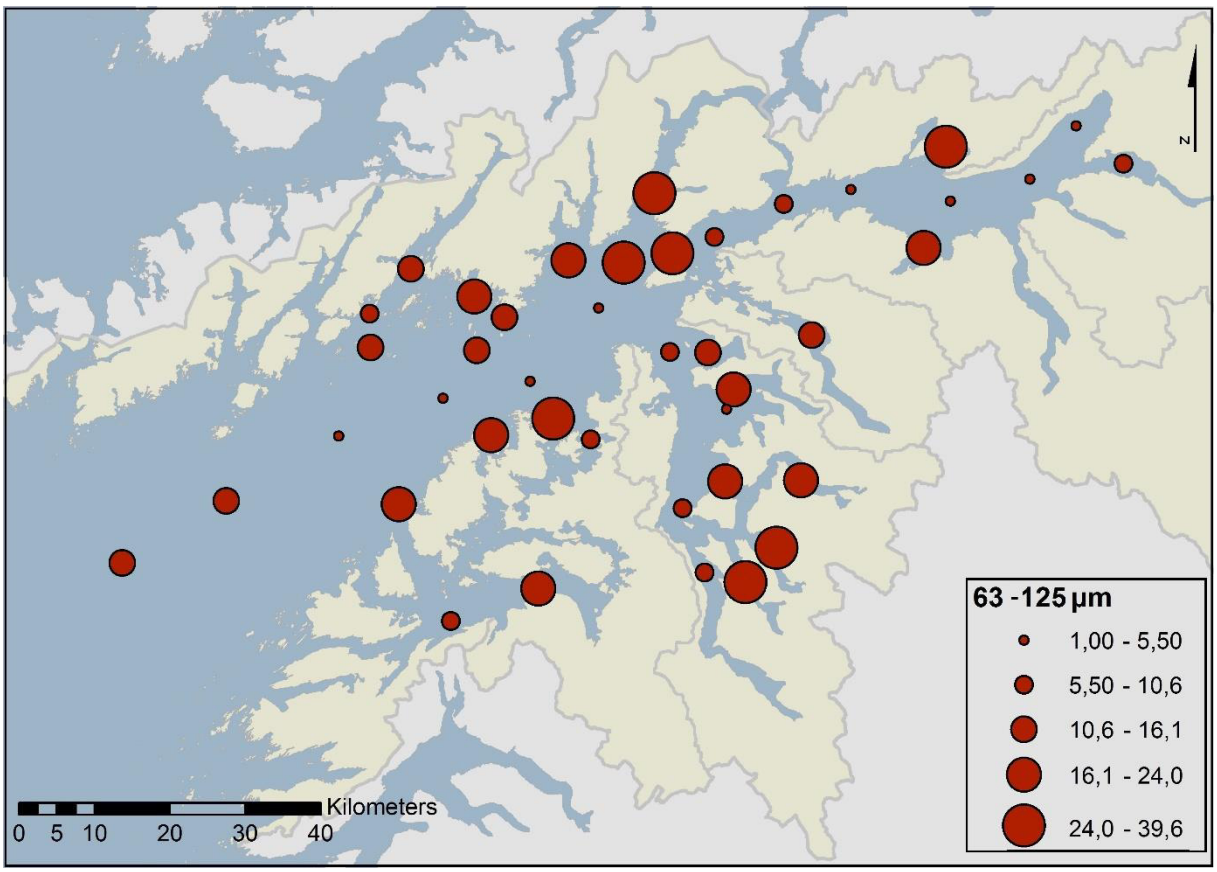

Figure 24: Distribution of the grain size fraction 63-125 µm.

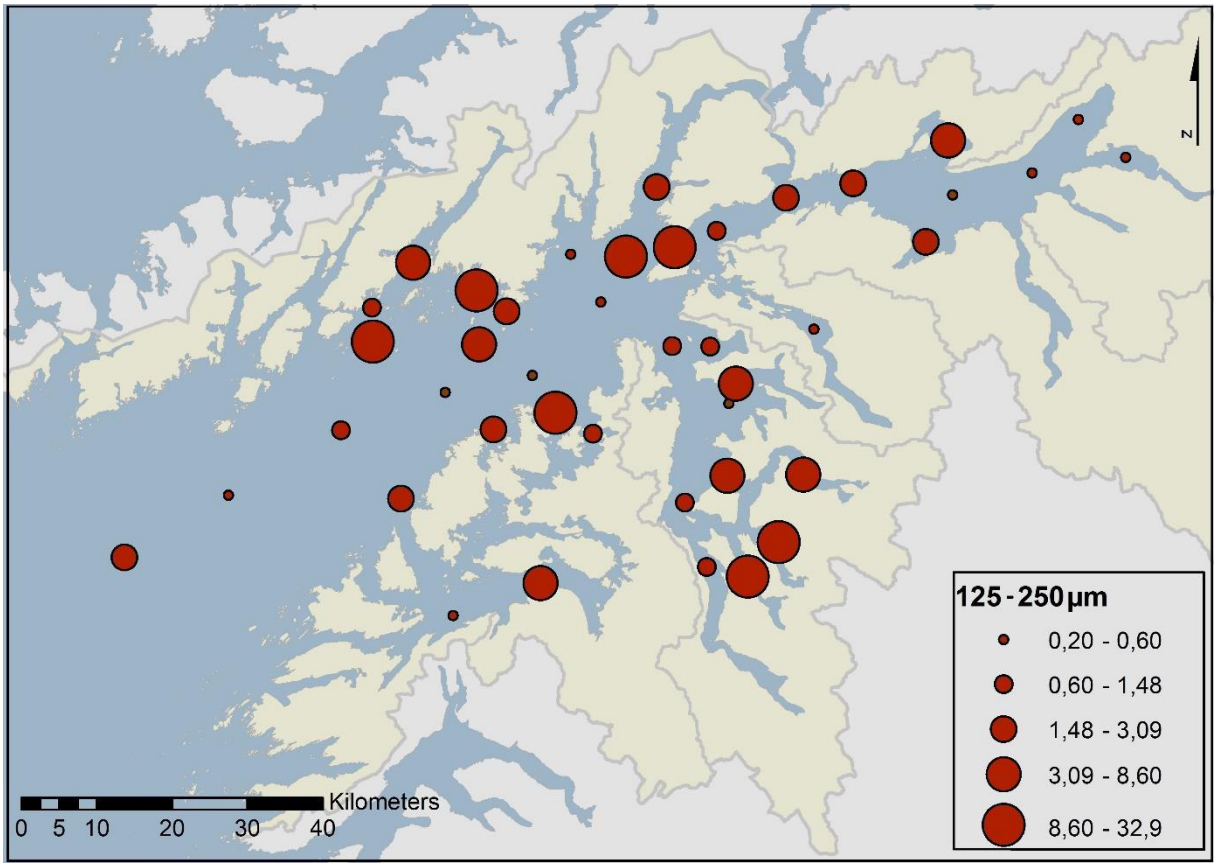

Figure 25: Distribution of the grain size fraction 125-250 µm.

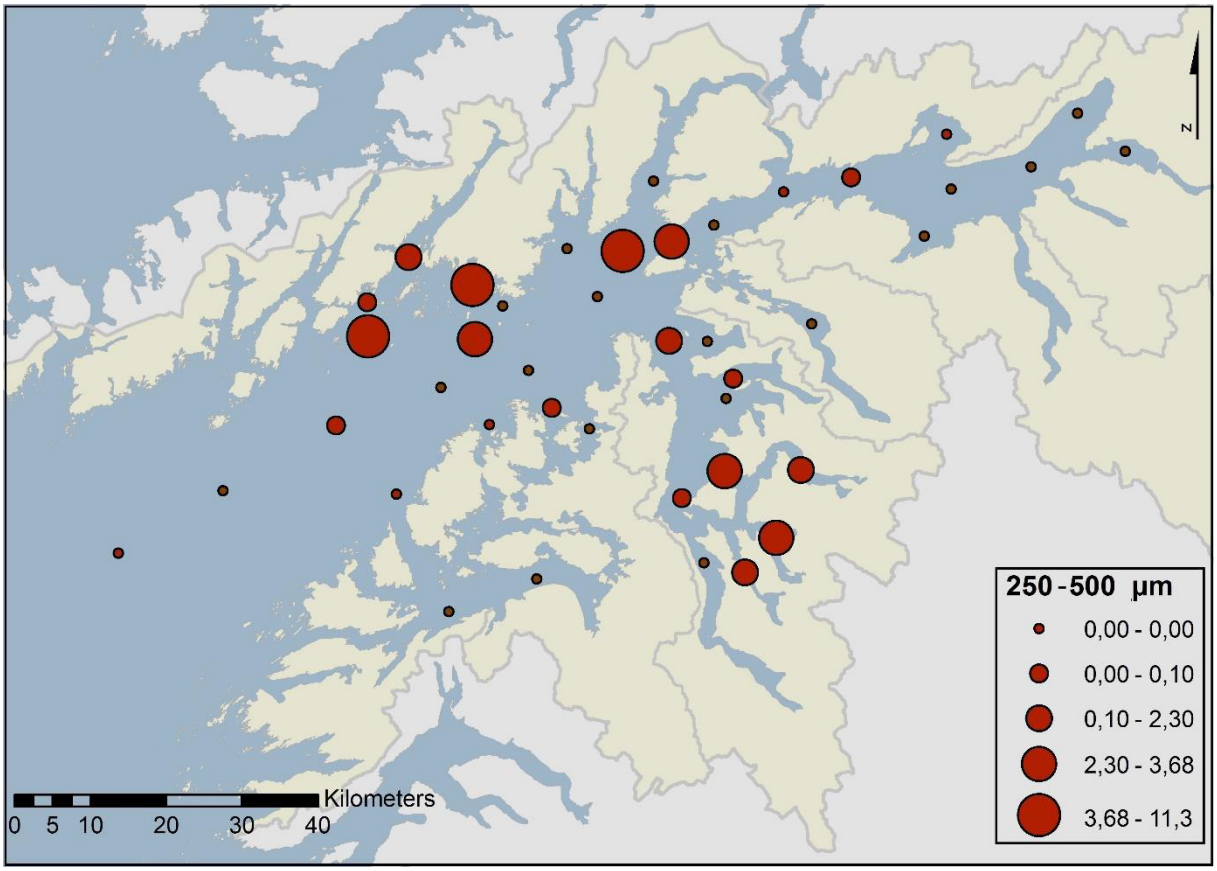

Figure 26: Distribution of the grain size fraction 250-500 µm.

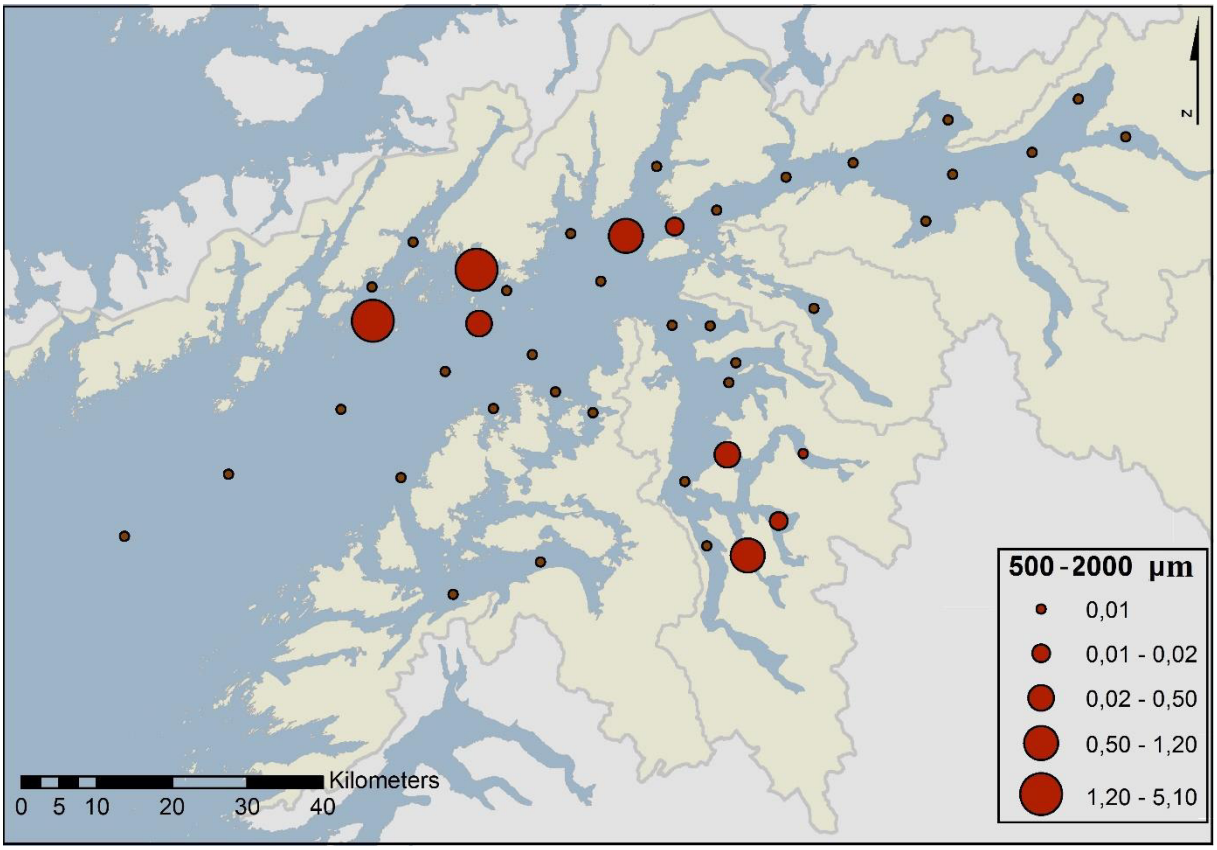

Figure 27: Distribution of the grain size fraction 500-2000 µm.

4.3 Total carbon, total organic, and total inorganic carbon

Values for C_{tot} vary between 1.2% (station 22) and 11% (station 39) with an average of 3.7% (Appendix Table 2). Highest concentrations can be found in samples near the northern and southern shore in the central part of the Vestfjord (Fig. 28), whereas lowest values are presented in the inner parts of the Tysfjord and Ofotfjord. A slightly increasing trend from the innermost part towards the outer part of the fjords can be observed. An exception of this trend comprise sediments from the outermost stations of the Vestfjord (station 31, 32, 33, 30) (Fig. 29, 15) which indicate relative low values <2.9%. C_{org} concentrations reveal values between 0.5% (station 12) and 4.5% (station 32) with an average of 1.5% (Appendix Table 2). C_{inorg} values range between 0.2% (station 22) and 9.9% (station 39) with an average value of 2.2% (Appendix Table 2). A distinct distribution pattern can be observed by a proximal to distal trend. Highest values can be found in the upwelling areas in the central part of the Vestfjord, whereby lowest values are distributed in the inner part of the Ofotfjord, and the land-near parts in the Tysfjord (Fig. 30). The organic fraction of carbon accounts for 10.1% to 82.8% of the C_{tot}, whereby C_{inorg} accounts for 17.2% to 89.9% of the C_{tot}.

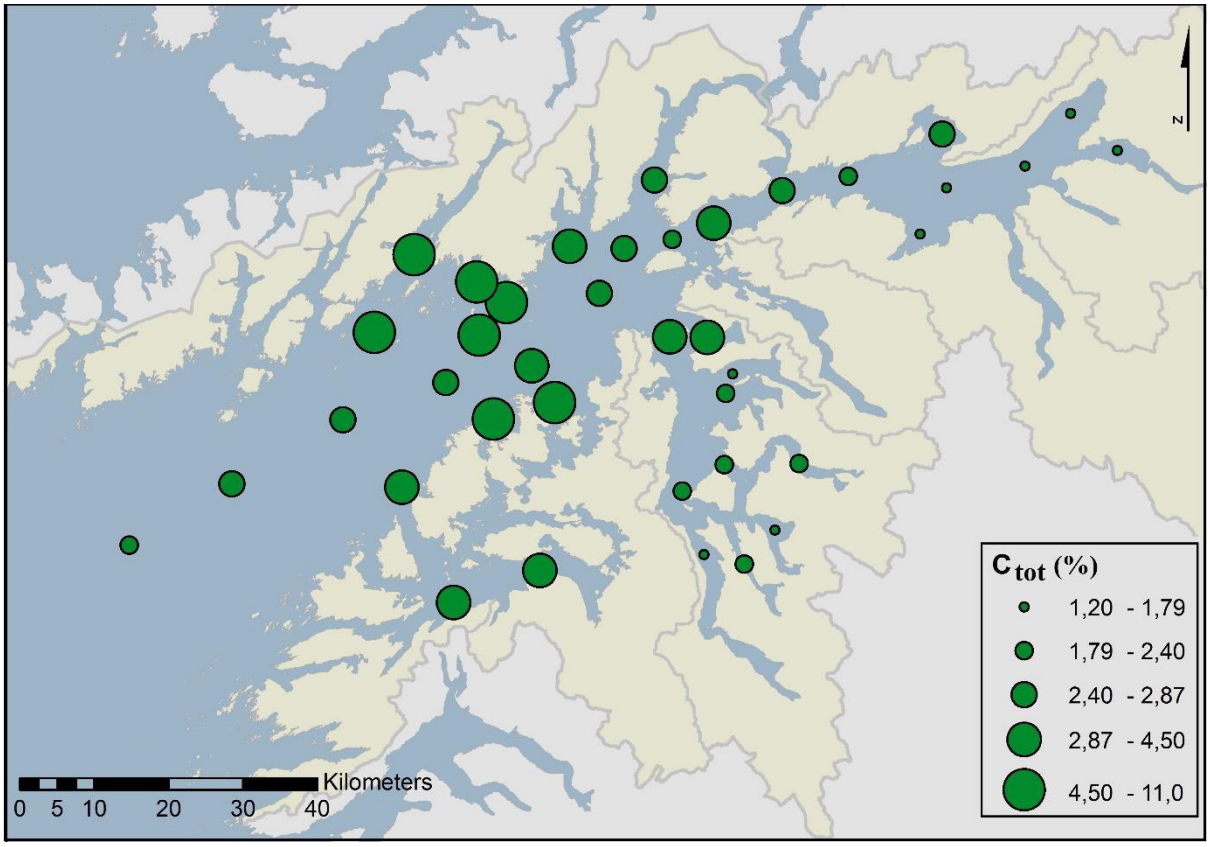

Figure 28: Distribution of the total carbon.

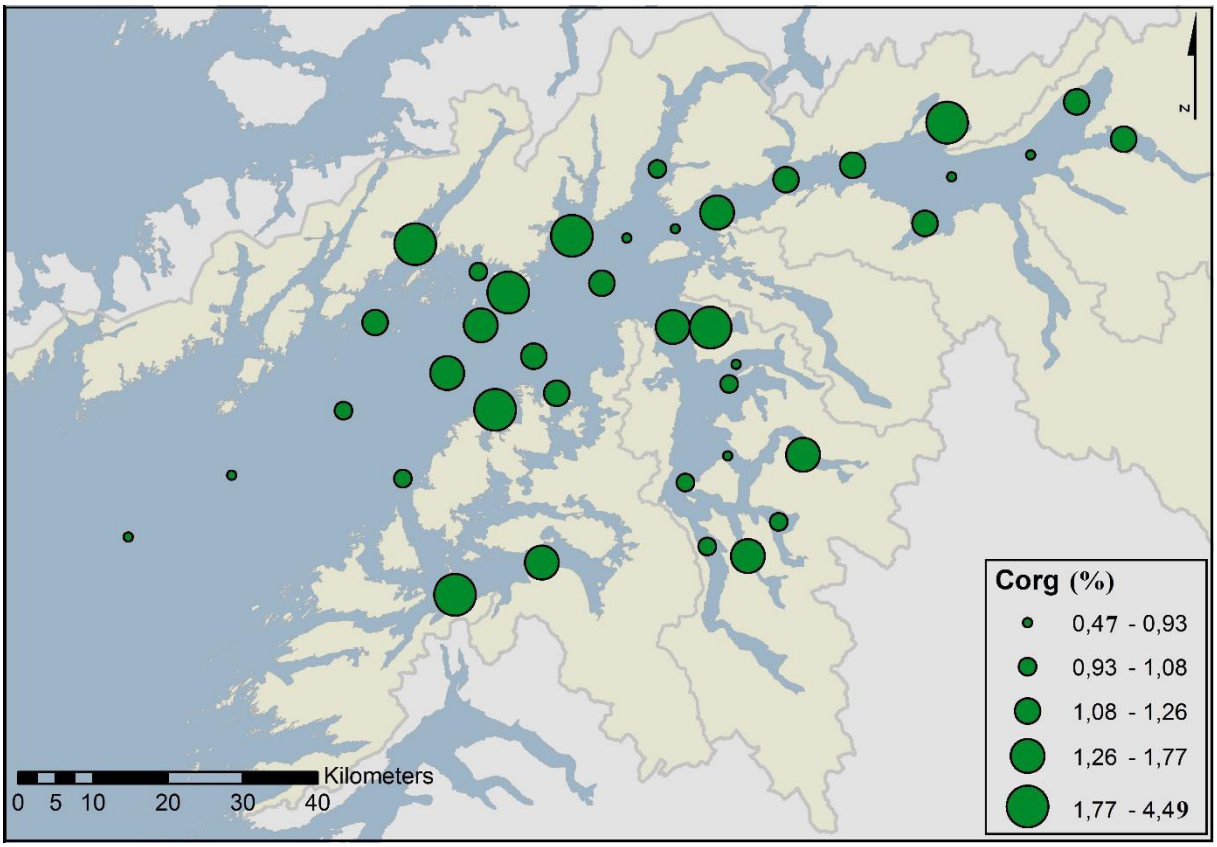

Figure 29: Distribution of the organic carbon.

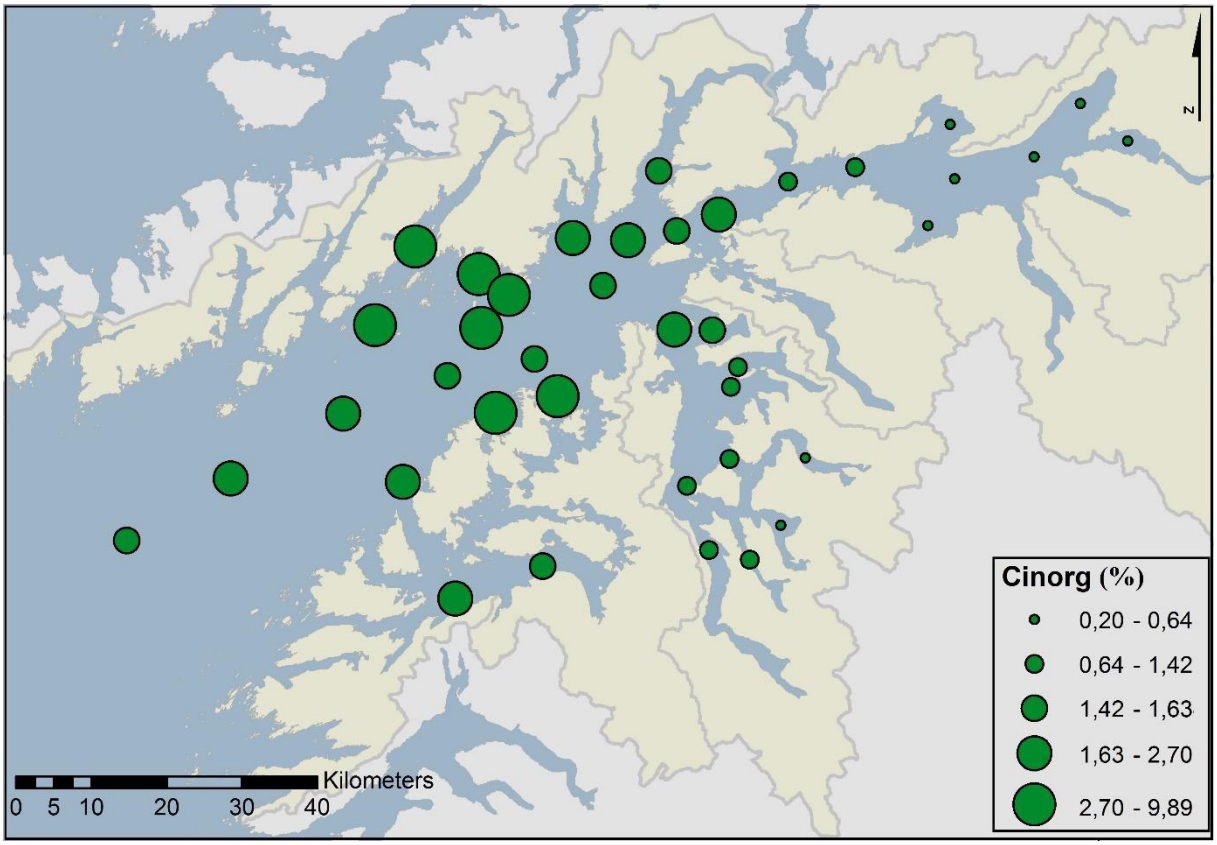

Figure 30: Distribution of the inorganic carbon.

4.4 Stable carbon isotope ratios

Stable organic carbon isotope values ($\delta^{13}C_{org}$) in the study area range between -23.83‰ (station 24) and -20.87‰ (station 26) and show an average value of -21.62‰ (Appendix Table 2). The spatial distribution of $\delta^{13}C_{org}$ is presented in Figure 31 and the values decrease from the outer part of the Vestfjord towards the inner part of the Ofotfjord. The distribution in the Tysfjord demonstrates no distinct pattern, as relatively high and low values exist in the inner and outer part of the fjord (Fig. 31). Lowest values characterize the inner parts of the Tysfjord and Ofotfjord.

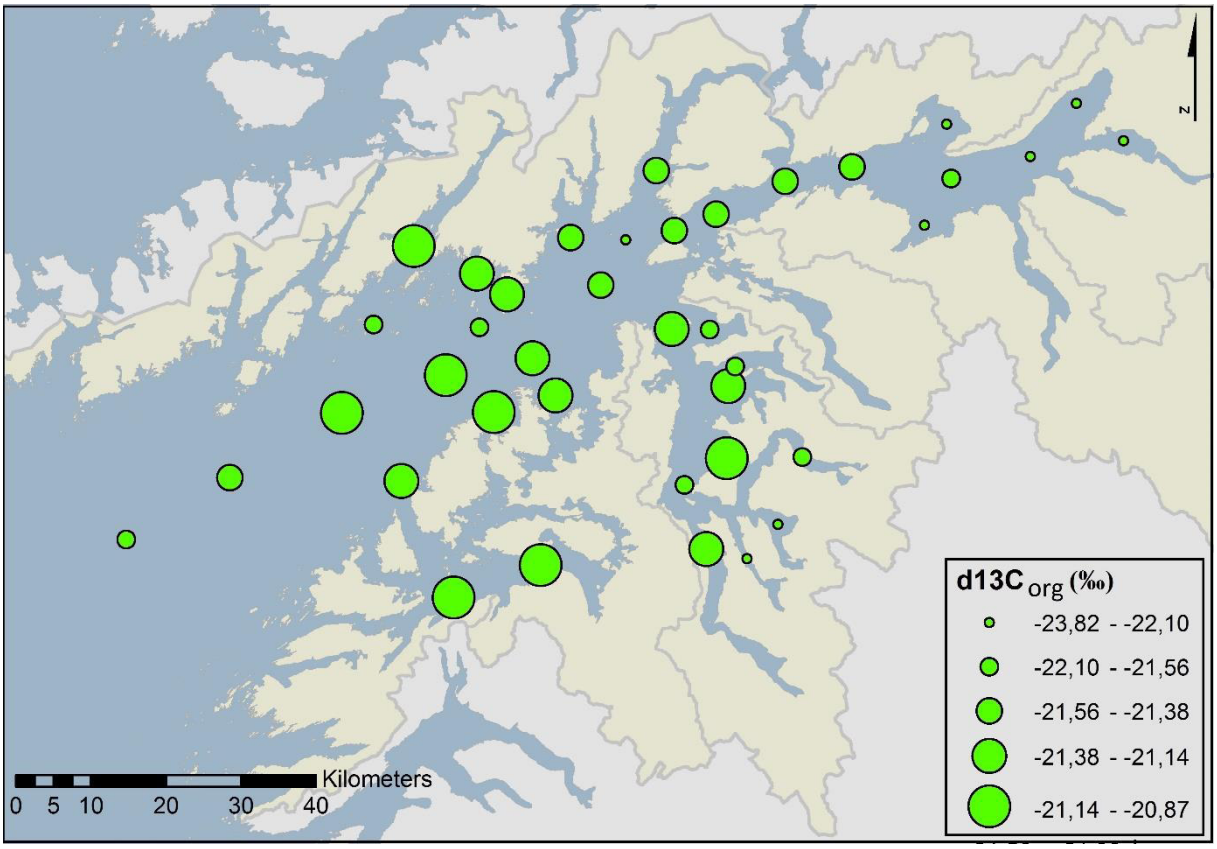

Figure 31: Distribution of the stable carbon isotope fraction $\delta^{13}C_{org}$.

4.5 Total nitrogen (N_{tot}), total organic nitrogen (N_{org}), and total inorganic nitrogen (N_{inorg})

Total nitrogen concentrations vary from 0.1% (station 12) to 0.7% (station 38) with an average value of 0.2% (Appendix Table 2). The values show a complex and unevenly distributed pattern (Fig. 32). N_{inorg} contents are very small ranging between 0.01% and 0.02%. No clear spatial distribution pattern can be distinguished. The proportion of N_{inorg} within the concentrations of N_{tot} has an average percentage of 7.7% with highest values of 16.1% (station 30) and lowest values of 2.38% (station 38). N_{org} contents reveal values between 0.1% (station 12) and 0.6% (station 38) with an average of 0.2% (Appendix Table 2). The organic nitrogen accounts for 83.9% to 97.6% of N_{tot} with an average of 92.3%. Concentrations illustrate no distinct distribution (Fig. 33).

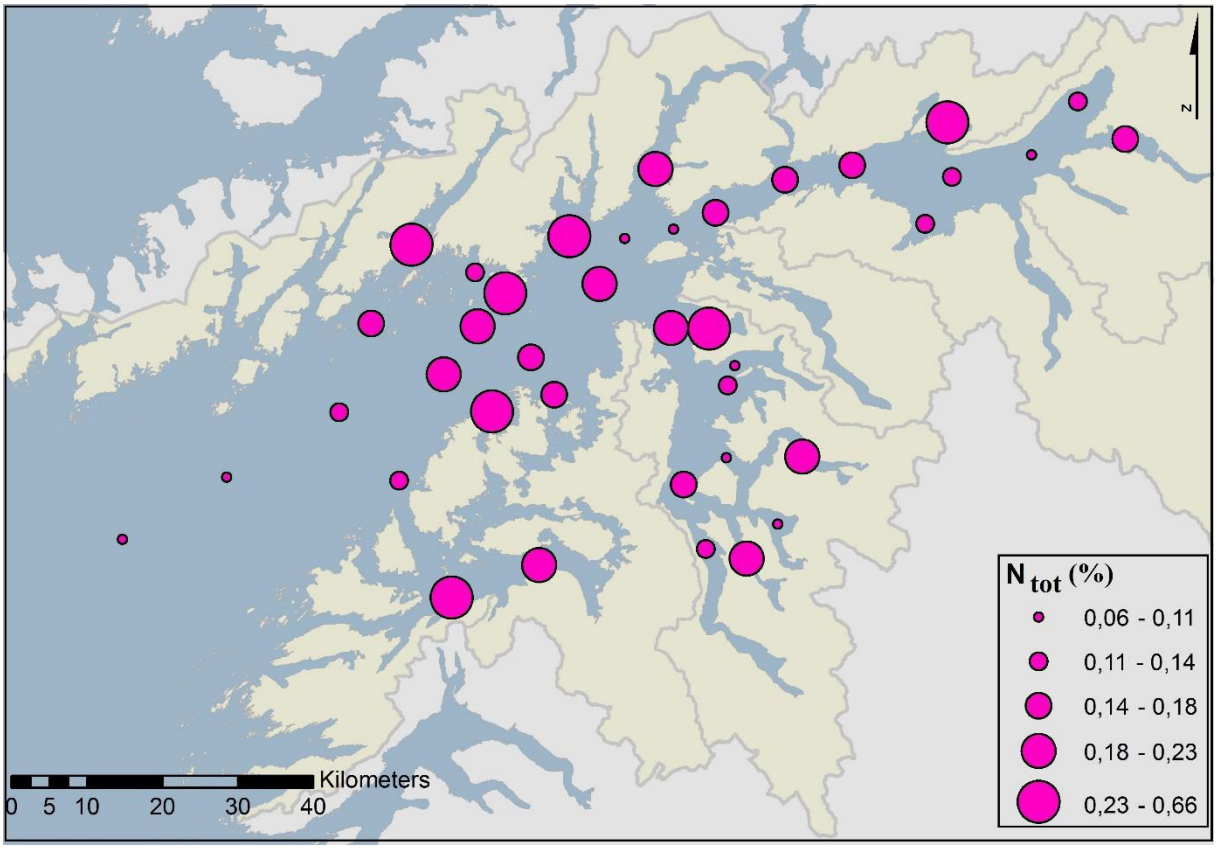

Figure 32: Distribution of the total nitrogen.

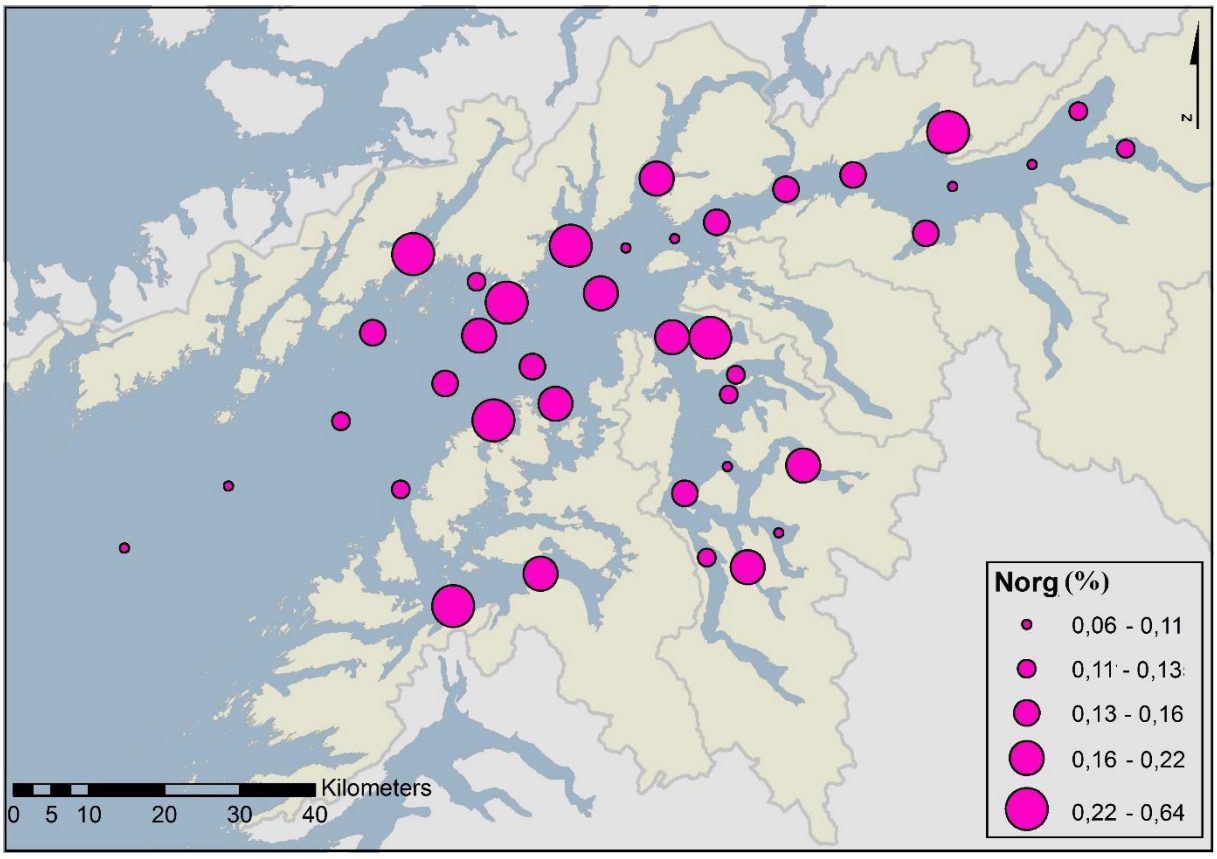

Figure 33: Distribution of the organic nitrogen.

4.6 Stable nitrogen isotope ratios

The nitrogen stable isotope content of the organic material ($\delta^{15}N_{org}$) ranges between 4.69‰ for sample station 22 and 6.9‰ for station 12 with an average of 6.14‰ of all samples (Appendix Table 2). The concentrations show a slightly distinct spatial distribution pattern with lowest values in the innermost fjord parts of the Ofotfjord and Tysfjord, and highest values in the deepest parts of the Vestfjord (Fig. 34).

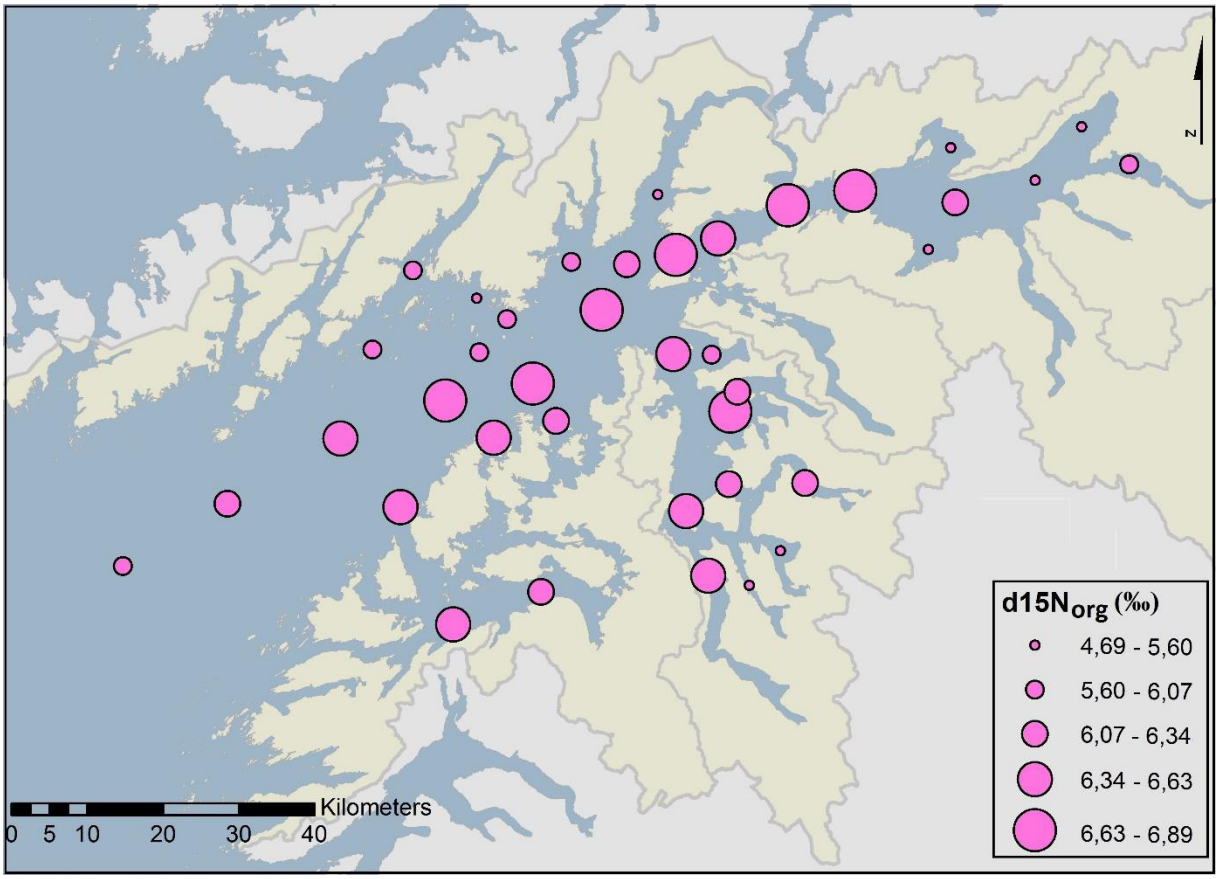

Figure 34: Distribution of the stable organic nitrogen isotopes.

4.7 Carbon versus nitrogen

The Pearson correlation coefficient (r) for C_{org} and N_{org} is calculated as 0.99 (n = 39) (Fig. 35a). The correlation between C_{org} and N_{tot} is also r = 0.99 (n = 39) (Fig. 35b). The distribution of C_{org}/N_{tot} shows no distinct pattern, but a rather complex picture with high and low values presented in inner and outer fjord parts (Fig. 36). Values vary between 5.6 and 9.2 (Appendix Table 2). The spatial distribution of C_{org}/N_{org} ratios is presented in Figure 37. Values show a relative evenly distributed pattern with an increase of concentrations towards the inner part of the fjords as well as to the open ocean. Highest values of up to 9.9 (station 15) occur in samples

in the inner parts of the Ofotfjord and Tysfjord (Appendix Table 2). Lowest values of 5.8 (station 10) are distributed in the upwelling areas of the Vestfjord. C_{org}/N_{org} ratios have an average value of 7.9 (Appendix Table 2). They are inverse to N_{org}/C_{org} ratios.

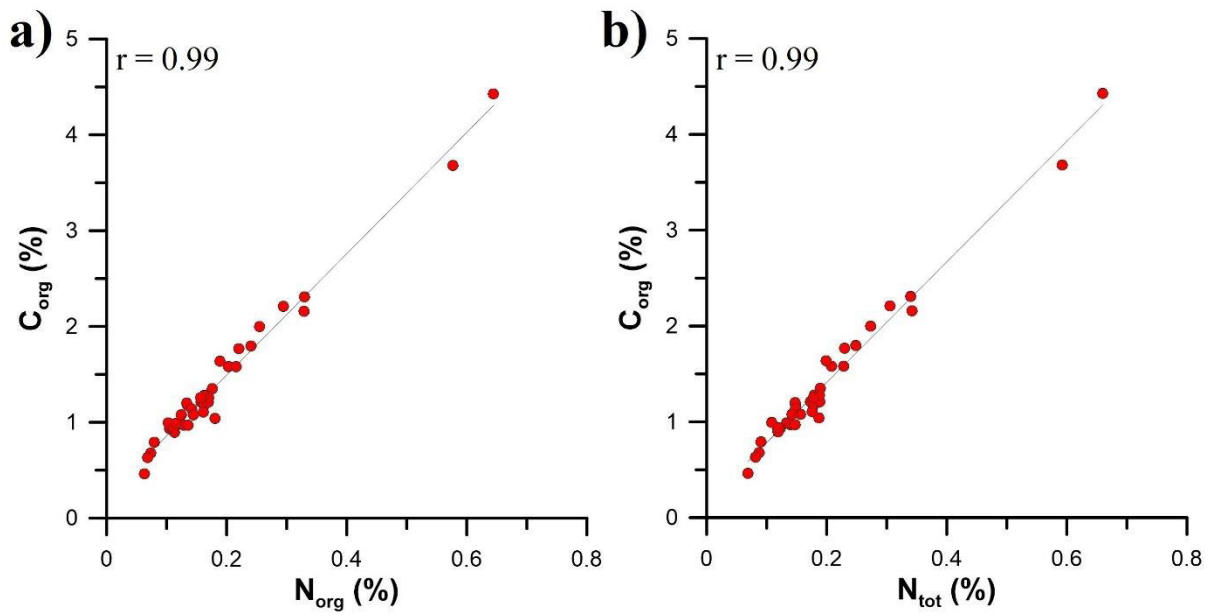

Figure 35: Correlation between a) C_{org} and N_{tot} and b) C_{org} and N_{org}.

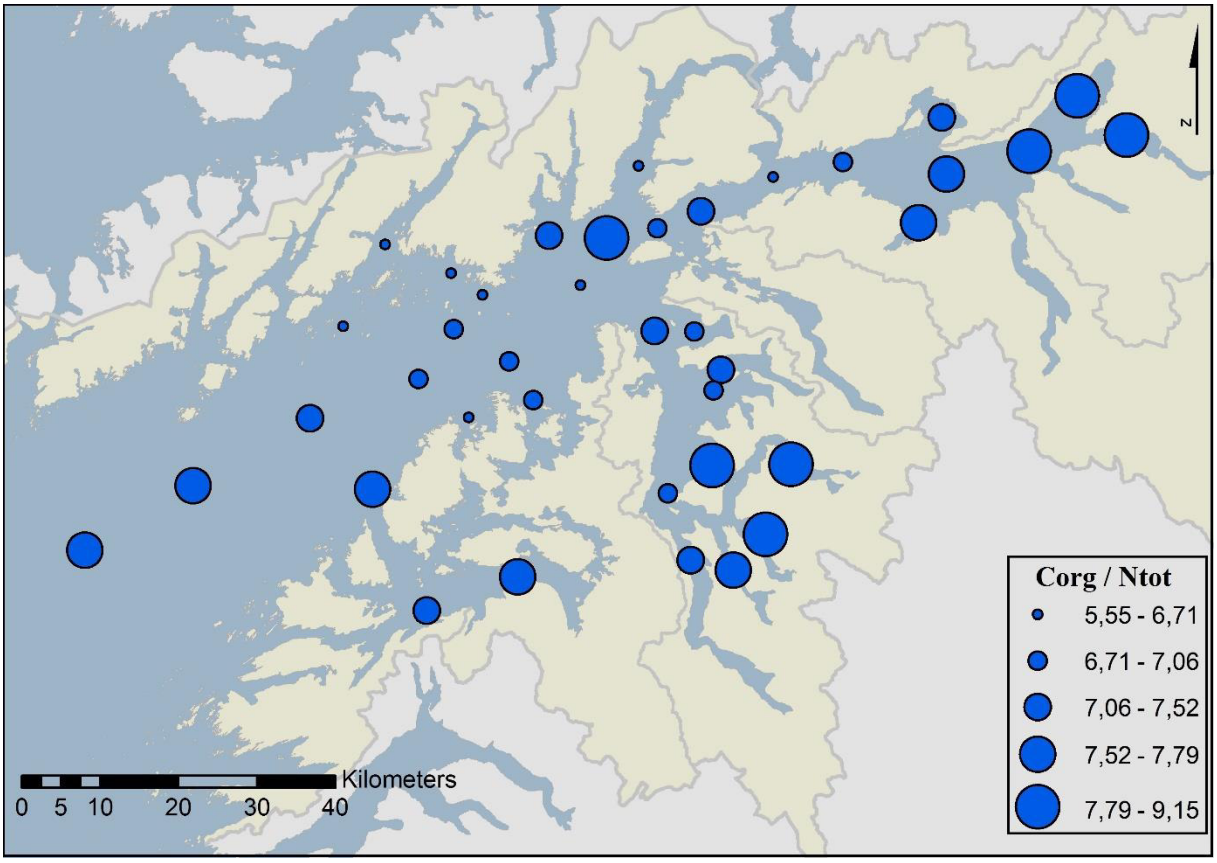

Figure 36: Distribution of C_{org}/N_{tot}.

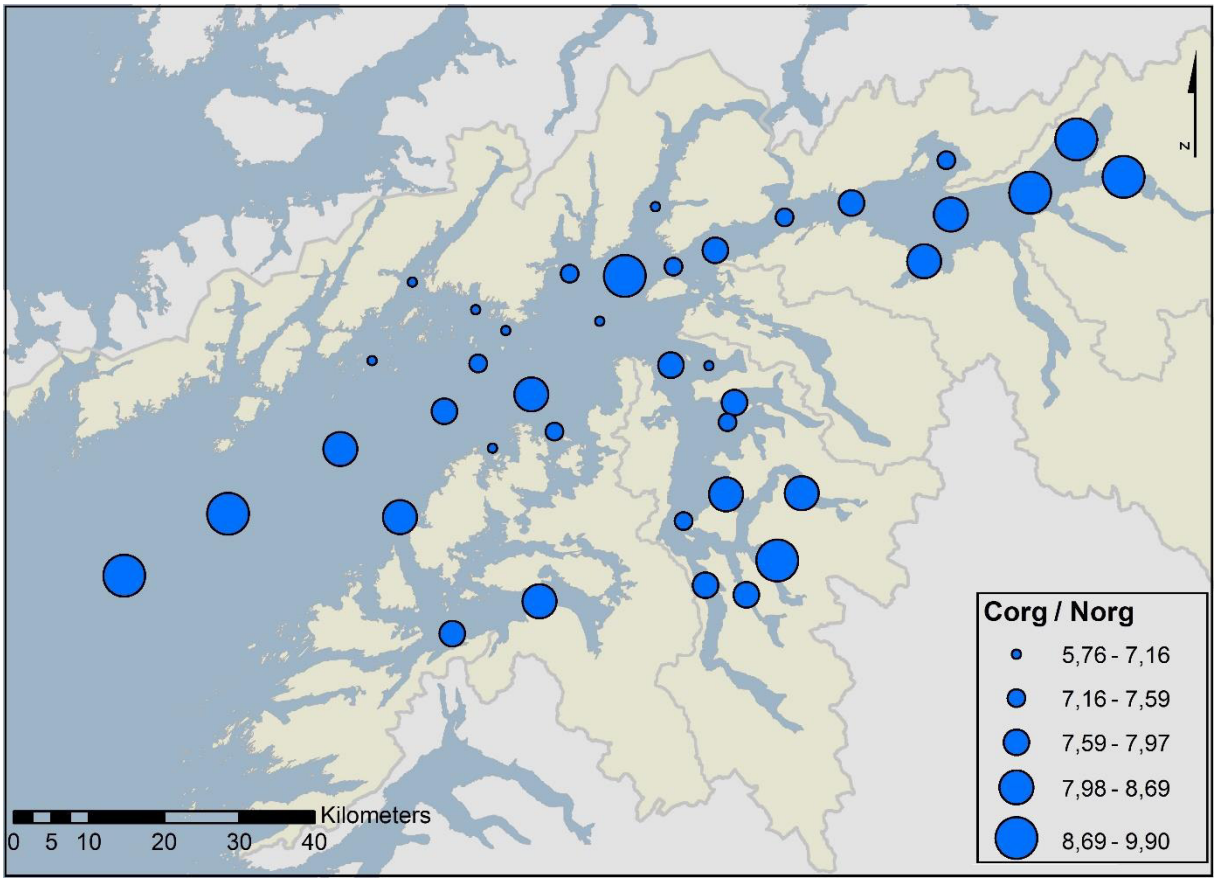

Figure 37: Distribution of Corg/Norg.

4.8 Calcium and calcium carbonate

Calcite measurements from the University of Bremen and $CaCO_3$ analyses from the NGU display a strong relation (r = 0.96, n = 40) as illustrated in Figure 38a. Calcium contents taken by the ALS laboratories and $CaCO_3$ measurements from the NGU are also strongly correlated, r = 0.99 (n = 40) (Fig. 38b). Ca distribution follows largely the spatial distribution of the $CaCO_3$ with a strong proximal to distal trend (Fig. 39) and highest values located in the outer parts of the Vestfjord (Ca = 31.9%, station 39; $CaCO_3$ = 82.4%, station 39). Lowest values are presented in the inner parts of the Ofotfjord and Tysfjord (Ca = 1.7%, station 1; $CaCO_3$ = 1.7%, station 24).

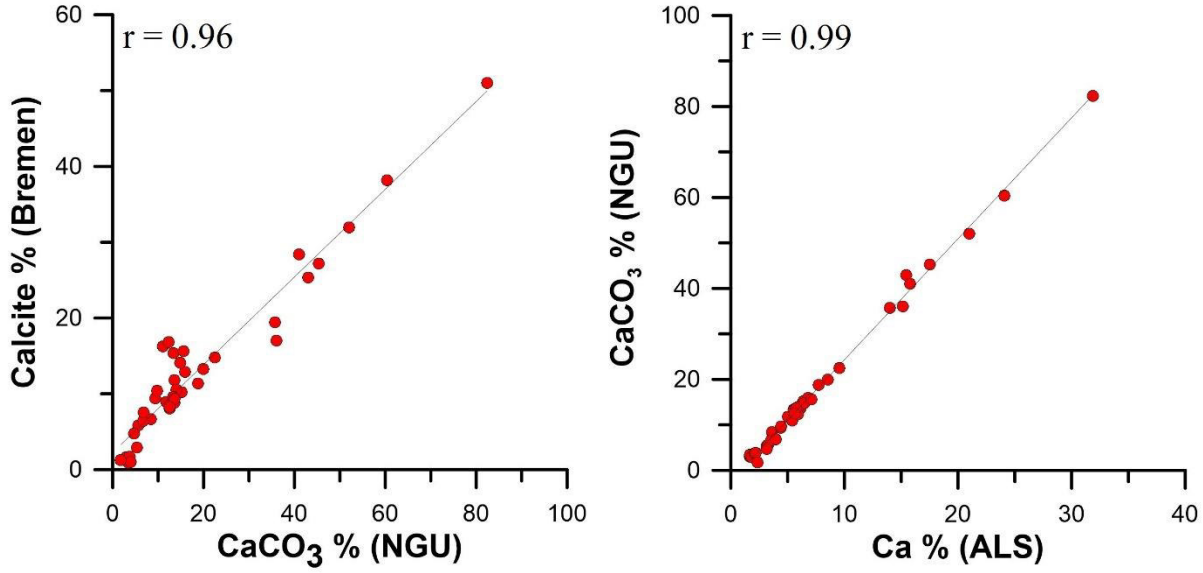

Figure 38: Correlation between $CaCO_3$ measurements from the NGU and calcite analyses from the University of Bremen (a), and correlation between calcite measurements from the ALS laboratories and $CaCO_3$ analyses by the NGU (b).

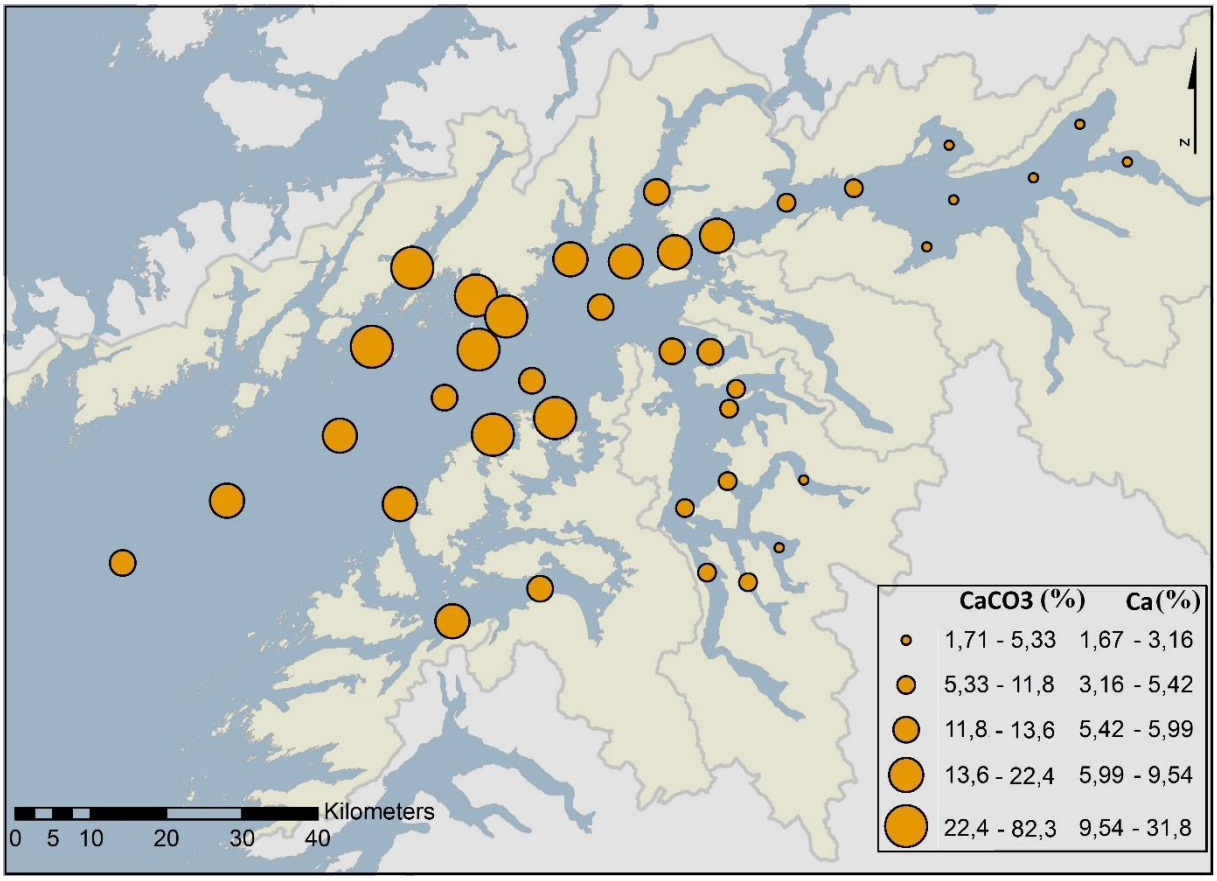

Figure 39: Distribution of the calcium carbonate and calcium.

5 Discussion

The following discussion is divided in four major parts focusing on the different environmental and sedimentological characteristics of the study area. The first part deals with the bulk inorganic composition of the 42 surface sediment samples and focuses on the bulk mineral assemblages, the grain size fractions, and elemental ratios that are commonly used for tracing terrigenous sediment sources. Secondly, the sources and pathways of OM are evaluated by applying numerous bulk parameters and proxies for distinguishing marine versus terrestrial OM. The third part deals with the size and characteristics of the drainage area, whereas the fourth part concentrates on Ca and $CaCO_3$ concentrations used as proxies for marine productivity.

For some parts of this chapter the Vestfjord, Ofotfjord, and Tysfjord are separated from each other and divided into inner, middle and outer fjord basin (Fig. 40). This separation is made due to an easier classification and merging of the different values and to combine values that belong to the same fjord.

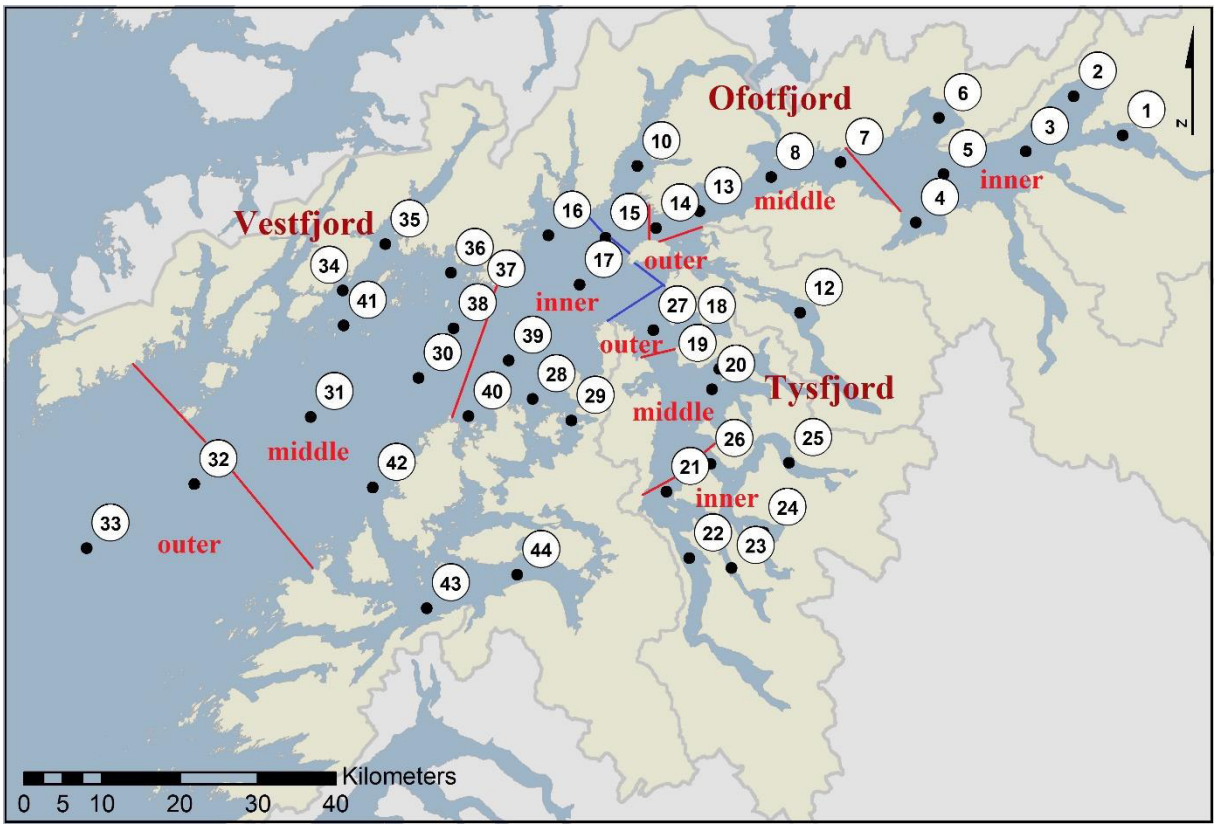

Figure 40: Classification and separation of the Vestfjord, Ofotfjord, and Tysfjord. The blue lines show the separation of the fjords due to the entrance sills. The red lines illustrate the subdivision of the individual fjords into inner, middle and outer fjord part for the Ofotfjord (stations 1-15), the Tysfjord (stations 18-27), and the Vestfjord (stations 16, 17 and 28-44).

5.1 Inorganic sediment composition

5.1.1 Mineral assemblages and grain sizes

Mineral assemblages of phyllosilicates, plagioclases, and illite/mica in the study area are highly variable over relatively short distances and follow no distinct distribution patterns (Fig. 17-21). The minerals are consistent with the surrounding bedrock geology of the Lofoten Islands and the mainland of Norway as they were part of the metamorphic bedrock, which consist, amongst others, of quartzo-feldspatic gneisses, graphitic schists or marble (Ramberg et al., 2008). Gaillardet et al. (1999) reported that homogeneity in a fjord sediment distribution is explained by the effective mixing of source rocks and soils due to comparatively long river transports. Thus, transport distances result in the smoothing of different chemical compositions in the material (Gaillardet et al., 1999). However, the inhomogeneous distribution pattern for the bulk mineralogy in the study area (Fig. 17-21) might be explained by the small drainage area which is predominantly restricted by its mountainous character and hence by relatively short transport distances of the riverine systems discharging from the area. In addition, the high topographic relief effects river characteristics as the rivers are dominantly defined by nearly straight channels with high gradients and relatively short lengths compared for example to meandering channels with low gradients and long-lasting channels (e.g. Culbertson et al., 1967). Thus, the rivers of the catchment area most likely are fed by low amounts of material and effective mixing of bedrock material might be insignificantly compared to other fjord systems. This is supported for example by the relatively homogenous distribution patterns of the bulk mineralogical composition in the Trondheimsfjord (e.g. Gaillardet et al., 1999; Faust et al., 2014b). The comparatively short transport lengths, high gradients and straight river channels therefore cause an ineffective mixing of terrestrial material transported by rivers towards the fjords and result in inhomogenous distribution patterns and an overall weak contribution for the terrigenous material to the fjords.

Grain size fractions in the study area show indistinct distribution patterns by comparing both the clay (<2 µm) and the silt (2-63 µm) fraction with the very fine to very coarse sand fraction (>63 µm) (Fig. 22-27). Slightly following the regional bathymetry (Fig. 9), smallest grain sizes are predominant in the deepest parts of the Vestfjord, Tysfjord, and Ofotfjord. Finest grain sizes of clay and silt mostly concentrate on the middle and outer parts of the fjords (Fig. 22, 23), whereas fine to coarse sands are more abundant in the inner basins, in the upwelling areas of the Vestfjord, as well as close to the entrance sills of the Ofotfjord and Tysfjord where the fjords merge (Fig. 24-27). The overall distribution of the grain sizes includes local variations for

individual stations and is influenced by different features and parameters like the local bathymetry and the distance to the shore (e.g. Skei, 1983; Howe et al., 2010). The latter is important as smaller grains are transported longer predominantly in a brackish surface plume towards the open ocean compared to coarser grain sizes that are deposited directly in shore-near locations (Hoskin et al., 1978). Regional differences in current velocities and flow directions as well as inflowing tidal currents that effect the occurrence of local restricted and temporary eddies and upwelling/downwelling effects highly influence the distribution pattern (e.g. Skei 1983 and references therein; Svendsen et al., 2002).

The Ofotfjord is mostly characterized by the silt grain size fraction with highest concentrations in the inner fjord and decreasing grain sizes towards the outer fjord (Fig. 22-27). Sandy particles between 63 and 250 µm are only minor presented (Fig. 24, 25). However, highest values for these fractions are abundant at sample station 4 and 6 in the middle part of the Ofotfjord. It is presumable that the strong occurrences of fine to medium sand in this spot are caused by the deposition of sediments with relatively short transport distances due to their near-shore location compared to other stations in the Ofotfjord (e.g. Skei, 1983; Howe et al., 2010). The proximity to the land increases the possibility for coarser material to be deposited (e.g. Howe et al., 2010).

In addition, grain sizes increase towards the merging of the Vestfjord and Ofotfjord (station 10, 14, and 15, Fig. 22-27) which is indicated by the predominance of medium to coarse sands (Fig. 26, 27). The rising in grain sizes is most likely effected by the proximity to the entrance sill that has been deposited as a terminal moraine consisting of morainal, rocky and glacio-fluvial material (e.g. Fløistad et al., 2009). Concentrations of medium to coarse sands are highly increased compared to adjacent stations. This might indicate that the surface sediment sample from station 15 is directly taken from the sill (Fig. 26, 27). Stations 14 and 10 likely are influenced by the coarser material as well as submarine slides seemed to occur in this area (Fløistad et al., 2009). Fløistad et al. (2009) reported that predominantly the distal parts of both the Ofotfjord sill (threshold) and the Tysfjord sill have been remobilized by sliding processes immediately after the glacial retreat in this area. Small-scaled earthquake activities due to the isostatic rebound might be the most likely triggering mechanism of the slides transporting high amounts of sediments from the sills (Fløistad et al., 2009). Sediment instability was most likely effected by rapid deposition of the glacio-marine material and the development of excess pore pressure (Fløistad et al., 2009). As the isostatic post-glacial uplift of Fennoscandia still proceeds (e.g. Fjeldskaar 1994 and references therein) it might be possible that seismic activity (small earthquakes) and thus small-scale sliding still occurs. This would be consistent with the

increased grain sizes at the stations 15, 10 and 14 (Fig. 24-27). In addition, it is possible that the exchange of water masses and the presence of strong currents in proximity to the sill result in outwashing of finer material and hence in the relative increase of the residual coarser material. Mitchelson-Jacob and Sundby (2001) reported that the bathymetric steering of the Tennholmen Ridge at the entrance of the Vestfjord (Fig. 9) forces inflowing currents through deeper parts of the fjord resulting in strong winnowing and outwashing of fine material.

Furthermore, material presumably is transported towards deeper fjord parts while originating from the island Barøya which is enclosed between the Vestfjord, Ofotfjord and Tysfjord (e.g. Fig. 8). Stations 14, 15, and 17 (Fig. 14) are closely located to this island. As submarine slides already can occur at a main slip plane gradient angle of 1° or less (e.g. Canals et al., 2004), it leads to the assumption that slides launching from the submarine extension of Barøya might be common in this area resulting in the deposition of coarser material. In addition, the presence of coarser grain sizes most likely is effected by the circulation of surface water masses originating from the presence of prevailing SW or NE wind patterns (Furnes and Sundby, 1981). As the island of Barøya is surrounded by relatively shallow water depths, it might be that surface water currents effect the sedimentary deposits of the island and hence cause erosion and winnowing of those sediments (e.g. Furnes and Sundby, 1981).

The grain size distribution in the Tysfjord represents a strong proximal to distal gradient with largest grain sizes of fine to coarse sand in the inner fjord part (Fig. 25-27). Grain sizes are decreasing towards the outer fjord. Clay and silt fractions dominate the deep parts of the Tysfjord and slightly follow the bathymetry (Fig. 9, 22, 23) and the water depth with a Pearson correlation coefficient of $r = 0.7$ ($n = 10$) for clay and $r = 0.5$ for silt. Compared to the inner part of the Ofotfjord, the inner part of the Tysfjord is characterized by higher concentrations of medium to coarse sands (Fig. 26, 27). This difference between the fjords and the increase in grain sizes might be caused by higher water depths (Appendix Table 1) and the relative proximity to the mountain range located south of the Tysfjord (Fig. 9). Transport distances from those mountains are shorter than the distances from the mountains located near the Ofotfjord (Figure 9). The proximity of the fjord to the mountains is important as coarse-grained material is mostly deposited close to river mouths entering the fjords, whereas finer material is capable to be transported over longer distances (e.g. Hoskin et al., 1978).

Sediments in the Vestfjord are characterized by high concentrations of clay and silt in the deepest parts of the fjord (Fig. 9, 22, 23). Sandy material is present near the shorelines, whereas

both sand and clay occur in the shallow upwelling areas of the Vestfjord, located on the eastern side of the city Svolvær (Fig. 9). Highest amounts of the coarse sand fraction occur at the stations 41 and 36 (Fig. 14; Appendix Table 1). Effected by relatively shallow water depths of 59 m (station 36) to 185 m (station 34) in this area (Appendix Table 1), coarser material might be preferentially deposited due to comparatively short transport distances (e.g. Hoskin et al., 1978). In addition, $CaCO_3$ concentrations are highest with 82.4% and 60.4% at the stations 41 and 36 (Appendix Table 2). The high concentrations of Ca and $CaCO_3$ at these stations (Fig. 39) might demonstrate the presence of carbonate aquatic productivity of marine organisms producing biogenic shells (see chapter 5.4). Carbonate productivity is strongly connected to the availability of high nutrient concentrations transported by freshwater runoff from the drainage area or Atlantic deep water masses to the areas (e.g. Eilertsen, 1993). Nutrient-rich water masses also indicate the presence of currents and hence the mixing of water masses. Therefore, the relatively coarse-grained material also may result from comparative strong currents at the stations. These currents might cause outwashing of fine material as the shallow water depth, the proximity to the shore, and the high concentrations of $CaCO_3$ are indicators for a fast flowing flow regime which is affected by SW or NE winds transporting Atlantic nutrient-rich water masses into the fjords that cause vertical mixing of upper water layers (Furnes and Sundby, 1981). The vertical mixing likely occurs as upwelling at stations 36 and 41 (e.g. Mitchelson-Jacob and Sundby, 2001; Furnes and Sundby, 1981).

5.1.1.1 Correlation between grain size fractions and the water depth

By comparing any grain size fraction with the water depth in the fjords, correlations are relatively weak with $r = 0.52$ ($n=42$) for the clay fraction (<2 µm), $r = 0.32$ ($n=42$) for the silt fraction (2-63 µm) and $r = -0.41$ for the fine sand fraction (63-125 µm) (Fig. 41a, b, c). These findings are in agreement with the general indistinct distribution patterns of the grain sizes in the fjords which do not follow the bathymetry due to several parameters that influence the distribution. Those parameters are for example current velocities and flow directions, the presence of upwelling, the size and characteristics of the drainage area, seasonal variations of freshwater supply from rivers and glaciers, and transport distances of the sedimentary material (e.g. Skei, 1983; Svendsen et al., 2002; Howe et al., 2010 and references therein). The contribution of marine produced material influences the grain size distribution as it strongly depends on the presence of nutrient-rich water masses transported into the fjords. Thus, it depends on the amount of marine organisms that occur in the water column and supplementary

being degraded by microorganisms and deposited in the sediments (e.g. Altabet and François, 1994). Furthermore, high amounts of MOM might cause dilution of terrestrial material as the relatively low content of terrigenous material decreases with increasing marine material supply.

The grain size distribution in the Vestfjord, Ofotfjord, and Tysfjord is highly variable and depends on numerous local and regional characteristics like the overall bathymetry and the oceanography. Grain size distribution depends on the size and properties of the drainage area and its topographical characteristics, as well as different sedimentation patterns influenced by marine and terrestrial sources.

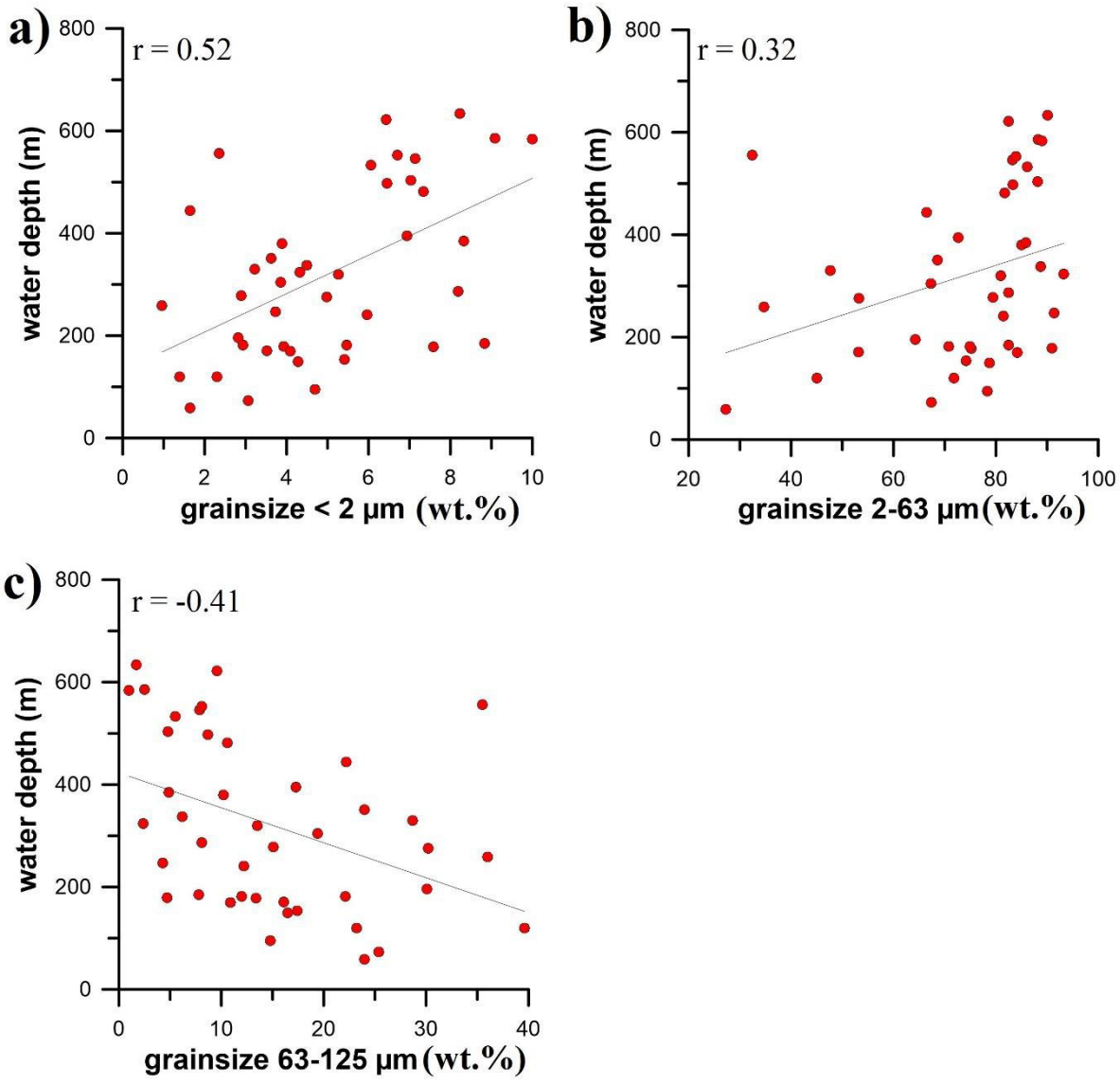

Figure 41: Grain size fractions versus water depth using grain sizes <2 µm (a), grainsizes 2-63 µm (b), and grain sizes 63-125 µm (c).

5.1.1.2 *Grain size fractions versus inorganic and organic carbon and nitrogen*

Only a weak correlation between C_{org}, C_{inorg}, N_{org}, $\delta^{15}N_{org}$, $\delta^{13}N_{inorg}$, and $\delta^{13}C_{org}$ with any grain size fraction was found ($r < 0.53$, $n = 42$). However, the N_{inorg} fraction is strongly connected to the clay fraction (<2 µm) with a Pearson correlation coefficient of $r = 0.84$, $n = 42$ (Fig. 42). Correlations with other grain size fractions are comparatively weaker with $r = 0.57$ for the silt fraction (2-63 µm) and $r = -0.75$ for very fine to fine sand (63-250 µm). Grain size fractions >63 µm are inverse to the values of the clay and silt fractions (<63 µm). Due to the strong connection to the clay the observations indicate a strong land-derived origin for N_{inorg}. This strong correlation between N_{inorg} and the clay fraction is consistent with previous studies by Schubert and Calvert (2001), Winkelmann and Knies (2005), Knies et al. (2007), and Faust et al. (2014a) who also found strong terrestrial sources of N_{inorg}.

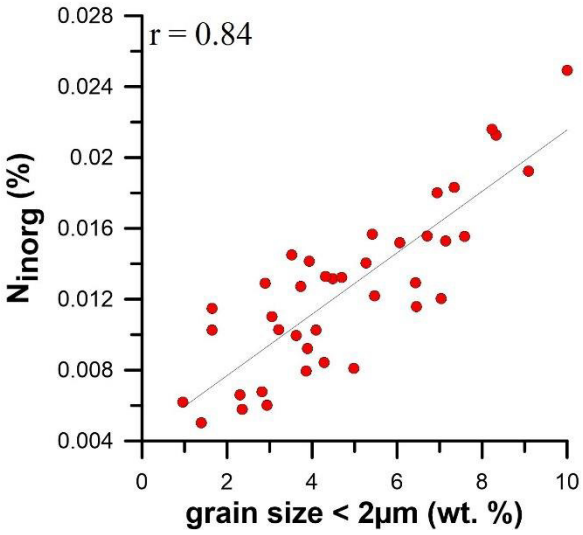

Figure 42: Correlation of the inorganic nitrogen versus the grain size fraction of clay (<2 µm).

However, N_{inorg} concentrations in the entire area are extraordinary low with 0.01 to 0.02% and a percentage of 7.7% for the proportion of N_{inorg} of the N_{tot} compared to the other studies who for example reported strong N_{inorg} proportions of up to 70% of the N_{tot} in the central Arctic Ocean (Schubert and Calvert, 2001). These small N_{inorg} concentrations are strongly affected by the small contribution of terrestrial material in general that is restricted by the mountainous topography of the drainage area and thus relatively short sediment transport distances. Furthermore, the relatively small drainage area/fjord surface area of almost 1:1 might cause relative dilution of terrigenous material by the dominant supply of MOM (see also chapter 5.3).

5.1.2 Elemental ratios as proxies for terrestrial sediment supply

5.1.2.1 Elemental compositions and selection of an element representative of the lithogenic fraction

In sedimentary geochemistry elemental ratios can be used to overcome dilution effects by biogenetic or organic phases (e.g. by carbonate) and to minimize grain size effects (e.g. by quartz) by using a normalizer which mainly is incorporated in a single grain size fraction (e.g. Calvert, 1976; Van der Weijden, 2002). Usually, normalization to aluminium (Al) is used to identify element enrichment in sediments by assuming that Al belongs to the lithogenic and terrestrial content of sediments (Calvert et al., 1993). Al is insensitive to changes regarding the sediment source, the catchment size, and hydrodynamic sorting in fjords (Bertrand et al., 2012). Variations in the ratios can be interpreted in terms of the texture and mineralogy of sediments (Calvert, 1976). In addition, Al-based ratios might identify potential land sources for the terrigenous fraction and likely are used as proxies for terrestrial sediment supply to the sediment samples (e.g. Faust et al., 2014a).

By correlating Al to the different grain size fractions of the study area, only relatively weak Pearson correlation coefficients were found. The grain size fraction of silt (2-63 µm) reveals a correlation of r = 0.36 (Fig. 43), whereas the correlations to clay (<2 µm) and very fine to coarse sand (>63 µm) are negligible small as well with r < -0.33.

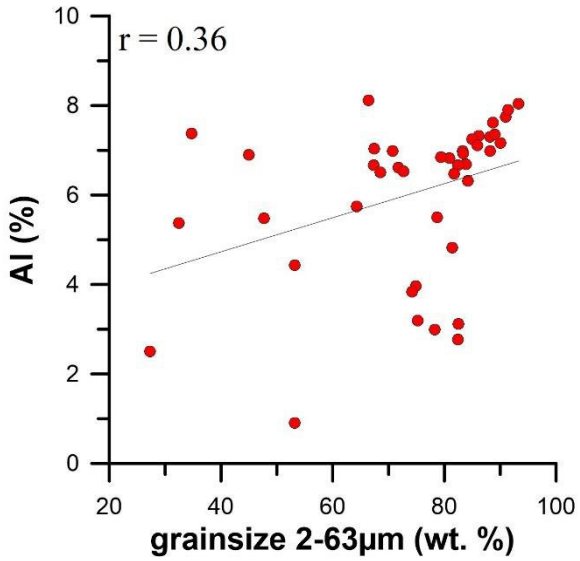

Figure 43: Correlation between Al and the grain size fraction 2-63 µm.

As correlations between Al and the grain size fractions are generally weak, the element is not related to just one single grain size fraction as reported for example in Faust et al. (2014a).

Thus, the elemental ratios cannot be used for investigating potential land sources for the terrestrial sediment fraction. Due to dilution effects and grain size independence, calculations are sensitive to hydrodynamic and sedimentological changes (Bertrand et al., 2012).

However, the normalization to Al might be used for distinguishing whether other elements have similar sources like Al (Calvert et al., 1993). By correlating Al with Ca, iron (Fe), potassium (K), silicon (Si), and strontium (Sr) (Appendix Table 3), the ratios indicate high relations with r = -0.91 for Al/Ca, r = 0.9 for Al/Fe, r = 0.93 for Al/K, r = 0.85 for Al/Si, and r = -0.89 for Al/Sr with n = 42 (Fig. 44a, b, c, d, e). Fe, K, and Si have strong proportional correlations to Al illustrating that the elements have similar sources. This has been reported by Calvert et al. (1993), Karageorgis et al. (2005), and Faust et al. (2014). As Al is related to the terrestrial fraction, Fe, K, and Si also have terrestrial sources due to their positive correlation (e.g. Calvert et al., 1993). This as well is consistent with the observation that Fe is a highly lithophile and immobile element used as an indicator for the terrigenous fraction (e.g. Haug et al., 2001). The terrestrial sources for Fe, Si, and K are comparable to observations obtained by Calvert et al. (1993) and Karageorgis et al. (2005).

In addition, Fe, K and Si are common elements that are incorporated in typical minerals of the bedrock geology in the drainage area (e.g. Ramberg et al., 2008). For example, K occurs in potassium feldspar ($K[AlSi_3O_8]$ and illite (K,H_3O) $Al[(OH)_2Si_3AlO_{10}]$) which can be a dominant K source in marine sediments and in sediments deposited in upwelling areas or restricted basins (e.g. Martinez et al., 1999; Shimmield, 1992). The bedrock material around the study area consists for example of quartzo-feldspathic gneisses (Ramberg et al., 2008) which might illustrate one of the K (and Si) sources. Furthermore, as Si is a major constituent of quartz (SiO_2), it is present in the bedrock material as this mostly consists of (Precambrian) gneisses and granites (e.g. Ramberg et al., 2008). However, the elemental composition of the terrigenous derived material has no great influence on the sedimentary record of the surface sediment samples due to the insignificant low contribution of terrigenous material in general. This is consistent with observations concerning the organic fraction (see chapter 5.2) which strongly dilutes the terrigenous material.

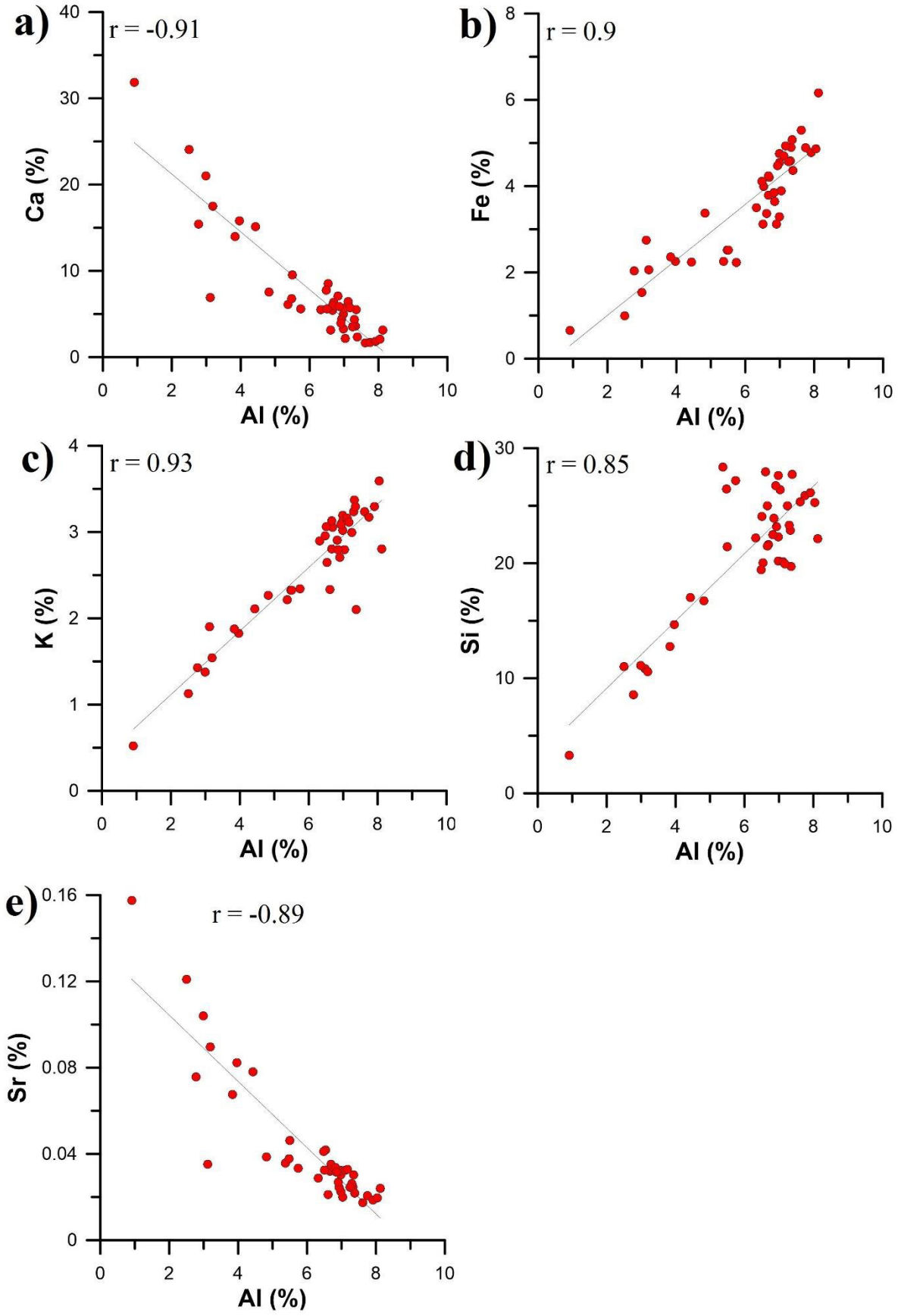

Figure 44: Elemental ratios normalized to aluminium. Ca vs. Al (a); Fe vs. Al (b); K vs. Al (c); Si vs. Al (d); and Sr vs. Al (e).

In contrast, Ca and Sr are inversely proportional to Al (Fig. 44 a, e) with r = -0.91 and r = -0.89, respectively. This may indicate that Sr and Ca are originated due to the influence of a marine environment. As Ca and Sr are strongly correlated to each other with r = = 0.99 (n = 42) it is assumable that they have same sources. The findings are consistent with the previously reported strong correlation between Ca and Sr which emerges due to geochemical similarities (Shankar et al., 1987). Calvert et al. (1993) and Karageorgis et al. (2005) further demonstrate that the distribution of Sr strongly is controlled by the presence of biogenic carbonate minerals (calcite and aragonite) that build up the tests of foraminifera and coccoliths, whereas a small contribution from bedrock material like plagioclase feldspars might also be possible. It is reasonable that Sr in the study area also is dominated by the presence of biogenic carbonate minerals due to the strong correlation between Sr and Ca and the fact that Ca is as well strongly connected to the carbonate fraction (see chapter 5.4).

To summarize, the elemental ratios normalized to Al illustrate that Fe, K, and Si are of terrigenous origin, whereby Ca and Sr are originated from marine environments. Al is highly independent of grain sizes and hence affected by dilution effects. Therefore, Al-based ratios cannot be used as proxies to identify potential land sources or to track terrestrial sediment supply to the samples as Al is sensitive to changes regarding the sediment source, the catchment size, and hydrodynamic sorting (e.g. Bertrand et al., 2012).

5.2 Sources and pathways of organic matter

The following discussion deals with several potential proxies for distinguishing between MOM and TOM by investigating the carbon and nitrogen content of the surface sediment samples. The use of several proxies is important as numerous parameters increase the reliability of the observations (e.g. Meyers, 1997).

5.2.1 Measurements and distribution of carbon and nitrogen concentrations

5.2.1.1 Carbon concentrations

For exact measurements of C_{tot} and C_{org} contents, it is important to prove the conformity of the different analyses which were performed by applying numerous measuring instruments at different laboratories (Appendix Table 2). Figure 45a and b illustrates the correlations between the different measurements. The connection between the C_{tot} content analysed by the ALS

Global laboratories and the NGU (Fig. 45a) reveals a strong value of r = 0.99 (n=42). By correlating C_{org} values (Fig. 45b) obtained by the NGU and IsoAnalytical, the Pearson coefficient is weaker with r = 0.81 (n=42). The measurements are reliable due to their relatively strong correlations. Thus, they can be well used for further interpretations. For those analyses, values performed by the NGU are used for the distribution patterns of C_{org}, C_{inorg}, and C_{tot} concentrations as well as for the utilization of C_{org}/N_{org} and N_{org}/C_{org} ratios.

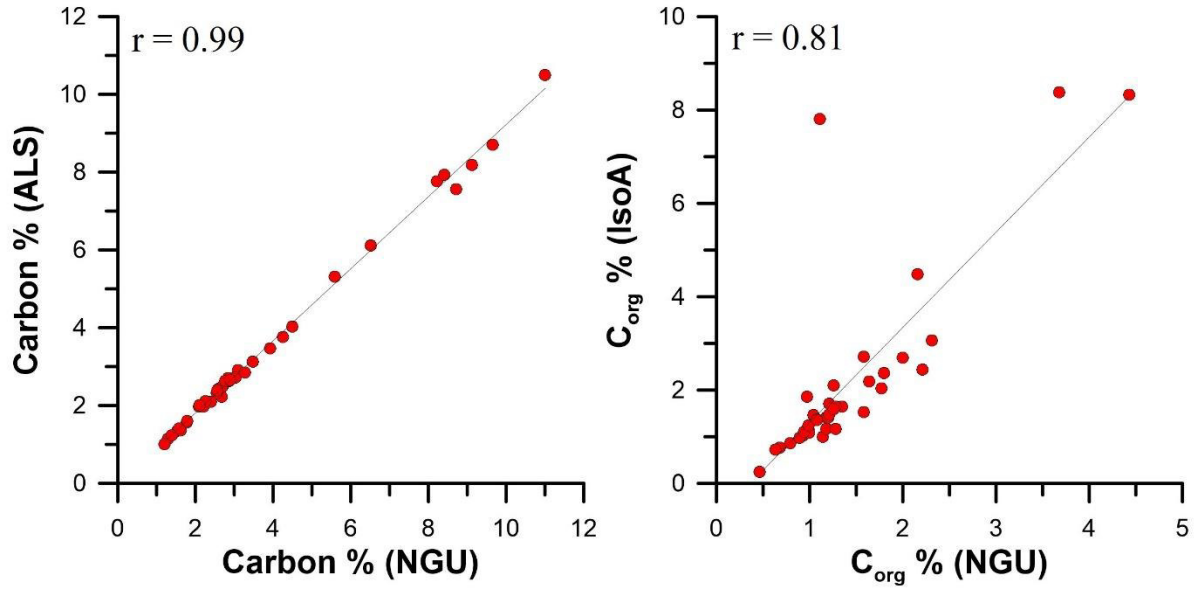

Figure 45: Correlations between a) C_{tot} measured by the NGU and ALS Global labratories, b) C_{org} measured by IsoAnalytical and the NGU.

The distribution pattern of C_{inorg} ($CaCO_3$) shows that the concentrations are strongly affected by marine sources as the values are highest in the outermost part of the Vestfjord and decrease towards the shore and the inner parts of the Ofotfjord and Tysfjord (see also chapter 5.4). C_{tot} concentrations also increase towards the open ocean with a highest value of 11% at station 41 (Fig. 28). The values indicate marine sediment sources in general due to the mixing of inorganic material ($CaCO_3$) that is strongly influenced by a marine environment and due to highly variable organic sources which are presented in the indistinct distribution of C_{org} (Fig. 28). The alternating C_{org} concentrations might be caused by the mixed input of various sources probably effected by differences in fractionation processes both on land and in aquatic environments (e.g. Meyers 1997) and by specific characteristics of individual marine species like phytoplankton (e.g. Sverdrup, 1953; Bordovskiy, 1965). Phytoplankton is controlled by several parameters like the intensity of sunlight, solar radiation, temperature, salinity and the abundance of nutrients in the marine realm which highly depends on freshwater supply from the drainage area and wind-driven vertical mixing of water masses (e.g. Fischer, 1939; Sverdrup, 1953).

Thus, several chemical and biological parameters further might influence the variable distribution of the carbon content.

5.2.1.2 Nitrogen concentrations

Concerning the nitrogen content it is important to distinguish between the organic and inorganic fraction of the nitrogen, as N_{inorg} may be influenced by ammonium (NH_4^+) in the terrestrial fraction of the clay minerals (e.g. Müller, 1977). In the study area, N_{inorg} is relatively low with values between 0.01 and 0.02%. A distribution pattern for N_{inorg} is not presented due to the lack of material as only a minor fraction of N_{inorg} has been remained during analysis after the removal of N_{org} from the N_{tot} content. Hence, the small amounts of N_{inorg} make it difficult to obtain reliable nitrogen analyses. N_{org} is defined by relatively high proportions of 83.9% - 97.6% and an average percentage of 92.3% of the N_{tot} content. This demonstrates that N_{tot} and N_{org} are similar within a small range of values and in their chaotic distributions which likely are influenced by the mixing of various material and by variations in nutrient availability and the uptake of nutrients during fractionation processes in the water column (Wada et al., 1987a).

Furthermore, as it has been presented in the results, the regression between C_{org} and N_{tot}, as well as the regression between C_{org} and N_{org} both have strong correlations of r = 0.99 indicating that the total amount of nitrogen is chiefly organic and that sources of nitrogen and carbon are mostly the same and of marine origin. To sum up, N_{inorg} and thus the terrestrial fraction of the material is extraordinary low for the surface sediment samples, whereas the proportions of N_{org} are almost identical with the N_{tot} fraction.

5.2.2 C/N and δ13Corg as proxies for marine versus terrigenous organic material

5.2.2.1 C/N and $\delta^{13}C_{org}$

The following chapter deals with carbon-to nitrogen ratios and $\delta^{13}C_{org}$ values. C_{org}/N_{org} ratios and $\delta^{13}C_{org}$ are used to estimate relative contributions of marine versus terrigenous OM (e.g. Goñi et al., 1997; Winkelmann and Knies, 2005; Sepúlveda et al., 2011). Contrary to C_{org} and N_{org} values only, the parameters are independent of changes in the sedimentation rate. Several studies have been performed to identify the variabilities for marine and terrestrial derived OM (Goñi et al., 1997; Karageorgis et al., 2005; Winkelmann and Knies, 2005; Perdue and Koprivnjak, 2007; Knies and Martinez, 2009; Sepúlveda et al., 2011; Bertrand et al., 2012;

Faust et al., 2014a/b). The studies have shown that C/N ratios and $\delta^{13}C_{org}$ are reliable proxies to distinguish between the different sediment sources.

C/N ratios are usually proxies for discriminating autochthonous (marine) from allochthonous (terrigenous) OM in sediments (e.g. Stein, 1991; Sepúlveda et al., 2011; Faust et al., 2014a/b). C_{org}/N_{org} ratios are favoured over C_{org}/N_{tot} ratios, as too much N_{inorg} might be bound as ammonium (NH_4^+) in the lattice structure of the clay minerals (especially illite) of the terrigenous fraction. It is important to distinguish between N_{inorg} and N_{org} because high proportions of illite can strongly dilute the organic signal (Müller, 1977). Furthermore, due to mathematical reasons, N/C ratios are used instead of C/N ratios (Perdue and Koprivnjak, 2007). Marine derived OM usually is indicated by C/N ratios between 4 and 10, whereas terrestrial derived OM show values >20 (Meyers, 1994; Meyers 1997). Differences between those values are affected by the composition of the OM. Marine produced algae and microorganisms are protein-rich (nitrogen-rich) and related to the absence of cellulose and lignin (causing relatively low values), whereas terrestrial vascular vegetation is cellulose-rich and contains a high proportion of carbon (relatively high values) which is needed to fight the effects of gravity (Meyers and Teranes, 2002).

The $\delta^{13}C_{org}$ also reflects quantitative proportions of marine versus terrigenous OM due to the fractionation of ^{12}C and ^{13}C during photosynthesis (e.g. Hayes, 1993; Schubert and Calvert, 2001). Average $\delta^{13}C_{org}$ signatures for marine derived OM are -20‰ to -22‰ (Meyers, 1994), whereas depleted values of approx. -27‰ are characteristic for TOM derived from plants using the C_3 pathway (O´Leary, 1981; Meyers, 1994). In the study area, C_3 pathways are preferred as the admixture of C_4 plant debris is of less insignificance in higher latitudes (Teeri and Stowe, 1976).

5.2.2.2 The distribution of C_{org}/N_{org} and $\delta^{13}C_{org}$

C_{org}/N_{org} values in the study area vary between 5.8 and 9.9 with an average value of 7.9. The values indicate an overall strong marine originated sediment supply to the surface sediments, as MOM usually show values between 4 and 10 (Meyers, 1994). As C_{org}/N_{tot} ratios have similar values between 5.6 and 9.2 with an insignificant small range of values (Appendix Table 2), it is obvious that C_{org}/N_{org} ratios are just slightly affected by the N_{inorg}. The $\delta^{13}C_{org}$ signatures show comparatively enriched values between -23.83‰ and -20.87‰ with an average concentration of -21.62‰ for the entire study area. These values are also well within the range

of marine influence, as MOM usually is defined by $\delta^{13}C_{org}$ values between -20‰ and -22‰ (Meyers, 1994). For the following analysis and more detailed investigations, the Vestfjord, Ofotfjord, and Tysfjord are presented separately from each other (Fig. 40).

5.2.2.2.1 The Ofotfjord

C_{org}/N_{org} ratios in the Ofotfjord show an overall decreasing trend from the innermost fjord part (C/N: 9, station 2) towards the merging with the Vestfjord and Tysfjord (C/N: 5.8, station 10) (Appendix Table 2). All ratios are indicative for enhanced input of MOM, with an increase in MOM towards the entrance sill. The $\delta^{13}C_{org}$ values vary between -23.20‰ (station 1) and -21.39‰ (station 8) (Appendix Table 2) and show an increasing trend of marine derived sediment input towards the outer fjord part.

Station 15 which is located close to the entrance sill of the fjord has to be seen separately as it shows a relatively high C_{org}/N_{org} ratio of 9.9 and $\delta^{13}C_{org}$ value of -22.11‰ that indicate comparatively high terrigenous derived input compared to adjacent stations. Due to the bathymetrical height of the sill, steering of water mass exchange on top of the ridge and currents at the sides may have caused outwashing of the sedimentary fine-grained fraction leaving coarser material on top of the sill (e.g. Svendsen et al., 2002). In addition, it might be possible that coarser material is transported towards the sill by inflowing rivers and being deposited on top of the sill or on its slopes. The presence of the sill therefore most likely causes the high $\delta^{13}C_{org}$ values and low C_{org}/N_{org} ratios at this station indicating a relative stronger supply of terrigenous material due to the proximity of morainal and glacio-marine material.

5.2.2.2.2 The Tysfjord

The Tysfjord is characterized by C_{org}/N_{org} ratios ranging between 7 (station 18) and 9.7 (station 24) and by $\delta^{13}C_{org}$ values of -23.83‰ (station 24) to -20.87‰ (station 26) (Appendix Table 2 and Fig. 31, 37). A decreasing trend in C_{org}/N_{org} and an increasing gradient for $\delta^{13}C_{org}$ concentrations can be observed from the inner part of the fjord towards the outer fjord, although the gradients are not as distinct as in the Ofotfjord. This might be due to shorter sediment transport distances between the land-near inner fjord part and the merging of the fjords and hence result in the relative increase of terrestrial input.

5.2.2.2.3 The Vestfjord

The Vestfjord is defined by C_{org}/N_{org} ratios that range between 6.4 (station 35) and 9.3 (station 32) (Appendix Table 2). The $\delta^{13}C_{org}$ values vary between -22.05‰ (station 41) and -20.94‰ (station 35). Concentrations are in the range of values from the Ofotfjord and Tysfjord. Lowest values for C_{org}/N_{org} ratios and relatively high $\delta^{13}C_{org}$ values are observed in the assumed upwelling areas in the central part of the Vestfjord (stations 28, 30, 35, 36, 37, 38, 40, 41; Fig. 9, 31, 37). The values reflect predominant influences of MOM. Due to the coastal upwelling of nutrient-rich deep-water masses in this area caused by SW winds also transporting high amounts of primary producers into the fjords (Furnes and Sundby, 1981; Asplin et al., 1999), large amounts of phytoplankton and Northeast Arctic cod eggs preferably spawned by the cod in these areas are piled up (Ellertsen et al, 1981; Sundby and Solemdal, 1984). The high availability of marine organisms increase the contribution of MOM in the water column and the dominating concentrations of MOM thus are presented in the surface sediment samples.

Stations 31, 32, and 33 (Fig. 15) which are located in the outermost part of the Vestfjord, show an increase in C_{org}/N_{org} ratios (8.5; 9.3; 9.3) and slightly decline in $\delta^{13}C_{org}$ values (-21.09‰, -21.42‰, -21.57‰) (Figure 31, 37). This relative increase in TOM might be caused by alteration effects within the sediments as reported previously by Müller (1977) and Altabet and François (1994). Due to microbial degradation of OM by marine micro-organisms, an enrichment in the heavier ^{13}C compared to the ^{12}C is present in the sediments, as a preferentially removal of the lighter isotopes occurs during degradation processes (Altabet and François, 1994). Therefore, the heavier isotope fraction ^{13}C is relatively enriched in the sediments compared to the ^{12}C which results in lower $\delta^{13}C_{org}$ values. Furthermore, the decrease in N_{org} and hence the increase in C_{org}/N_{org} ratios is effected by the preferential diagenetic degradation and uptake of nitrogen comparatively to carbon by benthic organisms in the water column (Müller, 1977; Altabet and François, 1994). Higher rates of microbial degradation might be predominant at these stations compared to other samples, as degrading processes increase with time. Due to relatively low sedimentation rates compared to inner fjord parts (e.g. Skei, 1983; Hedges et al., 1997), the depositional environment is comparatively calm. Thus, degradation preferentially can take place (e.g. Freudenthal et al., 2001).

In addition, the local bathymetry might play an important role due to decreasing water depths in this part of the Vestfjord compared to adjacent sample stations (Appendix Table 1). Decreasing water depth increases the influence from the land. Furthermore, it is presumable that sedimentary erosion and outwashing of finer material by inflowing currents are existent.

This is consistent with slightly increasing grain sizes for the stations 32 and 33 (Fig. 25, 26) that also indicate a stronger influence by terrestrial sources.

The overall distribution pattern and the concentration of $\delta^{13}C_{org}$ and C_{org}/N_{org} show strong influences of MOM for all three main fjords. Concentrations are highly affected by regional and local circulation patterns and depend on both the Norwegian Atlantic Current and the Norwegian Coastal Current entering the fjords (e.g. Eggvin, 1931; Geddes and Scott, 1994). Local bathymetry and topography are important as they control circulation patterns and tidal currents in the area for example due to the presence of the entrance sills located at the merging of the three main fjords (Fløistad et al., 2009). NE and SW wind patterns as well as frequently occurring eddies influence the amount of carbon and nitrogen contents due to the interaction between water layers and the atmosphere, and cause mixing of water masses which strongly is connected to the amount of marine organisms in the water column and thus in deposited sediments.

5.2.3 $\delta^{15}N_{org}$ as a proxy for tracking nutrient utilization in marine environments.

5.2.3.1 The general utilization of $\delta^{15}N$

The stable nitrogen isotope content is another proxy commonly used to distinguish between MOM and TOM (e.g. Sepúlveda et al., 2011; Schubert and Calvert, 2001). It has been used as an indicator for tracking nutrient utilization and fractionation by phytoplankton in the euphotic water column of nitrate replete environments (e.g. Wada and Hattori, 1991; Calvert et al., 1992; Altabet and François, 1994; Schubert and Calvert, 2001; Knies et al., 2007), as well as for tracking changes in denitrification (e.g. Altabet et al., 1995) and N_2-fixation processes (e.g. Haug et al., 1998). Furthermore, $\delta^{15}N_{org}$ concentrations can be used to identify Atlantic water inflow into fjords (e.g. Schubert and Calvert, 2001).

The $\delta^{15}N$ is part of the marine nitrogen cycle (Fig. 7) which further belongs to the global nitrogen cycle. The isotopic signatures of $\delta^{15}N$ depend on the isotopic composition of nitrogenous substrate and on the degree of isotope fractionation of the N_{inorg} pool during nitrate (NO_3^-) uptake by phytoplankton (Wada and Hattori, 1991) or during fractionation by land plants. Typically, $\delta^{15}N$ signatures for MOM range between 4‰ and 8‰, whereas terrestrial derived OM, produced by plants using the C_3 pathway, reveal average values of 0.4‰ (Peters et al., 1978). Isotopic differences are effected by MOM being isotopically heavier due to fractionation during nutrient uptake, and TOM being relatively lighter since fractionation there

is low or absent (Wada et al., 1987a). In the photic zone, the uptake of light $^{14}NO_3^-$ is preferred by phytoplankton leading to lower $\delta^{15}N$ values for the organisms and hence isotopically light MOM, whereas ^{15}N is enriched in the residual dissolved NO_3^- (higher $\delta^{15}N$) within the water column (e.g. Wada and Hattori, 1991). Under nutrient (nitrate) replete conditions the physical supply of nitrate exceeds the biological demand in the water column and the settling OM is depleted in the heavy isotope (lower $\delta^{15}N$) (Farrell et al., 1995). During nitrate deplete conditions, the supply is lower than the biological demand, thus, OM is enriched in the heavy isotope which results in high $\delta^{15}N$ values (Farrell et al., 1995). Denitrification is characterized by the conversion of NO_3^- to N_2 (Fig. 7) and might be another factor leading to changes in the sedimentary $\delta^{15}N$ composition (Altabet et al., 1995). It usually occurs in anaerobic environments and results in the enrichment of the ^{15}N fraction of surface waters and in low $\delta^{15}N$ values for the OM (e.g. Altabet et al., 1995). However, denitrification seems to be unlikely in the well oxygenated water masses of the fjords in the study area strongly affected by the inflowing Norwegian Atlantic Current and Norwegian Coastal Current. Furthermore, the high occurrence of primary producers indicate well oxygenated water masses as primary production highly depends on well-mixed water masses (e.g. Fischer, 1939; Furnes and Sundby, 1981). Considering the different environmental conditions and changes in nutrient availability, variations in the isotopic signal of nitrogen are possible to interpret.

5.2.3.2 Stable organic nitrogen $\delta^{15}N_{org}$ concentrations as an indicator for nutrient utilization and fractionation by marine organisms

5.2.3.2.1 The Ofotfjord and the Tysfjord

The isotopic signatures of $\delta^{15}N_{org}$ show relatively high values in the entire study area comparable to previous studies by Schubert and Calvert (2001) and Knies et al. (2007). Concentrations are highest in the deepest parts of the fjords with a decreasing gradient from the outer fjord towards the innermost part of the Tysfjord and Ofotfjord. Relative low values (4.69‰ to 6.50‰) for $\delta^{15}N_{org}$ are present in the inner part of the Tysfjord and Ofotfjord, as well as close to the fjord entrance sills (Fig. 34). The terrestrial supply in inner fjord areas is comparatively high (lower $\delta^{15}N_{org}$ values) compared to outer fjord parts, as fractionation is mainly controlled by the uptake of nitrogen by marine organisms changing the isotopic signatures towards higher values (e.g. Meyers 1997). This uptake by marine phytoplankton decreases towards the land as it is strongly connected to the inflow of Atlantic water masses

which decreases as well. The decreasing trend of Atlantic water inflow is for example presented in the $CaCO_3$ and C_{inorg} values, respectively (see chapter 5.4).

Furthermore, lower $\delta^{15}N_{org}$ values are more effected by fractionation by land plants (C_3) which increases towards the shore. The range of the values demonstrates that even the innermost fjord parts are highly influenced by MOM, although they show a decreasing trend towards more terrestrial derived material. This is consistent with observations obtained by Peters et al. (1978) who reported that the range for marine derived $\delta^{15}N$ values lies between 4‰ and 8‰. In addition, observations are comparable to Schubert and Calvert (2001) who found out that $\delta^{15}N$ values (4.6‰ to 13.1‰) are also increasing towards the open ocean which is mainly caused by the inflow of Atlantic water masses with relatively high amounts of nitrate intruding towards the coasts. Nitrate concentrations decrease progressively towards the shore due to the utilization by phytoplankton.

Increasing values from the innermost fjord basins towards the outer parts illustrate an increase in the influence of MOM which is mainly controlled by the inflow of Atlantic water and hence by the high supply of marine organisms and the uptake of nitrate by phytoplankton in the euphotic zone of the water column (e.g. Schubert and Calvert, 2001). Observations and the range of $\delta^{15}N_{org}$ values are consistent with previously described analyses by Schubert and Calvert (2001) and Knies et al. (2007) who found $\delta^{15}N_{org}$ values varying from 4.6‰ to 13.1‰, and 4.6‰ to 10.7‰, respectively. Schubert and Calvert (2001) separated the values by their location: Central Arctic Ocean and Yermak Plateau region. Thereby, the values in the Central Arctic Ocean have been found to be higher (7.1‰ – 13.1‰) compared to those from the Plateau region (4.6‰ – 10.7‰). The $\delta^{15}N_{org}$ values of the Central Arctic Ocean are higher than those from the study area (4.69‰ – 6.14‰) which are more in the range of those from the Yermak Plateau region and observations obtained by Knies et al. (2007). This is due to the proximity to the land which is closer in the Yermak region and in the area investigated by Knies et al. (2007) than in the Central Arctic Ocean. Thus, $\delta^{15}N_{org}$ values increase towards the open ocean and reflect the inflow of relatively nutrient- and nitrate-rich Atlantic waters. Schubert and Calvert (2001) found that the significant fraction of variance in the values is caused by changes in nitrate concentrations which further depend on nutrient utilization by phytoplankton (Schubert and Calvert, 2001).

In contrast to Schubert and Calvert (2001) and Knies et al. (2007) who investigated sediment samples from the Central Arctic Ocean and the continental margin off Spitsbergen, the samples of the study area have been taken in fjord environments. Most likely, $\delta^{15}N_{org}$ values of the study

area should reveal lower values compared to the sediments from the continental margin and the Central Arctic Ocean due to their proximity to the shore. However, $\delta^{15}N_{org}$ concentrations in the study area are relatively high due to the extremely high influence of Atlantic water masses and the comparatively low input of terrigenous material. This agrees with observations concerning the C_{org}/N_{org}, $\delta^{13}C_{org}$ and $CaCO_3$ contents (see chapter 5.2.2 and 5.4).

5.2.3.2.2 The Vestfjord

The upwelling areas in the Vestfjord are characterized by relative low $\delta^{15}N_{org}$ values ranging between 5.38‰ and 6.08‰ (stations 35, 36, 37, 38, 41) as illustrated in Fig 35. The values likely are highly influenced by the steady replenishment of nutrient-rich Atlantic water masses which flow into the fjords and pile up in the upwelling area, subsequently increasing the occurrences of marine organisms (Furnes and Sundby, 1981). The high abundance of nutrients is utilized by marine organisms which favour the uptake of ^{14}N and are buried in the sediments afterwards. Lowest $\delta^{15}N_{org}$ values in local upwelling cells are also investigated by Knies et al. (2007) off Spitsbergen who reported that comparatively low nutrient utilization is the main reason for low $\delta^{15}N_{org}$ values in the underlying sediments of the upwelling areas.

The three outermost stations in the Vestfjord (station 31, 32, 33) are characterized by decreasing $\delta^{15}N_{org}$ concentrations with values between 6.63‰ (station 31) and 5.77‰ (station 33) (Appendix Table 2). As these stations are highly influenced by the inflow of Atlantic water and thus by the uptake of nitrate by marine organisms, they commonly should have higher isotopic values. One explanation for the relatively low concentrations is the presence of diagenetic effects within the sediments. These are caused by bacterial degradation while settling in the water column and during early diagenesis in the sediments (Altabet and François, 1994; Freudenthal et al., 2001). During anoxic decay processes, $\delta^{15}N$ values are decreasing due to bacterial growth adding ^{15}N depleted biomass (OM) to the residual material by using soluble nitrogenous compounds (e.g. Wada et al., 1980; Libes and Deuser, 1988; Lehmann et al., 2002).

In addition, it is assumable that the local bathymetry (Fig. 9) at the sample stations influences the OM and $\delta^{15}N_{org}$ values probably due to a decrease in water depth compared to nearby stations and due to possible bathymetric steering and thus an increase in sedimentary erosion and outwashing of finer material. This is consistent with the slightly increasing grain sizes for stations 32 and 33 (Fig. 25, 26) as well as C_{org}/N_{org} and $\delta^{13}C$ which also indicate relative higher contribution of terrigenous material (see chapter 5.2.2.2.3).

All $\delta^{15}N_{org}$ values in the study area are relatively high compared to previous studies (Schubert and Calvert, 2001; Knies et al., 2007) and therefore strongly influenced by the mixing of different species-related MOM sources with increasing values towards the open ocean. The mixing of terrestrial and marine OM is slightly consistent with Peters et al. (1978) who concluded that it is the dominant process that determines $\delta^{15}N$ signatures in coastal sediments leading to values that vary between 4‰ and 8‰. However, the influence of MOM in general is comparatively high compared to the low contribution of terrigenous material which is caused by the high inflow of Atlantic water masses and hence nitrogen uptake by phytoplankton. The more nitrate is utilized by phytoplankton, the higher the values. Furthermore, the input of terrestrial material is strongly restricted by the small drainage area. This is consistent with analyses of N_{tot} and N_{org}, relatively high C_{org}/N_{org} ratios, as well as high $\delta^{13}C_{org}$ signatures for the study area since all parameters show an increased influence in marine derived material. Furthermore, the isotopic nitrogen observations are comparable to $\delta^{15}N$ signatures obtained by Schubert and Calvert (2001) and Knies et al. (2007) who reported similar values. Therefore, the utilization of $\delta^{15}N_{org}$ concentrations from surface sediment samples is another parameter proofing the strong supply of MOM into the sediments of the study area.

5.2.4 Using cross-correlations of organic carbon ($\delta^{13}C_{org}$) with nitrogen ($\delta^{15}N_{org}$) isotopes, and C/N ratios with $\delta^{13}C_{org}$ and $\delta^{15}N_{org}$ to quantify proportions of OM

5.2.4.1 Combining $\delta^{13}C_{org}$ and $\delta^{15}N_{org}$ as a proxy to identify the mixing of TOM and MOM

The correlation of $\delta^{13}C_{org}$ and $\delta^{15}N_{org}$ can be used for evaluating the technique for its ability to identify the marine versus terrigenous sources of the OM (e.g. Wada et al., 1987; Peters et al., 1978). It allows a more definitive assignment to the origin of the MOM than it could be identified by applying the isotopes separately (Peters et al., 1978).

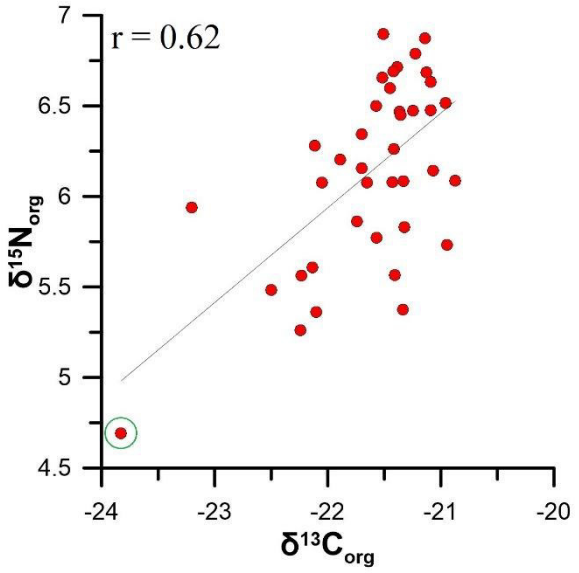

Figure 46: Correlation between stable organic carbon isotopes and stable organic nitrogen isotopes. The green cycle indicates station 24.

The relationship between $\delta^{13}C_{org}$ and $\delta^{15}N_{org}$ is plotted in Figure 46 and presents a relatively weak correlation of r = 0.62 (n = 39). The coherence illustrates a strong mixing of various marine environments with slightly small amounts of terrestrial material. It indicates local differences in nutrient availability and fractionation effects during the fixation of carbon and nitrogen by marine organisms. Although all values are highly influenced by marine material, one sample represents an exception (station 24) (Fig. 46). This sample is located in the inner part of the Tysfjord and represents comparatively low $\delta^{13}C_{org}$ values of -23.83‰ and 4.69‰ for $\delta^{15}N_{org}$ which indicate slightly stronger influences of terrigenous material compared to all other samples. By excluding the values for station 24, the correlation between $\delta^{13}C_{org}$ and $\delta^{15}N_{org}$ gets even weaker with r = 0.47 (n = 38). The value is consistent with the relatively high C_{org}/N_{org} ratio of 9.7 at this station which is the second highest in the entire study area (Appendix Table 2). The relatively higher influence of terrestrial material at this station might be affected by its relative proximity to the mountain range in the south and thus due to short transport distances. Although the sample illustrates stronger terrestrial sediment supply, it is still highly in the range of MOM.

In addition, the plot illustrates that the majority of the values is included into the range for MOM strongly influenced by the presence of nutrient uptake by phytoplankton and thus fractionation processes as marine $\delta^{15}N_{org}$ concentrations are in the range of 4‰ and 8‰ (Peters et al., 1978). Terrestrial derived values would be much lower with values approx. around 0.4‰. Similarly, $\delta^{13}C_{org}$ signatures are also in the range for MOM - these are defined between -20‰

and -22‰ (Meyers, 1994) - whereas TOM has an endmember value of -27‰ (O´Leary, 1981; Meyers, 1994) which is much higher than the values in the study area.

The findings are not consistent with previous studies obtained by Peters et al. (1978), Knies (2005) and Wada et al. (1987a) who concluded that the mixing of terrigenous and marine OM is the dominant process in coastal environments like fjords and strongly is affected by nutrient availability and by the uptake of these nutrients by phytoplankton. However, the sediment samples in the study area are just slightly effected by equal mixing processes as the contribution of MOM strongly dominates the insignificantly small supply of TOM. Therefore, the surface sediment samples of the Vestfjord, Ofotfjord and Tysfjord are different to other fjord systems as they mostly are influenced by marine sources and their characteristic species-related differences.

5.2.4.2 N/C ratios versus $\delta^{13}C$ and $\delta^{15}N$ to classify the values in a range of possible endmembers

Another proxy commonly used to quantify the proportions of marine C_{org} in sediment samples is performed by using the cross-correlation between N_{org}/C_{org} and $\delta^{13}C_{org}$ (e.g. Schubert and Calvert, 2001; Winkelmann and Knies, 2005). The parameters in the graph are normalized to the C_{org} content as the ^{12}C of the $^{13}C/^{12}C$ ratios composes approx. 99% of the C_{org} (Jasper and Gagosian, 1990). By using this relation, it is possible to establish a terrestrial and marine endmember binary system as presented in several previous studies (e.g. Schubert and Calvert, 2001; Winkelmann and Knies, 2005; Knies et al. 2007; and Knies and Martinez, 2009). For mathematical reasons and to reach a graphical linear relation of the values, N_{org}/C_{org} ratios are used instead of C_{org}/N_{org} ratios (Perdue and Koprivnjak, 2007).

The correlation between $\delta^{13}C_{org}$ and N_{org}/C_{org} is presented in Figure 47a and indicates a weak coherence of r = 0.4 (n = 39). As illustrated in the data plot, the composition of the overall OM input into the fjords shows a highly variable pattern leading to the assumption that sedimentation is not consistent with a balanced mixing of MOM produced by primary producers and C_3-photosynthetic TOM. As discussed previously, the admixture of C_4 plants is insignificant for the study area (Collins and Jones, 1986). The imbalance is mainly caused by the predominant high proportion of MOM because terrigenous input is negligible low and hence not represented as a proper endmember in the plot. Proper endmember values would give more insights into the overall sedimentary environment of the terrestrial and marine realm and to distinguish more precisely between those environments. Based on the plot, no real defined

endmember values can be distinguished as reported previously by Schubert and Calvert (2001), Winkelmann and Knies (2005) or Faust et al. (2014a) who all found endmember values within a similar range.

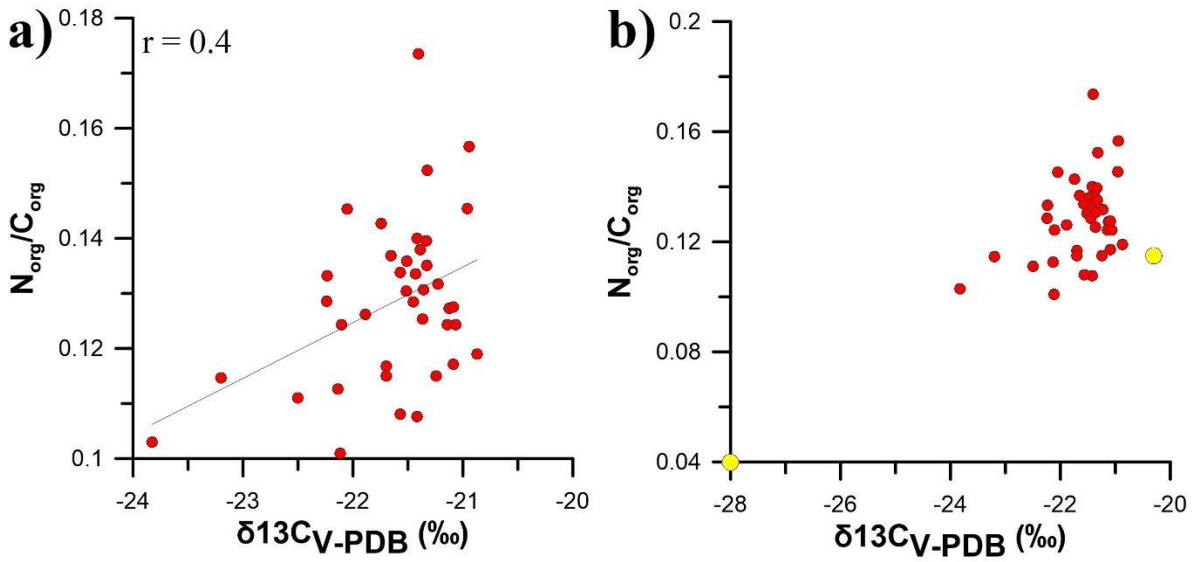

Figure 47: Cross-correlation between a) the N_{org}/C_{org} ratio and the $\delta^{13}C_{org}$ signatures and b) the N_{org}/C_{org} ratio and the $\delta^{13}C_{org}$ signatures including a common terrestrial and marine endmember (Faust et al., 2014a).

By using the terrestrial endmember defined as -28‰ for $\delta^{13}C_{org}$ and 0.04 for the N_{org}/C_{org} ratio and the marine endmember of -20‰ for $\delta^{13}C_{org}$ and 0.12 for N_{org}/C_{org} which were obtained by Faust et al. (2014a), an assumed two-endmember plot can be produced (Fig. 47b). The endmember values of Faust et al. (2014a) are in the range of common endmembers and comparable to Knies (2005), Winkelmann and Knies (2005), and Knies and Martinez (2009). As presented in Figure 47b, it is obvious that all values from the surface sediment samples of this study are highly influenced by marine sources as they are closely located to the common marine endmember obtained by Faust et al. (2014a) for the Trondheimsfjord. However, it is presented that some of the values from the study area are slightly more controlled by terrigenous sources than other values although this happens in a very small range.

For an overall overview of the different marine and terrigenous environments which likely are presented in the study area, a cross-correlation diagram with $\delta^{13}C_{org}$ and $\delta^{15}N_{org}$ values versus C_{org}/N_{org} and N_{org}/C_{org} ratios is shown in Figure 48a and b. Possible endmember values and their ranges are presented in the boxes, whereas the samples of the study area are illustrated by the red dots. Typical endmember values from several studies are presented in Table 2. As illustrated in Figure 48a and b, C_{org}/N_{org}, $\delta^{13}C_{org}$ and $\delta^{15}N_{org}$ from the study area are mostly in the range of freshly deposited MOM indicated by C_{org}/N_{org} ratios of 8-10 (Meyers, 1997). C_{org}/N_{org} ratios in

the study area have an average of 7.88 which is slightly below the values proposed by Meyers (1997). This might be caused by the sample stations in the upwelling areas of the Vestfjord as those values are comparatively lower compared to the remaining values of the Vestfjord, Tysfjord and Ofotfjord area and thus decreasing the entire average values. The lowest value in the upwelling area of the Vestfjord is located at station 35 with C_{org}/N_{org} = 6.4 which is below the range proposed by Meyers (1997) but slightly higher than the values for the phyto- and zooplankton with C_{org}/N_{org} ratios of 4-6 (Meyers, 1997). Therefore, it is assumable that C_{org}/N_{org} ratios in the upwelling areas show the mixing of both marine sources. This mixing might be effected by the upwelling of nutrients and the high amounts of phytoplankton present at this spot depending on parameters like temperature, salinity or light-intensity (e.g. Jasper and Gagosian, 1990).

Table 2: δ13Corg, δ15Norg, and Corg/Norg ratio ranges for different environments and sources of OM including the corresponding references.

Environment/ sources	**$\delta^{13}C$**	**$\delta^{15}N$**	**C_{org}/N_{org}**	**References**
marine phyto- and zooplankton	-22‰ to -19‰	3‰ to 8‰	4 - 6	Meyers 1997
freshly deposited marine OM	-22‰ to -19‰	3‰ to 8‰	8 - 10	Meyers 1997
C3 plants (terrestrial OM)	-32‰ to -26‰	approx. 0.4‰	20 – 50	Meyers 1994, 1997
riverine OM	-35‰ to -25‰	approx. 5‰	11 - 13	Meyers 1997
lacustrine algae	-30‰ to -25‰	approx. 0.4‰	5 - 10	Meyers 1994, 1997

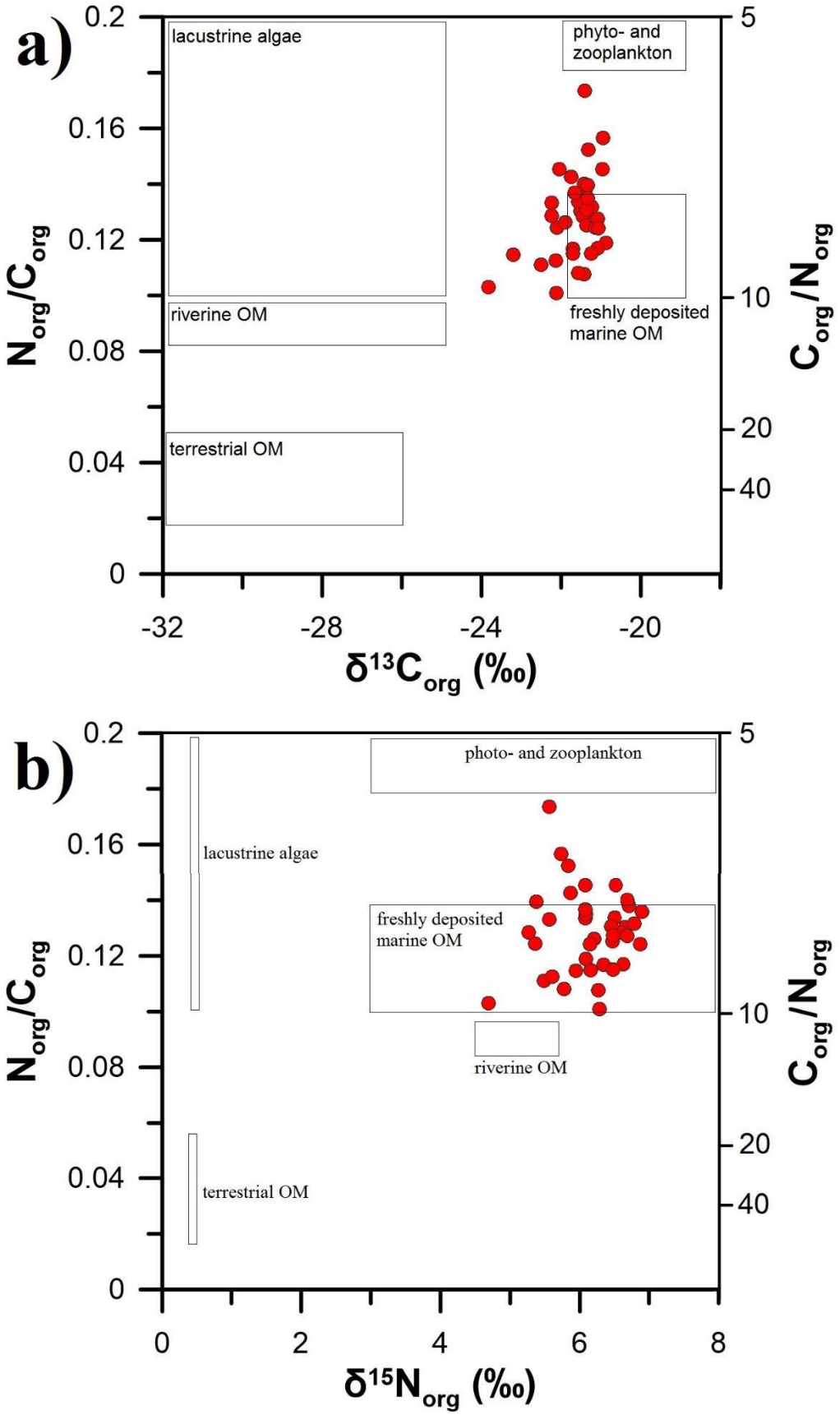

Figure 48: Correlation of a) δ13Corg and b) δ15Norg to Corg/Norg and the inverse Norg/Corg. Possible endmember values and their ranges are presented in the boxes.

The correlations between $\delta^{13}C_{org}$ and $\delta^{15}N_{org}$ versus C_{org}/N_{org} illustrate the dominant proportion of MOM for the surface sediment samples of the entire study area. Most of the sediments are in the range of freshly deposited MOM with weak influence of terrigenous material and phyto- and zooplankton both in the upwelling areas and close to the shorelines of the inner fjord parts in the Ofotfjord and Tysfjord. The observations are consistent with previously presented parameters like $\delta^{13}C_{org}$ and $\delta^{15}N_{org}$ contents, C_{org}/N_{org} ratios, and C_{org} and N_{org} concentrations, which all are highly affected by the contribution of MOM. Due to this high supply of MOM, it is difficult to define an appropriate value for the terrestrial endmember as the samples are just slightly influenced by the input of terrigenous material compared to the marine derived material input. A proper end-member sampling and analysis in more terrestrial derived environments like discharging rivers in the area would have been essential to assign reliable values for terrestrial sources.

5.3 The size of the drainage area as an indicator for the terrestrial sediment supply

The drainage area of the Vestfjord, Ofotfjord, Tysfjord, and tributary fjords has a total extent of 7 118 km^2 (Fig. 8). The drainage area/fjord surface area ratio is calculated as 47.23% for the fjord surface and 52.77% for the land. The catchment area and thus the contribution of terrigenous derived material into the fjords are strongly influenced by the steep mountain ranges of the Lofoten archipelago and by the mountains in the southern parts of the area as size and topography of a drainage area primarily control the sediment discharges of most rivers (Milliman and Syvitski, 1992). The high topographic, mountainous character of the area leads to the inhomogenous distribution of the sediments in the entire area (see chapter 5.1) as effective mixing of source rocks and soils is strongly limited by the short transport distances (Gaillardet et al., 1999). In addition, the catchment area is characterized by several small rivers entering the fjords. In contrast, the Trondheimsfjord drainage area (Fig. 49), for example, is defined by six large rivers entering the fjord (Sakshaug and Sneli, 2000; Faust et al., 2014b). Those rivers are not restricted by such high mountains and hence have relatively long transport distances following in a more distinct distribution pattern with increasing grain sizes from the inner part of the fjord towards the outer part (Faust et al., 2014a).

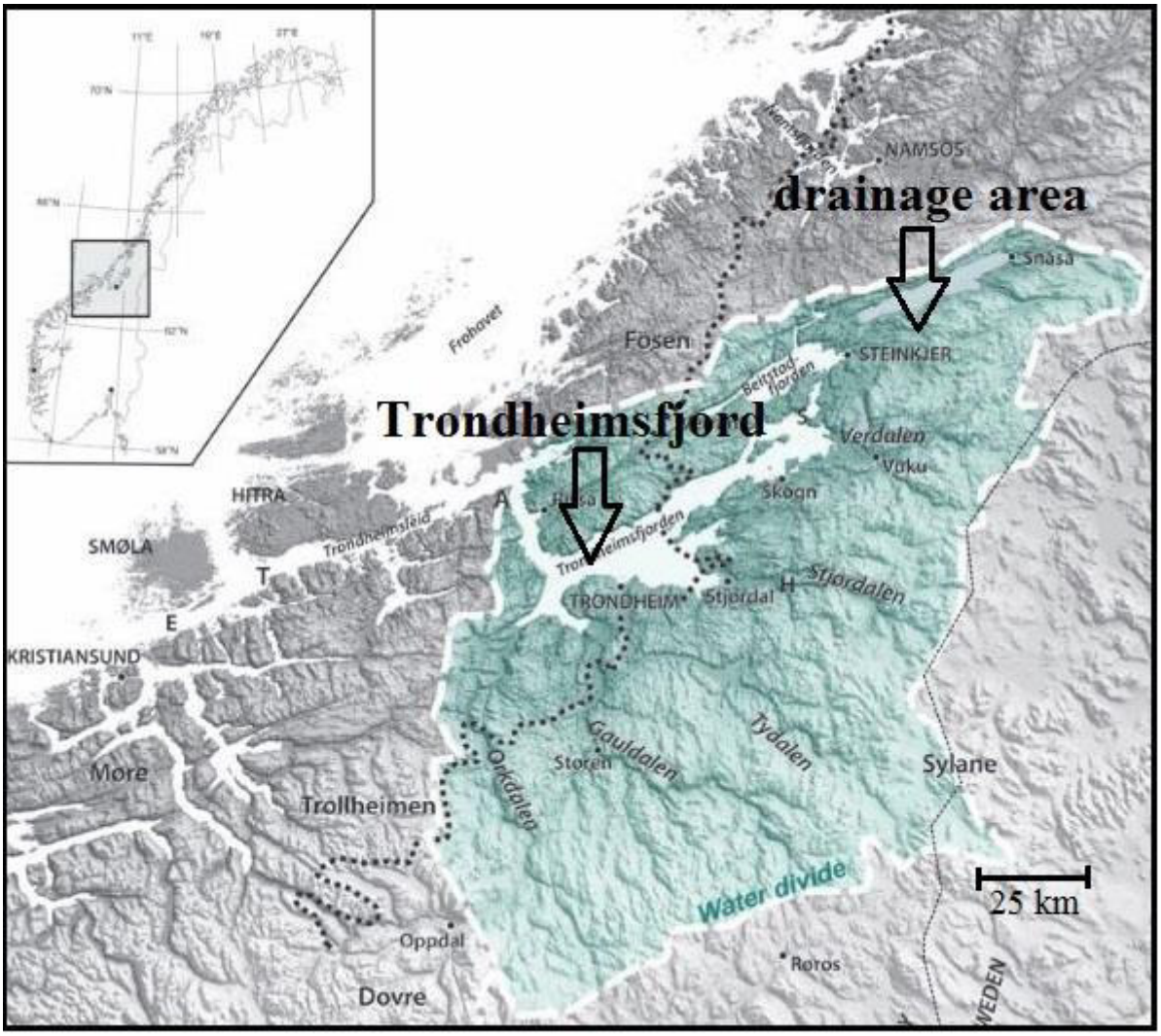

Figure 49: Location and drainage area of the Trondheimsfjord. Modified after Rise et al., 2006.

The drainage area for the Trondheimsfjord has a total extent of 20 000 km^2 (Rise et al., 2006). The size correlates with a drainage area/fjord surface area ratio of 92.9% for the land and 7.1% for the fjord surface. By comparing the Trondheimsfjord and the fjords of the study area with each other, it is evident that the size of the fjord surface area in the study area is relative larger in contrast to its drainage area than the fjord surface area of the Trondheimsfjord compared to its catchment area. The relation between fjord and land area is almost 1:1 in the study area illustrating that the drainage area has nearly the same size as the fjords (Fig. 8). This leads to a relative low contribution of terrigenous material as the high amounts of marine material produced by marine organisms decrease the effect of the terrestrial matter. Thus, terrigenous material has an extraordinary small impact on the general sedimentary content of the surface samples. In contrast, the Trondheimsfjord drainage area/fjord surface area ratio indicates relative higher supply of terrigenous material due to the small proportion of the fjord surface area compared to the catchment area, and hence the relatively small contribution of MOM.

Therefore, terrestrial derived sediment input into the fjords of the study area is comparatively low compared to both - the supply of terrestrial matter into the Trondheimsfjord and the amount of marine derived material that is produced in the fjords of the study area. The observations are consistent with the general relatively small contribution of terrigenous material illustrated by N_{inorg} and the bulk inorganic material as well as by the high amount of MOM shown by C_{org}/N_{org}, $\delta^{13}C_{org}$ and $\delta^{15}N_{org}$ (see chapter 5.2).

The North Atlantic Oscillation (NAO) which describes the most robust periodical mode of atmospheric circulation variability in the North Atlantic region and the Norwegian Atlantic Current (NAC) both have strong influences on the Norwegian coastal climate (e.g. Hurrell, 1995; Dickson et al., 2000). Hurrell (1995) reported an effect of the NAO on the transport and convergence of atmospheric moisture which further can be related to changes in precipitation on land. As the NAO and the inflowing NAC are present at the Norwegian coast and thus also in the fjords of the study area, precipitation, temperatures and wind intensities most likely are effected by variabilities in atmospheric pressure and by the inflowing Atlantic water masses of the NAC and Norwegian Coastal Current (e.g. Hurrell, 1995).

Precipitation in the study area ranges between 855 mm/year for Narvik and 1 500 mm/year for Svolvær (Norwegian Meteorological Institute, 2015) and is responsible for river runoff and hence supply of terrigenous material to the fjords. In addition, annual mean temperatures vary from 3.6°C for Narvik to 4.6°C for Svolvær (Norwegian Meteorological Institute, 2015). Both precipitation and temperatures are in the range of those for the Trondheimsfjord region with annual mean precipitation of 1 100 mm/year and average winter temperatures of -4.6°C (Faust et al., 2014b). Faust et al. (2014b) reported that changes in the regional temperature, precipitation and river runoff are strongly related to variabilities of the NAO. As temperature and precipitation strongly control the intensity of terrigenous weathering and erosion (e.g. Syvitski, 2002), the contribution of terrestrial derived material has been reported to be able to record past NAO changes in the Trondheimsfjord (Faust et al., 2014b). Given the similar characteristics of both areas, the reconstruction would also be possible in the study area by using longer core samples.

In addition, temperature and precipitation of the study area have relatively small values compared to Patagonian fjord systems (Silva et al., 2011; Sepúlveda et al., 2011; Bertrand et al., 2012) where the mean annual precipitation is 3 000 mm/year with a mean annual temperature of 10°C (Sepúlveda et al., 2011). Inner parts of Patagonian fjords are surrounded

by dense vegetation characteristic of cold, wet climate regimes in the form of temperate evergreen forests (e.g. Villagrán, 1988). This also is in contrast to the fjords of the study area, where the vegetation cover is relatively sparse and dominated by periglacial mountain plants (e.g. Vorren and Moe, 1986). Generally, high precipitation and warm temperatures are strongly connected to relative high rates of chemical weathering (Nesbitt et al., 1996). Thus high erosion rates and meltwater discharges in spring and summer lead to the increase of terrigenous sediment supply to river systems and marine environments (e.g. Pollack, 1999).

Therefore, precipitation, temperature and short transport distances in the study area are parameters most likely influencing the terrestrial sediment supply into the fjords (e.g. Hurrell 1995; Syvitski, 2002). This leads to the comparatively weak contribution of the terrigenous fraction as precipitation and temperatures are relative low (Norwegian Meteorological Institute, 2015) and the vegetation cover is sparse compared to other fjord systems (e.g. Sepúlveda et al., 2011). Investigations concerning the precipitation and annual mean temperatures are consistent with the overall low terrestrial sediment supply observed by the contribution of the bulk elemental composition which is extremely low (see chapter 5.1) and by $\delta^{13}C_{org}$, $\delta^{15}N_{org}$, and C_{org}/N_{org} which present an overall high supply of MOM compared to the terrestrial matter. However, size and topography of the drainage area are of more importance controlling sediment discharges than net precipitation and river runoff that play a minor role (Milliman and Syvitski, 1992).

Moreover, the presence of the three main glaciers (Kitjejekna, Storsteinsfjellbre, Frostisen) in the area (Fig. 10) probably could contribute to increased terrestrial sediment supply (e.g. Greve and Blatter, 2009 and references therein). This likely can be illustrated by comparing sample stations from the inner fjord part close to the glaciers (e.g. stations 4, 23, 24, 25) with other inner fjord stations that are located further away from the glaciers. As there is no significant difference in concentrations of the bulk inorganic material, it is assumable that the influence of the glaciers is not significant due to short transport distances and the restricted area of the glaciers.

In summary, the contribution of terrestrial material into the fjords of the study area is relatively small compared to the supply of marine derived material. This may be due to the size and the topography of the drainage area which are most influencing on sediment discharges (Milliman and Syvitski, 1992). Thus transport distances are strongly limited by the mountainous character. Precipitation and temperature are also comparatively low compared to other fjord systems (e.g.

Sepúlveda et al., 2011) leading to decreasing rates of weathering and erosion. However, precipitation, temperatures and river runoff are of minor influence for the sediment supply (Milliman and Syvitski, 1992) as only 52.77% of the area are defined by land compared to 47.23% for the fjord surface area. Hence, the percentage of terrestrial material entering the fjords is decreased compared to the contribution of marine material.

The observations are in contrast to the overall strong mixing between terrestrial and marine sources in coastal environments which has been observed by Peters et al. (1978), Knies (2005), Wada et al. (1987). Moreover, Schubert and Calvert (2001), Winkelmann and Knies (2005), Sepúlveda et al. (2011), Silva et al. (2011), and Faust et al. (2014a/b) reported a relatively balanced contribution of both terrestrial and marine material into sediment samples. This is contrary to the sediment samples of the study area since those are highly dominated by MOM compared to the low contribution of terrigenous material resulting in an imbalanced contribution between marine and terrestrial material.

5.4 Calcium and calcium carbonate: Proxies for marine productivity

Ca distribution follows strongly the spatial distribution of the $CaCO_3$ (Fig. 39, 50) which both illustrate a clear distal to proximal trend with highest values in the outer part of the Vestfjord and decreasing values towards innermost parts of the Ofotfjord and Tysfjord. This demonstrates that both parameters presumable are highly influenced by marine sources. Moreover, $CaCO_3$ and Ca are both inorganic in origin as the $CaCO_3$ is calculated from $CaCO_3 = (C_{tot} - C_{org}) \times 8.33$ which is the C_{inorg}. The correlation between Ca and C_{inorg} confirms this statement due to a correlation coefficient of $r = 0.99$.

The findings are consisting with observations obtained by correlating $CaCO_3$ to elements like Si, Sr, Fe and Al. The different correlations are relatively strong with $r = -0.95$ ($n = 40$) for Al, $r = -0.93$ ($n = 40$) for Si, $r = -0.79$ ($n = 40$) for Fe, and $r = 0.99$ ($n = 40$) for Sr (Fig 51a, b, c, d). As previous discussed in chapter 5.1.2, Al, Fe and Si are strong indicators for terrestrial sources, whereby Sr is an indicator for marine derived material as its distribution is reported to be controlled by the presence of biogenic carbonate minerals (calcite and aragonite) representing the tests of marine organisms like foraminifera and coccoliths (Calvert et al., 1993; Karageorgis et al., 2005). The strong correlation between Sr and Ca (hence $CaCO_3$) is justified by the substitution of Sr and calcite due to strong geochemical similarities (e.g. Shankar et al., 1987).

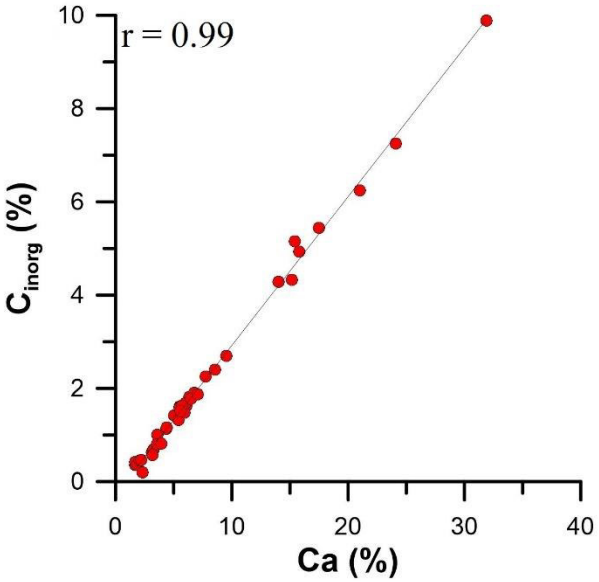

Figure 50: Correlation between calcium and the total inorganic carbon.

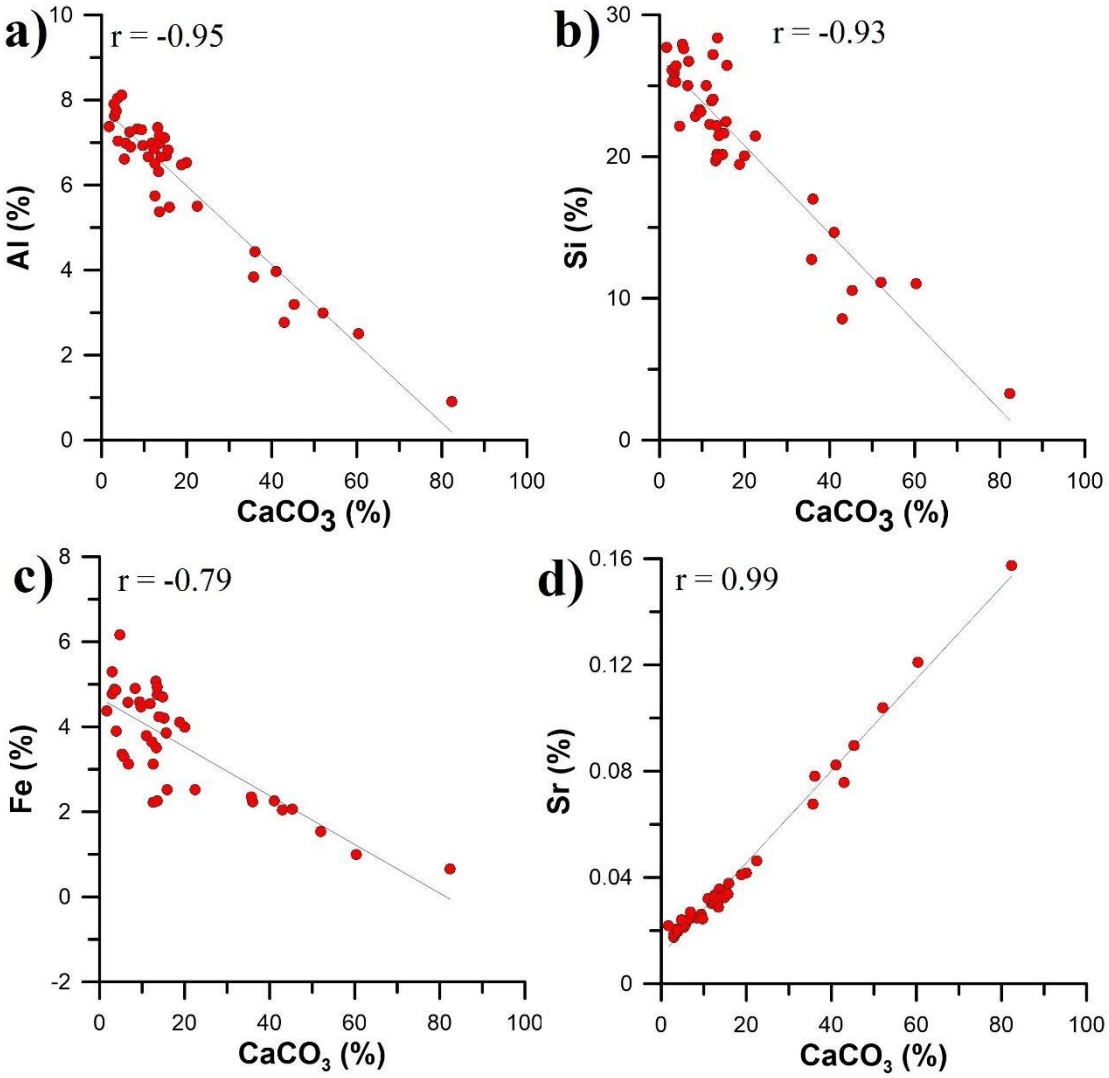

Figure 51: Correlation between $CaCO_3$ and Al (a), Si (b), Fe (c), and Sr (d).

High concentrations of $CaCO_3$ in outer fjord environments and the absence in inner fjord parts (Fig. 39) illustrate that the entire $CaCO_3$ most likely originates from carbonate aquatic productivity. Main contributors of the carbonate might be biogenic shells and shell fragments from diverse marine organisms illustrated by the concentrations of calcite and aragonite (Fig. 19, 21; Appendix Table 4) as similarities are consistent with previous studies of Calvert et al. (1993), Karageorgis et al. (2005), and Faust et al. (2014a) who reported that $CaCO_3$ mainly consists of biogenic shell material. In addition, the distribution of $CaCO_3$ may be used to identify the inflow and the influence of North Atlantic water masses into the fjords as concentrations are decreasing towards the inner fjord parts of the Tysfjord and Ofotfjord (Fig. 39).

Although Ramberg et al. (2008) and Melezhik et al. (2002) reported that calcitic and dolomitic marble are predominant in the Ofotfjord region it is reasonable that these possible Ca sources are insignificant for the composition of the fjord sediments due to the general small contribution of terrestrial material that is strongly diluted by the dominant MOM. The low contribution of terrigenous material and thus of calcium-rich materials is supported by observations concerning the bulk mineral composition (see chapter 5.1) and N_{inorg} (see chapter 5.2.1.2) as well as by the relatively small drainage area compared to the fjord surface area and relatively short sediment transport distances (see chapter 5.3). Although it might be possible that small increases in the distribution for the Ca content are present, it is not visible in the pattern due to the extremely small amounts of terrigenous material in general. However, the overall distribution patterns highly illustrate that Ca and $CaCO_3$ are of marine origin due to the strong gradient with increasing values from the innermost fjords towards the outer fjord parts (Fig. 39). Therefore, terrestrial calcium-bearing sources have no strong influence on Ca and $CaCO_3$ contents and hence most likely are negligible.

The upwelling areas in the central part of the Vestfjord show highest values for both Ca and $CaCO_3$ (up to 44.6% for Ca, and 82.4% for $CaCO_3$) as presented in Appendix Tables 2 and 3. As those comparatively high values are consistent with the high concentrations of aragonite (Fig. 21, 39), the parameters are strongly connected to each other in this area. The amounts of aragonite in the entire study area concentrate on the upwelling areas in the Vestfjord (Fig. 21) with values up to 16%, whereas other fjord parts do not contain any aragonite. As reported in previous studies (e.g. Faust et al., 2014a), the occurrence of aragonite is strongly connected to the distribution of Lophelia pertusa, a deep-water coral that is abundant at the Norwegian coast and in Norwegian fjords (e.g. Fosså et al., 2002). Fosså et al. (2002) present the distribution of

the deep-water coral along the Norwegian coast also with regard to the Vestfjord close to the upwelling areas. Thus, the presence of aragonite can indicate the occurrence of eroded remnants of the deep-water coral Lophelia pertusa.

6 Conclusion

This Master thesis provides an insight into the recent sedimentation patterns in the Vestfjord, Ofotfjord, Tysfjord and tributary fjords in northern Norway. The sedimentary environment is characterized by a strong contribution of MOM in contrast to a relatively small supply of terrestrial derived material. The bulk mineral composition and the grain size fractions are characterized by highly variable distributions probably caused by relatively short sediment transport distances due to the small size and the mountainous character of the drainage area. In addition, the distributions are affected by local and regional differences in the oceanography which strongly depends on differences in current velocities and flow directions, the presence of upwelling areas, local bathymetry, and the inflow of Atlantic water masses. Elemental ratios normalized to Al illustrate that Fe, K, and Si are of terrestrial origin and Ca and Sr presumably are of marine origin. As Al is independent of grain sizes and sensitive to dilution effects, hydrodynamic sorting, and the size of the catchment area, the element cannot be used as a proxy for potential land sources or to track terrestrial sediment supply to the samples.

Marine derived OM dominates the total OM content of the surface sediments. $\delta^{13}C_{org}$ and C_{org}/N_{org} ratios demonstrate an overall dominant influence of MOM due to relatively high $\delta^{13}C_{org}$ values (average -21.62‰) and comparatively low C_{org}/N_{org} ratios (average 7.9). The values correspond with relatively high $\delta^{15}N_{org}$ concentrations (average 6.14‰). All proxies illustrate a predominant high proportion of MOM with decreasing values from the outermost part of the Vestfjord towards inner fjord parts of the Ofotfjord and Tysfjord. In addition, $\delta^{15}N_{org}$ reflects the inflow of Atlantic water masses into the fjords.

The correlation between $\delta^{13}C_{org}$ and N_{org}/C_{org} also demonstrates the predominance of MOM. The weak correlation and highly variable values indicate that sedimentation is not characterized by a balanced mixing between both MOM produced by primary producers and C_3-photosynthetic TOM. Instead, it shows that the material is dominated by marine derived sources which dilute the insignificant small supply of terrigenous material. The weak correlation further is affected by species-related characteristics of marine organisms that cause differences in fractionation and uptake of nutrients in the water column and strongly influence the supply of MOM. The observations are consistent with correlations between $\delta^{13}C_{org}$ and $\delta^{15}N_{org}$ versus C_{org}/N_{org} indicating that the dominant proportion of the sediments is in the range of freshly deposited MOM and just slightly affected by terrestrial sources.

The land area/fjord surface area ratio is 1:1 for the study area which illustrates that the drainage area has a similar size like the fjord surfaces resulting in a relatively low proportion of the drainage area compared to the total area and compared to other fjord systems with a relatively larger land area in contrast to their fjord surface area. This leads to the comparatively low supply of terrestrial derived material into the sediments which is in contrast to the high concentrations of MOM. The dominant contribution of MOM dilutes the insignificantly small amount of terrestrial material. In addition, the relatively small drainage area and its mountainous character mainly control the short sediment transport distances and the relatively low contribution of terrestrial material into the fjords. Precipitation, temperatures, and wind intensities are influenced by variabilities in atmospheric circulation patterns and oceanic currents entering the fjords which results in comparatively weak rates of weathering and erosion in the drainage area leading as well to the small supply of terrestrial matter.

The high occurrences of primary productivity also show that MOM is dominant in the fjords as it is proportional to the presence of nutrients in the water column and the inflow of nutrient-rich Atlantic water masses. Plankton blooms occur frequently which increases the supply of MOM buried in the sediments. Especially in the upwelling areas in the central part of the Vestfjord, primary productivity leads to relatively high nutrient utilization (high $\delta^{15}N$) causing heavier $\delta^{13}C_{org}$ values. Furthermore, $CaCO_3$ is a good proxy for marine biogenic carbonate productivity which is the main $CaCO_3$ source.

All investigated parameters are affected by local characteristics of the bathymetry and oceanography. Coastal upwelling occurs in the central part of the Vestfjord and results in the increase of MOM since nutrient-rich deep water masses pile up and support the growth of primary producers. NE and SW wind patterns and frequently occurring eddies affect the inflow of Atlantic water masses and the availability of marine organisms which further influence carbon and nitrogen concentrations within the water column and the sediments due to fractionation processes and the uptake of nutrients by marine organisms.

The overall dominant contribution of MOM compared to the small amount of terrestrial derived material in the study area is in contrast to previous studies who reported a relatively balanced mixing of both allochthonous and autochthonous sources and the input of this material to marine sediments. Therefore, the sediment content indicates an imbalance in the supply of marine and terrestrial material that results in the predominance of MOM in the entire study area.

7 Outlook

This Master thesis provides an overview of inorganic and organic environmental processes in the Vestfjord, Ofotfjord, and Tysfjord fjord system in northern Norway. The obtained data may be used for further investigations concerning the general understanding of coastal environments and their interaction with the land. Investigations may provide deeper insights into carbon and nitrogen cycling and may help to identify past environmental and climatic processes as well as to predict future environmental processes concerning the fjords on a regional and global scale.

Detailed investigations regarding riverine sediment transporting and proper terrestrial end-member values (e.g. Sepúlveda et al., 2011; Bertrand et al., 2012; Faust et al., 2014a) might be assignable by using a wider range of sample stations with special regard to terrestrial sources and transport systems. Estimated terrestrial and marine endmember values and the results of this thesis in combination with analyses concerning other fjord systems could be used for establishing a global database which could reveal differences and similarities in these fjord systems from high-latitude regions with individual environmental settings. Comparisons could intensify analyses of the interaction between the Earth´s oceans, coastal environments and terrestrial landscapes as well as source-to-sink characteristics, transport mechanisms, and influencing parameters. Intensive source-to-sink analyses would help to identify response times of numerous proxies and thus provide better appreciation of seasonal variations in material supply (e.g. Faust et al., 2014b).

The North Atlantic Oscillation, the Norwegian Atlantic Current, and the Norwegian Coastal Current influence the Norwegian coastal climate and control the amount of precipitation, temperature, and wind intensity variabilities (Hurrell, 1995; Dickson et al., 2000). By analysing long sediment cores from the study area, the parameters contain information regarding environmental changes in the hinterland and oceanographic variability (e.g. Syvitski and Schafter, 1985). They could help to reveal a better understanding of past climate and environmental processes and to predict future climate change. Moreover, sedimentation rates could be used to identify local responses to short-term variabilities in the global climate and give insights into past climate conditions as parameters like the bulk inorganic composition, C/N ratios, $\delta^{13}C_{org}$, and $\delta^{15}N$ strongly are influenced by those climatic conditions and can illustrate changes by variabilities in their values.

Additional investigations concerning the OM in the study area might help to reconstruct sources in a detailed manner and to give further insights into the proportions of terrestrial versus marine

material. Analyses could be intensified by investigating biomarkers as for example long-chain alkenones (e.g. Eglinton and Eglinton, 2008) or steroids which are widespread in planktonic organisms (Hudson et al., 2001). N-alkanes, alkenones, and sterols may also be investigated as reliable data for MOM (e.g. Knies, 2005; Sepúlveda et al., 2011). A detailed identification of proportions of cod eggs and marine organisms in the water column and within the sediments could reveal more information about the influence of primary productivity with special regard to differences between benthic and planktic phytoplankton, and cod spawning grounds in the fjords (e.g. Sundby and Solemdal, 1984). Furthermore, it would be helpful to analyse the $CaCO_3$ production in the water column and buried sediments (e.g. Vorren and Plassen, 2002) as well as the relationship between surface nutrient utilization of dissolved nitrate (NO_3^-) and the sedimentary $\delta^{15}N$ (Altabet and François, 1994).

The comprehension of global burial processes and the role of the fjord as a potential storage site for carbon and nitrogen is indispensable for understanding past and future climate changes. The analysis of carbon and nitrogen accumulation and storage rates in sediments from coastal environments might therefore also help to give detailed insight into environmental processes.

8 References

Altabet, M.A., and R. Francois, 1994, Sedimentary nitrogen isotopic ratio as a recorder for surface ocean nitrate utilization, *Global Biogeochemistry Cycles*, 8, 103-116.

Altabet, M.A., R. Francois, D.W. Murray, and W.L. Prell, 1995, Climate-related variations in denitrification in the Arabian Sea from sediment 15N/14N ratios, *Nature*, 373, 506-509, doi: 10.1038/373506a0.

American Meteorological Societey, 2005:http://oceanmotion.org/html/background/upwelling-and-downwelling.htm (Accessed December 4th 2015)

Asplin, L., A.G.V. Salvanes, and J.B. Kristoffersen, 1999, Nonlocal wind-drinven fjord-coast advection and its potential effect on plankton and fish recruitment, *Fisheries Oceanography*, 8 (4), 255-263.

Atlas.nve.no: http://atlas.nve.no (Accessed January 14th 2016)

Bennet, M.R., 2003, Ice streams as the arteries of an ice sheet: Teir mechanics, stability and significance, *Earth-Science Reviews*, 61, 309-339, doi: 10.1016/S0012-8252(02)00130-7.

Bertrand, S., K.A. Hughen, J. Sepulveda, S. Pantoja, 2012, Geochemistry of surface sediments from the fjords of Northern Chilean Patagonia (44-47°S): spatial variability and implications for paleoclimate reconstructions, *Geochimica et Cosmochimica Acta*, 76, 125-146.

Bordovskiy, O.K., 1965, Sources of organic matter in marine basins, *Marine Geology*, 3, 5–31.

Broecker W.S., and E. Maier-Reimer, 1992, The influence of air and sea exchange on the carbon isotope distribution in the sea, *Global Biogeochemical Cycles*, 6 (3), 315-320.

Calvert, S.E., 1976, The mineralogy and geochemistry of near-shore sediments, *Chemical Oceanography*, ed. J.P. Riley, and R. Chester, London New York San Francisco.

Calvert, S.E., B. Nielsen, and M.R. Fontugne, 1992, Evidence from nitrogen isotope ratios for enhanced productivity during formation of eastern Mediterranean sapropels, *Nature*, 359, 223-225, doi: 10.1038/359223a0.

Calvert, S.E., T.F. Pedersen, and R.C. Thunell, 1993, Geochemistry of the surface sediments of the Sulu and South China Seas, *Marine Geology*, 114 (3-4), 217-231.

Canals, M., G. Lastras, R. Urgeles, J.L. Casamor, J. Mienert, A. Cattaneo, M. De Batist, H. Haflidason, Y. Imbo, J.S. Laberg, J. Locat, D. Long, O. Longva, D.G. Masson, N. Sultan, F. Trincardi, and P. Bryn, 2004, Slope failure dynamics and impacts from seafloor and shallow sub-seafloor geophysical data: case studies from the COSTA project, *Marine Geology*, 213 (1-4), 9-72.

Cho, Y.-G., C.-B. Lee, M.-S. Choi, 1999, Geochemistry of surface sediments off the southern and western coasts of Korea, *Marine Geology*, 159, 111–129.

Collins, R.P., and M.B. Jones, 1985, The influence of climatic factors on the distribution of C4 species in Europe, *Vegetatio,* 64 (2), 121-129.

Craig, H., 1957, Isotopic standards for carbon and oxygen and correction factors for mass-spectrometry analysis of carbon dioxide, *Geochimica et Cosmochimica Acta*, 12, 133-149.

Culbertson, D.M., L.E. Young, and J.C. Brice, 1967. Scour and fill in alluvial channels with particular reference to bridge sites. U.S. Geological Survey, *Open File Report*, 58.

Dahlgren, K.I.T., and T. Vorren, 2003, Sedimentary environment and glacial history during the last 40 ka of the Vøring continental margin, mid-Norway. *Marine Geology*, 193, 93–127.

Dickson, R.R., T.J. Osborn, J.W. Hurrell, J. Meincke, J. Blindheim, B. Adlandsvik, T. Vinje, G. Alekseev, and W. Maslowski, 2000, The Arctic Ocean response to the North Atlantic Oscillation, *Journal of Climate*, 13, 2671-2696.

Domack, W., and C.E. McClennen, 1996, Accumulation of glacial marine sediments in fjords of the Antarctic peninsula and their use as late Holocene paleoenvironmental indicatiors, Foundations for ecological research west of the Antarctic peninsula, *Antarctic research series*, 70, 135-154.

Dowdeswell, J.A., A. Elverhvi, and R. Spielhagen, 1998, Glacimarine sedimentary processes and facies on the polar north Atlantic margin, *Quaternary Science Reviews*, 17, 243-272.

Ellertsen, 1993, Spring blooms and stratification, Nature, 363, 24, doi: 10.1038/363024a0.

Eilertsen, H.C., and J.P. Taasen, 1984, Investigations on the plankton community of Balsfjorden, Northern Norway. The phytoplankton 1976–1978. Environmental factors, dynamics of growth, and primary production, Sarsia, 69 (1), 1-15, doi: 10.1080/00364827.1984.10420584.

Eggvin J., 1931, Litt om Vestfjordens vannmasser in skreitiden, Arsberetning vedr rende Norges Fiskerier.

Eglinton, T.I, and G. Eglinton, 2008, Molecular proxies for paleoclimatology, *Earth and Planetary Science Letters*, 275, 1-16.

Ellertsen, B., G.K. Furnes, P. Solemdal, and S. Sundby, 1981, Influence of wind induced currents on the distribution of cod eggs and zooplankton in Vestfjorden. *Proceedings from the Norwegian Coastal Current Symposium*, Geilo, Norway, 9-12 Sep. 1980, University of Bergen: 604-629.

Faust J.C., J. Knies, T. Slagstad, C. Vogt, G. Milzer, and J. Giraudeau, 2014a, Geochemical composition of Trondheimsfjord surface sediments: Sources and spatial variability of marine and terrigenous components, *Continental Shelf Research*, doi: 10.1016/j.csr.2014.07.008.

Faust, J.C., J. Knies, G. Milzer, and J. Giraudeau, 2014b, Terrigenous input to a fjord in central Norway records the environmental response to the North Atlantic Oscillation over the past 50 years, *The Holocene*, 1-8, doi: 10.1177/0959683614544052.

Farrell, J.W., T.F. Pedersen, S.E. Calvert, and B. Nielsen, 1995, Glacial-interglacial changes in nutrient utilization in the equatorial Pacific Ocean, Nature, 377, 514-517.

Fjeldskaar, W., 1994, Viscosity and thickness of the asthenosphere detected from the Fennoscandian uplift, *Earth and Planetary Science Letters* 126, 399-410.

Fisher, A.G.B., (1939), Production, primary, secondary and tertiary*, Economic Record*, 15 (1), 24-38.

Fløistad, K.R., J.S. Laberg, and T.O. Vorren, (2009), Morphology of Younger Dryas subglacial and ice-proximal submarine landforms, inner Vestfjorden, northern Norway, *Boreas*, 38 (3), 610-619.

Fosså, J.H., P.B. Mortensen, and D.M. Furevik, 2002, The deep-water coral Lophelia pertusa in Norwegian waters: distribution and fishery impacts, *Hydrobiologia*, 471 (1), 1-12, doi: 10.1023/A:1016504430684.

Freudenthal, T., T. Wagner, F. Wenzhöfer, M. Zabel, and G. Wefer, 2001, Early diagenesis of organic matter from sediments of the eastern subtropical Atlantic: evidence from stable nitrogen and carbon isotopes, Geochimica et Cosmochimica Acta, 65 (11), 1795-1808, doi: 10.1016/S0016-7037(01)00554-3.

Furnes and Sundby, 1981, Upwelling and wind induced circulation in Vestfjorden, The Norwegian Coastal Current.

Gaillardet, J., B. Dupré, and C.J. Allègre, 1999, Geochemistry of large river suspended sediments: Silicate weathering or recycling tracer? *Geochimica et Cosmochimica Acta*, 63 (23/24), 4037-4051.

Geddes, N.R., J.C. Scott, 1994, ROCKY WATER 93/6 Detailed ocean structure for the Vestfjord and adjacent regions, *Defence Research Agency Report* DRA/US/USSF/TM94021/1.0, 169.

Gedney, N., P.M. Cox, R.A. Betts, O. Boucher, C. Huntingford, and P.A. Stott, 2006, Detection of a direct carbon dioxide effect in continental river runoff records, *Nature*, 439, 835-838, doi: 10.1038/nature04504.

Gjevik, B., H. Moe, and A. Ommundsen, 1997, Sources of the Maelstrom, *Nature*, 388, 837–838.

Goñi, M.A., K.C. Ruttenberg, and T.I. Eglinton, 1997, Sources and contribution of terrigenous organic carbon to surface sediments in the Gulf of Mexico, *Nature,* 389, 275–278.

Govin, A., U. Holzwarth, D. Heslop, L. Ford Keeling, M. Zabel, S. Mulitza, J.-A. Collins, and C.M. Chiessi, 2012, Distribution of major elements in Atlantic surface sediments (36°N–49°S): Imprint of terrigenous input and continental weathering, *Geochemistry Geophysics Geosystems*, 13.

Greve, R., and H. Blatter, 2009, Dynamics of Ice Sheets and Glaciers, Springer, Berlin Heidelberg, doi: 10.1007/978-3-642-03415-2.

Hambrey, M., 1994, Glacial environments, UCL Press Limited, Vancouver

Haug, G.H., T.F. Pedersen, D.M. Sigman, S.E. Calvert, B. Nielsen, and L.C. Peterson, 1998, Glacial/interglacial variations in production and nitrogen fixation in the Cariaco Basin during the last 580 kyr, *Paleoceanography*, 13 (5), 427-432.

Haug, G.H., K.A. Hughen, D.M Sigman, L.C. Peterson, and U. Röhl, 2001, Southward migration of the intertropical convergence zone through the Holocene, Science, 293, 1304-1308.

Hayes, J.M., 1993, Factors controlling 13C contents of sedimentary organic compounds: principles and evidence. *Marine Geology*, 113, 111–125.

Hedges, J.I., R.G. Keil, 1995, Sedimentary organic matter preservation: an assessment and speculative synthesis, Marine Chemistry, 49 (2-3), 81-115, doi: 10.1016/0304-4203(95)00008-F.

Hedges, J.I., R.G. Keil, and R. Benner, 1997, What happens to terrestrial organic matter in the ocean? *Organic Geochemistry,* 27, 195–212.

Hoefs, J., 2009, Theoretical and experimental principles, Stable Isotope Geochemistry, Springer, 1-33.

Holtedahl, H., 1975, The geology of the Hardangerfjord, West Norway: *NGU Publikasjon*, 323, 87.

Hoskin, C.M., D.C. Burrell, and G.R. Freitag, 1978, Suspended sediment dynamics in Blue Fjord, Western Prince William Sound, Alaska, *Estuarine and Coastal marine Science,* 7, 1-16.

Howe, J.A., W.E.N. Austin, M. Forwick, M. Paetzel, R. Harland, A.G. Cage, 2010, Fjord Systems and Archives: A Review, 344, *Geological Society*, Special Publications, London, 5-15.

Hudson, E.D., C.C. Parrish, and R.J. Helleur, 2001, Biogeochemistry of sterols in plankton, settling particles and recent sediments in a cold ocean ecosystems (Trinity Bay, Newfoundland), *Marine Chemistry*, 76, 253-270.

Hurrell, J.W., 1995, Decadal trends in the North Atlantic Oscillation: Regional temperatures and precipitation, *Science*, 269 (5224), 676-679.

Jacobson, P., 1983, Physical oceanography of the Trondheimsfjord, *Geophysical and Astrophysical Fluid Dynamics*, 26, 3-26.

Jasper, J.P., and R.B. Gagosian, 1990, The sources and deposition of organic matter in the Late Quaternary Pigmy Basin, Gulf of Mexico. *Geochimica et Cosmochimica Acta*, 54, 1117–1132.

Jones, B., S. Boudjelas, E.G. Mitchelson-Jacob, 1997, Topographic steering of winds in Vestfjorden, Norway, *Weather*, 52 (10), 304–311.

Karageorgis, A.P., C.L. Anagnostou, and H. Kaberi, 2005, Geochemistry and mineralogy of the NW Aegean Seasurface sediments: implications for river runoff and anthropogenic impact, *Applied Geochemistry*, 20, 69–88.

Knies, J., 2005, Climate-induced changes in sedimentary regimes for organic matter supply on the continental shelf off northern Norway, *Geochimica et Cosmochimica Acta*, 69, 4631–4647.

Knies, J., S. Brookes, and C.J. Schubert, 2007, Re-assessing the nitrogen signal in continental margin sediments: New insights from the high northern latitudes. *Earth Planet*, Scientific Letters, 253, 471–484.

Knies, J., P. Martinez, 2009, Organic matter sedimentation in the western Barents Sea region: terrestrial and marine contribution based on isotopic composition and organic nitrogen content, *Norsk Geologisk Tidskrift*, 89, 79–89.

Laberg, J.S., T.O. Vorren, J. Mienert, D. Evans, B. Lindberg, D. Ottesen, N.H. Kenyon, and S. Henriksen, 2002a, Late Quaternary palaeoenvironment and chronology in the Trænadjupet Slide area offshore Norway. *Marine Geology*, 188, 35–60.

Laberg, J.S., T.O. Vorren, and S.-M. Knutsen, 2002b, The Lofoten Drift, Norwegian Sea, *in* Stow, D.A.W., Pudsey, C.J., Howe, J.A., Faugeres, J.-C., and Viana, A., eds., Deep-Water Contourite Systems: Modern Drifts and Ancient Series, Seismic and Sedimentary Characteristics: Geological Society of London Memoir 22, p. 57–64.

Laberg, J.S., R.S. Eilertsen, G.R. Salomonsen, and T.O. Vorren, 2007, Submarine push moraine formation during the early Fennoscandian Ice-Sheet deglaciation, Quaternary Research, 76, 453-462.

Laberg, J.S., R.S. Eilertsen, and T.O. Vorren, 2009, The paleo-ice stream in Vestfjorden, north Norway, over the last 35 k.y.: Glacial erosion and sediment yield, *Geological Society of America Bulletin*, 121 (3/4), 434-447.

Lange de, G.J., B. Van Os, P.A. Pruysers, J.J. Middelburg, D. Castradori, P. Van Santvoort, P.J. Müller, H. Eggenkamp, and F.G. Prahl, Possible Early Diagenetic Alteration of Paleo Proxies, in: Carbon Cycling in the Global Ocean: Constraints on the Ocean´s Role in Global Climate, 1994, 17, 225-258.

Lehmann, M.F., S.M. Bernasconi, A. Barbieri, and J.A. McKenzie, 2002, Preservation of organic matter and alteration of its carbon and nitrogen isotope composition during simulated and in situ early sedimentary diagenesis, *Geochimica et Cosmochimica Acta*, 66 (20), 3573-3584.

Libes, S.M., and W.G. Deuser, 1988, The isotope geochemistry of particulate nitrogen in the Peru upwelling area and the Gulf of Maine, *Deep Sea Research Part A*, 35 (4), 517-533.

Mariotti, A., 1983, Atmospheric nitrogen is a reliable standard for natural 15N abundance measurements, *Nature*, 303, 5919, 685-687.

Mariotti, A., F. Gadel, P. Giresse, and Kinga-Mouzeo, 1991, Carbon isotope composition and geochemistry of particulate organic matter in the Congo River (Central Africa): Application to the study of Quaternary sediments off the mouth of the river, *Chemical Geology: Isotope Geoscience section*, 86 (4), 345-357, doi: 10.1016/0168-9622(91)90016-P.

Martinez, P., P. Bertrand, G.B. Shimmield, C. Karen, F.J. Jorissen, J. Foster, and M. Dignan, 1999, Upwelling intensity and ocean productivity changes off Cape Blanc (northwest Africa) during the last 70,000 years: geochemical and micro-paleontological evidence, *Marine Geology*, 158, 57-74.

Melezhik, V.A., D. Robert, I.M. Gorokhov, A.E. Fallick, K.B. Zwaan, A.B. Kuznetsov, B.G. Pokrovsky, 2002, Isotopic evidence for a complex Neoproterozoic to Silurian rock assemblage in the North-Central Norwegian Caledonides. *Precambrian Research*, 114, 55–86.

Meyers, P.A., 1994, Preservation of elemental and isotopic source identification of sedimentary organic matter, *Chemical Geology*, 114, 289-302.

Meyers P.A., 1997, Organic geochemical proxies of paleoceanographic, paleolimnologic, and paleoclimatic processes, *Organic Geochemistry*, 27, 213-250.

Meyers, P.A., and J.L. Teranes, 2002, Sediment organic matter, *Developments in Paleoenvironmental Research*, 2, 239-269.

Milliman, J.D., and P.M. Syvitski, Geomorphic/Tectonic Control of Sediment Discharge to the Ocean: The Importance of Small Mountainous Rivers, *The Journal of Geology*, 100 (5), 525-544.

Mitchelson-Jacob, G., and S. Sundby, 2001, Eddies of Vestfjorden, Norway, *Continental Shelf Research*, 21 (16-17), 1901-1918.

Müller, P.J., 1977, C/N ratios in Pacific deep-sea sediments: Effect of inorganic ammonium and organic nitrogen compounds sorbed by clays, *Geochimica et Cosmochimica Acta*, 41, 765-776.

Muzuka, A.N.N., 1999, Isotopic compositions of tropical East African flora and their potential as source indicators of organic matter in coastal marine sediments, *Journal of Africal Earth Sciences*, 28 (3), 757-766, doi: 10.1016/S0899-5362(99)00044-5.

Nesbitt, H.W., G.M. Young, S.M. Lennan, and R.R. Keays, 1996, Effects of chemical weathering and sorting on petrogenesis of siliciclastic sediments, with implications for provenance studies, *Journal of Geology*, 104, 525-542.

Norwegian Institute of Marine Research, 2015: http://www.imr.no/forskning/forskningsdata/stasjoner/view?station=Skrova (Accessed November 20th 2015)

Norwegian Meteorological Institute: http://met.no/Klima/Klimastatistikk/Klimadata/ (Accessed November 28th 2015)

O´Leary, M.H., 1981, Carbon isotope fractionation in plants, *Phytochemistry*, 20 (4), 553-567.

Ostrom, N.E., S.A. Macko, D. Deibel, and R.J. Thompson, 1997, Seasonal variation in the stable carbon and nitrogen isotope biogeochemistry of a coastal cold ocean environment, *Geochimica et Cosmochimica Acta*, 61 (14), 2929-2942, doi: 10.1016/S0016-7037(97)00131-2.

Ottesen, D., J.A. Dowdeswell, and L. Rise, 2005a, Submarine landforms and the reconstruction of fast-flowing ice streams within a large Quaternary ice sheet: the 2,500 km-long Norwegian–Svalbard margin (57°N to 80°N), *Geol. Soc. Amer. Bull.* 117, 1033–1050.

Ottesen, D., L. Rise, J. Knies, L. Olsen, and S. Henriksen, 2005b, The Vestfjorden-Trænadjupet palaeo-ice stream drainage system, mid-Norwegian continental shelf, *Marine Geology*, 218 (1-4), 175-189, doi: 10.1016/j.margeo.2005.03.001.

Perdue, E.M., and J.-F. Koprivnjak, 2007, Using the C/N ratio to estimate terrigenous inputs of organic matter to aquatic environments, *Estuarine, Coastal and Shelf Science,* 73, 65-72.

Peters, K.E., R.E. Sweeney, and I.R. Kaplan, 1978, Correlation of carbon and nitrogen stable isotope ratios in sedimentary organic matter, *Limnology and Oceanography*, 23 (4), 598-604.

Pollack, J.M., 1961, Significance of compositional and textural properties of South Canadian River channel sands, New Mexico, Texas, and Oklahoma, *Journal of Sedimentary Petrology*, 31, 15-37.

Price, J.F., R.A. Weller, and R.R. Schudlich, 1987, Wind-driven ocean currents and Ekman transport, *Science*, 238, 1534-1538.

Ramberg, I.B., I. Bryhni, A. Nøttvedt, and K. Rangnes, 2008, The Making of a Land: Geology of Norway, *Geological Society of London*.

Rise, L., R. Bøe, H. Sveian, A. Lysså, and H.A. Olsen, 2006, The deglaciation history of Trondheimsfjorden and Trondheimsleia, Central Norway, *Norw J Geol* 86, 415-434.

Rokoengen, K., and J. Sættem, 1983, Shallow bedrock geology and Quaternary thickness off Northern Helgeland, Vestfjorden and Lofoten. *Continental Shelf Institute report* P-155/2/83.

Rundel, P.W., J.R. Ehleringer, and K.A. Nagy, 1989, Stable Isotopes in Ecological Research, 68, Springer-Verlag, New York Inc.

Sacket, W.M., 1964, The depositional history and isotopic organic carbon composition of marine sediments, *Marine Geology*, 2 (3), 173-185, doi: 10.1016/0025-3227(64)90038-6.

Sakshaug, E., Sneli, J.-A., 2000. Trondheimsfjorden. Tapir Forlag, Trondheim

Schubert, C.J., and S.E. Calvert, 2001, Nitrogen and carbon isotopic composition of marine and terrestrial organic matter in Arctic Ocean sediments: implications for nutrient utilization and organic matter composition, *Deep Sea Research Part I: Oceanographic Research Papers*, 48 (3), 789-810, doi: 10.1016/S0967-0637(00)00069-8.

Schwartz, D., A. Mariotti, R. Lanfranchi, and B. Gulliet, 1986, $^{13}C/^{12}C$ Ratios of soil organic matter as indicators of vegetation changes in the Congo, *Geoderma*, 39 (2), 97-103, doi: 10.1016/0016-7061(86)90069-8.

Sciencenotes.org: http://sciencenotes.org/printable-periodic-table/ (Accessed April 17th 2016)

Sepúlveda, J., S. Pantoja, and K.A. Hughen, 2011, Sources and distribution of organic matter in northern Patagonia fjords, Chile (44-47°S): A multi-tracer approach for carbon cycling assessment, Continental Shelf Research, 31, 315-329.

Sejrup, H.P., H. Haflidason, I. Aarseth, C.F. Forsberg, E. King, D. Long, and K. Rokoengen, 1994, Late Weichselian glaciation history of the northern North Sea, *Boreas* 23, 1–13.

Sejrup, H.P., E. Larsen, H. Haflidason, I.M. Berstad, B.O. Hjelstuen, H. Jonsdottir, E.L. King, J. Landvik, O. Longva, A. Nygard, D. Ottesen, S. Raunholm, L. Rise, and K. Stalsberg, 2003, Configuration, history and impact of the Norwegian Channel Ice Stream. *Boreas* 32, 18–36.

Shankar, R., K.V. Subbarao, and V. Kolla, 1987, Geochemistry of surface sediments from the Arabian Sea, *Marine Geology*, 76, 253-279, doi: 10.1016/0025-3227(87)90033-8.

Shimmield, G.B., 1992, Can sediment geochemistry record changes in coastal upwelling palaeoproductivity? Evidence from Northwest Africa and the Arabian Sea, 64, *Geological Society, Special Publications,* London, 29-46.

Silva J.A., and J.M. Bremner, 1966, Determination and isotope-ratio analysis of different forms of nitrogen in soils: 5. Fixed ammonium, *Soil Science Society of America*, 30 (5), 587-594, doi: 10.2136/sssaj1966.03615995003000050017x.

Silva, N., C.A. Vargas, and R. Prego, 2011, Land–ocean distribution of allochthonous organic matter in surface sediments of the Chiloé and Aysén interior seas (Chilean Northern Patagonia). *Continental Shelf Research,* 31, 330–339, doi: 10.1016/j.csr.2010.09.009.

Skei, J., (1983), Why sedimentologists are interested in fjords, *Sedimentary Geology*, 36 (2-4), 75-80.

Smith, R.W., T.S. Bianchi, and C. Savage, 2010, Comparison of lignin phenol sand branched / isoprenoid tetraethers (BIT index) as indices of terrestrial organic matter in Doubtful Sound, Fiordland, New Zealand, *Organic Geochemistry*, 41, 281–290.

Solemdal, P., S. Sundby, and P. Bratland, 1983, Spawning, distribution and drift of cod eggs in relation to hydrographic conditions off Lofoten and Vesteralen. *Contribution to the PINRO/HI-symposium in Leningrad 26-30* Sept. 1983.

Stein, R., 1991, Accumulation of Organic Carbon in Marine Sediments, 217 pp, Springer, New York.

Stein, R., R.W. MacDonald, 2004, The Organic Carbon Cycle in the Arctic Ocean, *Springer,* Berlin Heidelberg.

Still, C. J., J.A. Berry, G.J. Collatz, and R.S. DeFries, 2003, Global distribution of C_3 and C_4 vegetation: Carbon cycle implications, *Global Biogeochemical Cycles*, 17 (1), 6-1-6-14, doi: 10.1029/2001GB001807

Sundby, S., 1978, In/Outflow of coastal water in Vestfjorden, *International Council for the Exploration of the Sea.*

Sundby, S., and P. Solemdal, 1984, The egg production of Arcto-Norwegian Cod (Gadus Morhua L.) in the Lofoten area estimated by egg surveys, *Institute for Marine Research*, 1, 113-135.

Svendsen, J.P.M., A. Beszczynska-Møller, J.O. Hagen, B. Lefauconnier, V. Tverberg, S. Gerland, J.B. Ørbøk, K. Bischof, C. Papucci, M. Zajaczkowski, R. Azzolini, O. Bruland, C. Wiencke, J.-G. Winther, and W. Dallmann, 2002, The physical environment of Kongsfjorden Krossfjorden, an Arctic fjord system in Svalbard: *Polar Research*, 21, 133-166.

Syvitski, J.P.M., Burrell, D.C., and Skei, J.M., 1987, Fjords: Processes and products.

Syvitski, J.P.M., 1989, On the deposition of sediment within glacier-influenced fjords: Oceanographic controls, *Marine Geology,* 85, 301-329.

Syvitski, J.P.M., 2002, Sediment discharge variability in Arctic rivers: Implications for a warmer future, *Polar Research*, 21, 323-330.

Teeri, J.A., and L.G. Stowe, 1976, Climatic patterns and the distribution of C_4 grasses in North America, *Oecologia*, 23 (1), 1-12, doi: 10.1007/BF00351210.

Tissot, B.P., and D.H. Welte, 1984, Petroleum Formation and Occurence, Springer, Berlin Heidelberg, doi: 10.1007/978-3-642-96446-6.

Van der Weijden, C.H., 2002, Pitfalls of normalization of marine geochemical data using a common divisor, Marine Geology, 184 (3-4), 167-187, doi: 10.1016/S0025-3227(01)00297-3.

Vorren, T.O., 2003, Subaquatic landsystems: Continental margins, *in Evans*, D.J.A., ed., Glacial Landsystems: London, UK, Hodder Arnold, p. 289–312.

Vorren, K.D., and D. Moe, 1986, The early Holocene climate and sea-level changes in Lofoten and Vesterålen, North Norway, *Norsk Geologisk Tidsskrift,* 66, 135-143.

Vorren, T.O., and J.S. Laberg, 1996, Late glacial air temperature, oceanographic and ice sheet interactions in the southern Barents Sea region, *in* Andrews, J.T., Austin, W.E.N., Bergsten, H., and Jennings, A.E., eds., Late Quaternary Paleoceanography of the North Atlantic Margins: Geological Society of London Special Publication 111, p. 303–321.

Vorren, T., L. Plassen, 2002, Deglaciation and palaeoclimate of the Andfjord–Vågsfjord area, North Norway, *Boreas*, 31, 97–125.

Wada, E., E.D. Goldberg, Y. Horibe, and K. Saruhashi, 1980, Nitrogen isotope fractionation and its significance in biogeochemical processes occurring in marine environents, *Isotope marine chemistry*, 375-398.

Wada, E., M. Minagawa, H. Mizutani, T. Tsuji, R. Imaizumi, and K. Karasawa, 1987a, Biogeochemical studies on the transport of organic matter along the Otsuchi river watershed, Japan, Estuarine Coastal Shelf Science, 25, 321-336.

Wada, E., M. Terazaki, Y. Kabaya, and T. Nemoto, 1987b, 15 N and 13 C abundances in the Antartic Ocean with emphasis on the biogeochemical structure of the food web, *Deep Sea Research Part A. Oceanographic Research Papers*, 34 (5-6), 829-841, doi: 10.1016/0198-0149(87)90039-2.

Wada, E., and A. Hattori, 1991, Nitrogen in the Sea: Forms, Abundances, and Rate Processes, *CRC Press*, Ann Arbor.

Wakeham, S.G., and C. Lee, 1993, Production, transport, and alteration of particulate organic matter in the marine water column, in: M.H. Engel, S.A. Macko (Eds.), *Organic Geochemistry*, Plenum, New York, 145-169.

Wassmann, P., H. Svendsen, A. Keck, and M. Reigstad, 1996, Selected aspects of the physical oceanography and particle fluxes in fjords of northern Norway, *Journal of Marine Systems*, 8 (1-2), 53-71.

Winkelmann, D., and J. Knies, (2005), Recent distribution and accumulation of organic carbon on the continental margin west off Spitsbergen, Geochemistry, *Geophysics Geosystems*, 6, doi: 10.1029/2005gc000916.

9 Appendix

Table 1: Location of the surface sediment samples and grain size measurements performed by the Geological Survey of Norway (NGU).

NGU sample number	Sample	Station	zone	Latitude	Longitude	Water Depth (m)	Water content %	Grain size < 2 µm	< 63 µm	2-63 µm	63-125 µm	125-250 µm	250-500 µm	500-2000 µm
89751	0-2 cm	1	33N	68,4626	17,5998	338	60,0	4,49	93,2	88,71	6,2	0,6	0	0
89752	0-2 cm	2	33N	68,5095037	17,4518537	179	57,7	3,93	94,9	90,97	4,7	0,4	0	0
89753	0-2 cm	3	33N	68,4482417	17,2953835	247	53,9	3,73	95,1	91,37	4,3	0,6	0	0
89754	0-2 cm	4	33N	68,3710512	16,9447193	120	49,7	2,3	74,1	71,8	23,2	2,7	0	0
89755	0-2 cm	5	33N	68,4256035	17,0362685	324	56,7	4,32	97,6	93,28	2,4	0	0	0
89756	0-2 cm	6	33N	68,4905225	17,0269283	73	58,3	3,06	70,5	67,44	25,4	4,099	0,001	0
89757	0-2 cm	7	33N	68,4429165	16,7150895	533	64,3	6,06	92,2	86,14	5,5	2,2	0,1	0
89758	0-2 cm	8	33N	68,4279883	16,4970438	546	64,9	7,14	90,4	83,26	7,9	1,696	0,004	0
89759	0-2 cm	10	33N	68,4439642	16,0794615	196	46,1	2,82	67,1	64,28	30,1	2,8	0	0
89760	0-2 cm	12	33N	68,271171	16,5764062	241	81,0	5,97	87,4	81,43	12,2	0,4	0	0
89761	0-2 cm	13	33N	68,3905395	16,2706513	553	60,2	6,71	90,6	83,89	8,1	1,3	0	0
89762	0-2 cm	14	33N	68,3720485	16,1345608	556	38,7	2,36	34,8	32,44	35,5	27	2,68	0,02
89763	0-2 cm	15	33N	68,3618927	15,9762917	330	45,3	3,22	50,9	47,68	28,7	14,3	4,9	1,2
89764	0-2 cm	16	33N	68,3655228	15,7982452	150	58,0	4,28	83	78,72	16,5	0,5	0	0
89765	0-2 cm	17	33N	68,308263	15,8934465	586	69,0	9,09	97,3	88,21	2,5	0,2	0	0
89766	0-2 cm	18	33N	68,2532528	16,2423102	170	66,0	4,09	88,3	84,21	10,9	0,8	0	0
89767	0-2 cm	19	33N	68,2087635	16,3217512	182	50,1	2,94	73,7	70,76	22,1	4,19	0,01	0
89768	0-2 cm	20	33N	68,1853185	16,2981262	504	61,0	7,04	95,2	88,16	4,8	0	0	0
89769	0-2 cm	21	33N	68,0686918	16,1515028	498	63,2	6,45	89,8	83,35	8,7	1,48	0,02	0
89770	0-2 cm	22	33N	67,9915133	16,2174587	380	60,1	3,89	88,9	85,01	10,2	0,9	0	0
89771	0-2 cm	23	33N	67,9790642	16,3467778	120	53,8	1,39	46,4	45,01	39,6	10,7	2,3	1
89772	0-2 cm	24	33N	68,0193453	16,447145	259	51,0	0,96	35,7	34,74	36	24,6	3,68	0,02
89773	0-2 cm	25	33N	68,0987252	16,530535	444	62,1	1,65	68,1	66,45	22,2	8,6	1,09	0,01

89774	0-2 cm	26	33N	68,099625	16,2885627	305	52,4	3,86	71,2	67,34	19,4	6,3	3,07	0,03
89775	0-2 cm	27	33N	68,2547167	16,1205027	622	65,0	6,43	88,9	82,47	9,6	1,3	0,2	0
89776	0-2 cm	28	33N	68,1776708	15,7429595	276	53,9	4,98	58,2	53,22	30,2	11,56	0,04	0
89777	0-2 cm	29	33N	68,1522362	15,862123	287	86,4	8,19	90,7	82,51	8,1	1,2	0	0
89778	0-2 cm	30	33N	68,2030447	15,3914662	584	68,2	10	99	89	1	0	0	0
89779	0-2 cm	31	33N	68,158652	15,0566738	385	64,3	8,33	94,2	85,87	4,9	0,8	0,1	0
89780	0-2 cm	32	33N	68,0810752	14,6968413	320	54,7	5,27	86,2	80,93	13,5	0,3	0	0
89781	0-2 cm	33	33N	68,0062573	14,3690708	278	52,0	2,9	82,3	79,4	15,1	2,598	0,002	0
89782	0-2 cm	34	33N	68,3041293	15,1574888	185	78,0	8,83	91,3	82,47	7,8	0,85	0,05	0
89783	0-2 cm	35	33N	68,3570488	15,2906357	178	74,1	7,59	82,8	75,21	13,4	3,2	0,6	0
89784	0-2 cm	36	33N	68,3237972	15,4935652	59	41,9	1,65	28,9	27,25	24	32,9	11,3	2,9
89785	0-2 cm	37	33N	68,2985922	15,590241	95	57,2	4,7	83	78,3	14,8	2,2	0	0
89786	0-2 cm	38	33N	68,2598985	15,5011505	182	60,0	5,47	80,4	74,93	12	4	3,1	0,5
89787	0-2 cm	39	33N	68,2222988	15,6709518	634	66,2	8,23	98,3	90,07	1,7	0	0	0
89788	0-2 cm	40	33N	68,1584857	15,544411	154	74,6	5,42	79,6	74,18	17,4	2,998	0,002	0
89789	0-2 cm	41	33N	68,2637553	15,1595968	171	46,3	3,52	56,7	53,18	16,1	15,7	6,4	5,1
89790	0-2 cm	42	33N	68,077172	15,2476342	395	59,0	6,94	79,6	72,66	17,3	3,099	0,001	0
89791	0-2 cm	43	33N	67,9380288	15,411673	482	65,3	7,34	89,1	81,76	10,6	0,3	0	0
89792	0-2 cm	44	33N	67,9755303	15,6894982	351	58,3	3,63	72,2	68,57	24	3,8	0	0

Table 2: Total carbon and nitrogen analyses, stable carbon and nitrogen isotopic signatures measured by Organic, Iso-Analytical and the Geological Survey of Norway (NGU), and C/N and N/C ratios.

	Organic	Iso-Analytical						NGU						
NGU sample number	C %	Corg %	d13CV-PDBorg ‰	Norg %	d15NAirorg ‰	Ninorg %	d15NAirinorg ‰	Ctot %	Corg %	Cinorg %	CaCO3 %	Norg/Corg	Corg/Norg	Corg/Ntot
89751	1,35	1,41	-23,20	0,15	5,94	0,01	3,64	1,54	1,18	0,36	3,00	0,11	8,72	7,95
89752	1,37	1,42	-22,50	0,15	5,48	0,01	4,61	1,62	1,2	0,42	3,50	0,11	9,01	8,14
89753	1,15	1,03	-22,14	0,12	5,61	0,01	4,75	1,29	0,94	0,36	2,96	0,11	8,87	7,92
89754	1,57	1,00	-22,10	0,15	5,36	0,01	3,63	1,78	1,14	0,64	5,33	0,12	8,04	7,68
89755	1,24	1,03	-21,70	0,12	6,35	0,01	5,80	1,39	0,95	0,45	3,78	0,12	8,56	7,63
89756	2,23	2,44	-22,23	0,31	5,56	0,01	4,67	2,68	2,21	0,47	3,92	0,13	7,51	7,23
89757	2,05	1,47	-21,52	0,17	6,66	0,02	4,07	2,22	1,21	1,01	8,41	0,13	7,67	6,99
89758	2,43	1,17	-21,39	0,18	6,71	0,02	4,99	2,6	1,18	1,42	11,83	0,14	7,25	6,63
89759	2,33	1,47	-21,41	0,19	5,57	0,01	4,78	2,55	1,04	1,51	12,58	0,17	5,76	5,55
89760	6,17													
89761	2,92	1,17	-21,45	0,19	6,60	0,02	4,94	3,1	1,28	1,82	15,16	0,13	7,78	7,11
89762	1,99	0,25	-21,51	0,07	6,90	0,01	4,92	2,1	0,47	1,63	13,61	0,14	7,36	6,74
89763	2,49	0,87	-22,11	0,09	6,28	0,01	2,45	2,7	0,79	1,91	15,90	0,10	9,90	8,77
89764	4,03	2,36	-21,43	0,25	6,08	0,01	4,96	4,5	1,8	2,7	22,49	0,13	7,49	7,23
89765	2,71	1,71	-21,42	0,19	6,69	0,02	3,57	2,84	1,21	1,63	13,58	0,14	7,14	6,41
89766	3,48	3,07	-21,74	0,33	5,86	0,01	3,18	3,92	2,31	1,61	13,41	0,14	7,01	6,79
89767	1,42	0,98	-21,89	0,12	6,21	0,01	5,14	1,58	0,90	0,69	5,71	0,13	7,92	7,52
89768	1,97	1,17	-21,23	0,14	6,79	0,01	2,64	2,1	0,97	1,13	9,40	0,13	7,59	6,94
89769	2,09	1,37	-21,57	0,16	6,50	0,01	3,65	2,25	1,08	1,17	9,75	0,13	7,47	6,92
89770	1,61	1,16	-21,36	0,13	6,47	0,01	2,35	1,79	0,99	0,8	6,66	0,13	7,98	7,43
89771	2,1	1,53	-22,24	0,21	5,26	0,01	2,15	2,4	1,58	0,82	6,83	0,13	7,78	7,59
89772	1,01	1,08	-23,83	0,11	4,69	0,01	3,26	1,2	0,99	0,21	1,72	0,10	9,71	9,15
89773	1,98	2,19	-21,70	0,20	6,16	0,01	4,02	2,21	1,64	0,57	4,75	0,12	8,69	8,25

89774	2,11	1,11	-20,87	0,12	6,09	0,01	3,53	2,26	0,94	1,32	11,00	0,12	8,40	7,84
89775	2,72	1,65	-21,36	0,19	6,45	0,01	4,53	3,03	1,35	1,68	13,99	0,13	7,65	7,13
89776	5,32	2,10	-21,33	0,18	6,09	0,01	2,91	5,59	1,26	4,33	36,07	0,14	7,40	7,07
89777	6,02													
89778	2,64	1,65	-21,13	0,19	6,69	0,02	5,04	2,87	1,28	1,59	13,24	0,13	7,85	6,81
89779	2,63	1,25	-21,09	0,14	6,63	0,02	3,66	2,77	0,99	1,78	14,83	0,12	8,54	7,22
89780	2,39	0,77	-21,42	0,09	6,26	0,01	3,56	2,56	0,68	1,88	15,64	0,12	9,29	7,80
89781	2,01	0,73	-21,57	0,08	5,77	0,01	2,49	2,11	0,63	1,48	12,31	0,11	9,25	7,78
89782	8,71							9,65	4,49	5,16	42,98			
89783	8,19	8,38	-20,94	0,59	5,73	0,02	6,24	9,12	3,68	5,44	45,32	0,16	6,38	6,21
89784	7,77	1,86	-21,33	0,15	5,38	0,01	7,00	8,22	0,97	7,25	60,38	0,14	7,16	6,60
89785	7,93	4,48	-21,32	0,34	5,83	0,01	5,24	8,41	2,16	6,25	52,06	0,15	6,56	6,31
89786	6,12	2,72	-21,65	0,23	6,08	0,01	5,13	6,51	1,58	4,93	41,07	0,14	7,31	6,92
89787	2,66	1,59	-21,14	0,18	6,87	0,02	4,90	2,89	1,26	1,63	13,58	0,12	8,04	7,07
89788	7,57	8,33	-20,96	0,67	6,52	0,02	6,75	8,72	4,43	4,29	35,74	0,15	6,88	6,71
89789	10,5	7,81	-22,05	0,18	6,08	0,01	6,46	11	1,11	9,89	82,38	0,15	6,88	6,31
89790	3,13	1,36	-21,24	0,14	6,48	0,02	4,80	3,48	1,08	2,4	19,99	0,12	8,69	7,59
89791	3,76	2,70	-21,09	0,27	6,48	0,02	4,60	4,26	2	2,26	18,83	0,13	7,84	7,32
89792	2,85	2,04	-21,07	0,22	6,14	0,01	4,08	3,28	1,77	1,51	12,58	0,12	8,04	7,70

Table 3: Bulk elemental composition measured with X-ray fluorescence spectroscopy (XRF) by the ALS laboratories.

NGU sample number	Al %	Ca %	Fe %	K %	Si %	Sr %
89751	7,62	1,68	5,30	3,24	25,33	0,01
89752	7,75	1,69	4,89	3,17	25,90	0,01
89753	7,91	1,86	4,78	3,30	26,13	0,01
89754	6,62	3,14	3,36	2,33	27,95	0,03
89755	8,04	2,08	4,87	3,59	25,29	0,03
89756	7,04	2,19	3,90	2,80	26,41	0,03
89757	7,33	3,61	4,90	3,37	22,86	0,03
89758	6,99	5,031	4,55	3,20	22,30	0,03
89759	5,74	5,61	2,23	2,34	27,20	0,03
89760	4,83	7,54	3,38	2,27	16,73	0,04
89761	6,70	6,36	4,20	3,06	21,64	0,04
89762	5,37	6,11	2,26	2,22	28,37	0,03
89763	5,48	6,79	2,52	2,32	26,46	0,04
89764	5,50	9,54	2,52	2,32	21,45	0,04
89765	6,99	5,70	4,76	3,13	20,19	0,03
89766	6,32	5,52	3,50	2,90	22,20	0,03
89767	6,99	3,27	3,29	3,02	27,63	0,02
89768	7,30	4,38	4,59	3,24	23,32	0,03
89769	6,93	4,42	4,47	3,09	23,18	0,03
89770	7,25	3,54	4,57	3,00	25,01	0,02
89771	6,91	3,95	3,13	2,71	26,74	0,03
89772	7,38	2,34	4,37	2,10	27,72	0,02
89773	8,12	3,17	6,16	2,81	22,16	0,02
89774	6,67	5,42	3,79	2,81	25,01	0,03
89775	6,67	6,00	4,24	3,13	21,50	0,04
89776	4,44	15,15	2,24	2,11	17,01	0,07
89777	3,12	6,92	2,75	1,90	10,84	0,04
89778	7,36	5,52	5,08	3,30	19,73	0,03
89779	7,12	6,46	4,71	3,16	20,15	0,03
89780	6,83	7,09	3,85	2,91	22,48	0,04
89781	6,85	5,92	3,65	2,80	23,93	0,03
89782	2,77	15,44	2,04	1,43	8,58	0,07
89783	3,20	17,51	2,06	1,54	10,56	0,07
89784	2,50	24,09	1,00	1,13	11,03	0,10
89785	3,00	21,01	1,54	1,38	11,12	0,09
89786	3,97	15,79	2,26	1,83	14,68	0,07
89787	7,17	5,74	4,94	3,11	19,96	0,03
89788	3,84	14,00	2,36	1,88	12,76	0,06
89789	0,91	31,88	0,66	0,52	3,29	0,15
89790	6,54	8,54	3,99	2,65	20,05	0,04
89791	6,48	7,75	4,11	2,96	19,44	0,04
89792	6,51	5,60	3,12	3,06	24,07	0,02

Table 4: Bulk mineral assemblages analysed with X-ray diffraction (XRD) by the Universty of Bremen.

NGU sample number	Plagioclase	Calcite	Aragonite	Sum Illites & Micas	Sum Phyllosillicates
89751	19,02	1,13	0	10,69	34,30
89752	27,88	0,91	0	19,34	28,31
89753	27,23	1,68	0	13,09	26,40
89754	30,65	2,91	0	17,79	24,08
89755	28,25	1,76	0	23,70	32,13
89756	24,87	1,02	0	21,58	30,27
89757	18,29	6,67	0	14,67	36,65
89758	29,87	8,98	2,70	6,17	21,17
89759	27,47	8,06	0	6,76	11,82
89760					
89761	17,53	10,22	1,67	16,28	32,62
89762	28,60	8,87	0	7,79	12,75
89763	22,25	12,92	0	11,59	16,44
89764	23,97	14,79	0	8,33	12,06
89765	18,56	11,85	0	10,63	34,81
89766	31,55	15,39	0	13,77	17,79
89767	35,93	5,85	0	9,45	16,08
89768	22,35	9,39	0	10,08	22,19
89769	19,22	10,46	0	17,07	25,22
89770	24,86	6,42	0	24,62	30,66
89771	27,90	7,55	0	10,16	18,23
89772	26,79	1,25	0	13,02	19,17
89773	21,33	4,75	1,17	23,11	36,37
89774	19,20	16,27	0	12,36	17,65
89775	18,81	10,58	2,71	10,51	26,02
89776	22,61	17,03	7,18	7,19	12,80
89777					
89778	12,09	9,60	0	14,58	49,81
89779	17,58	14,13	0	10,10	33,43
89780	15,61	15,66	0	19,10	24,09
89781	22,40	16,85	0	13,14	20,16
89782	9,43	25,39	14,03	10,38	14,89
89783	21,72	27,18	16,05	4,59	9,34
89784	12,80	38,17	12,32	4,44	7,05
89785	16,27	31,98	9,52	9,13	13,58
89786	17,42	28,44	7,78	9,13	11,97
89787	17,06	9,37	0,85	16,91	44,03
89788	18,33	19,46	10,04	8,16	12,98
89789	2,26	51,04	10,97	2,63	12,77
89790	19,27	13,26	0	17,07	22,21
89791	23,01	11,39	4,37	11,22	21,19
89792	28,24	8,26	1,22	12,02	16,38

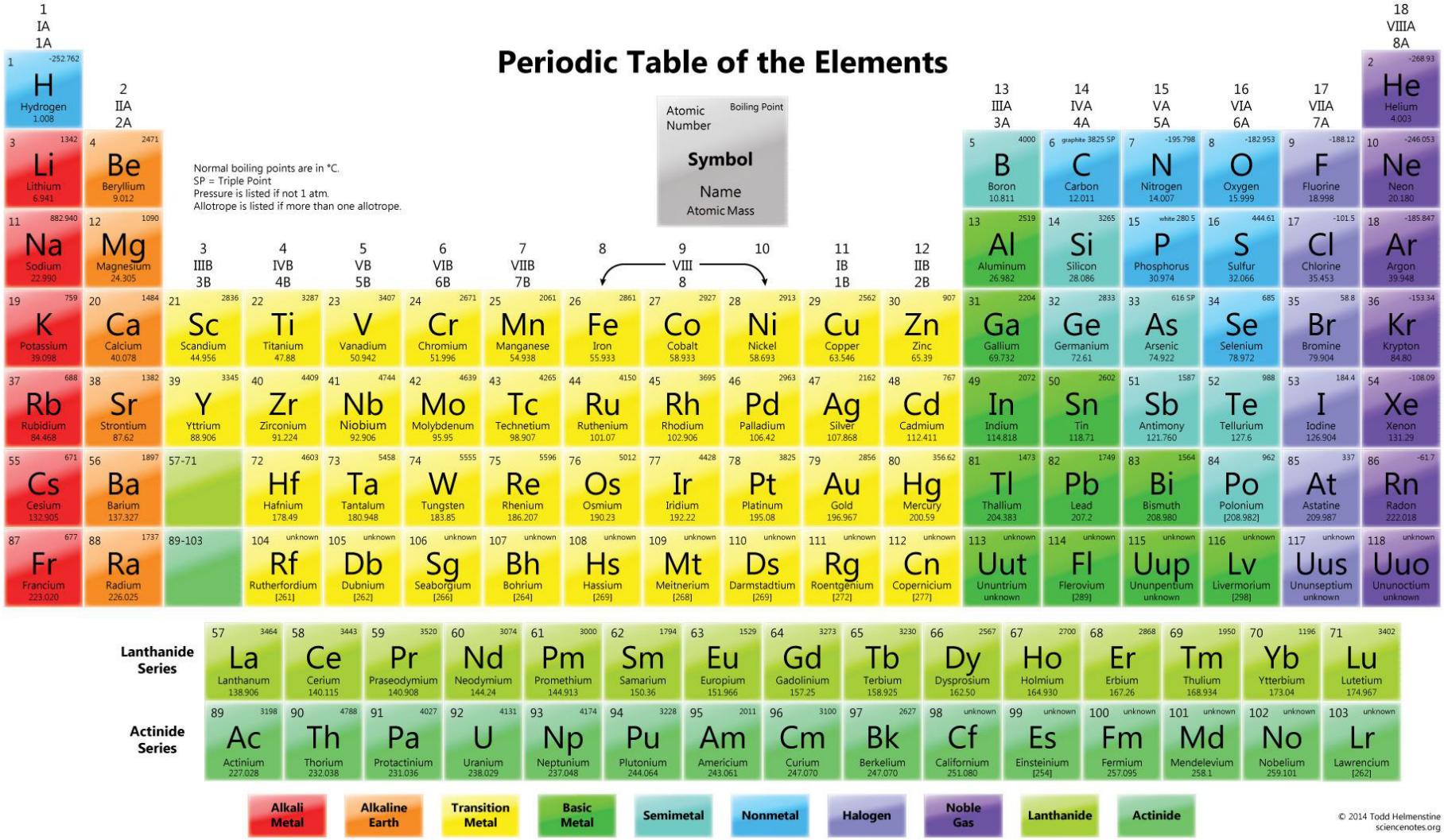

Figure 1: Periodic Table of the Elements taken from http://sciencenotes.org/printable-periodic-table.

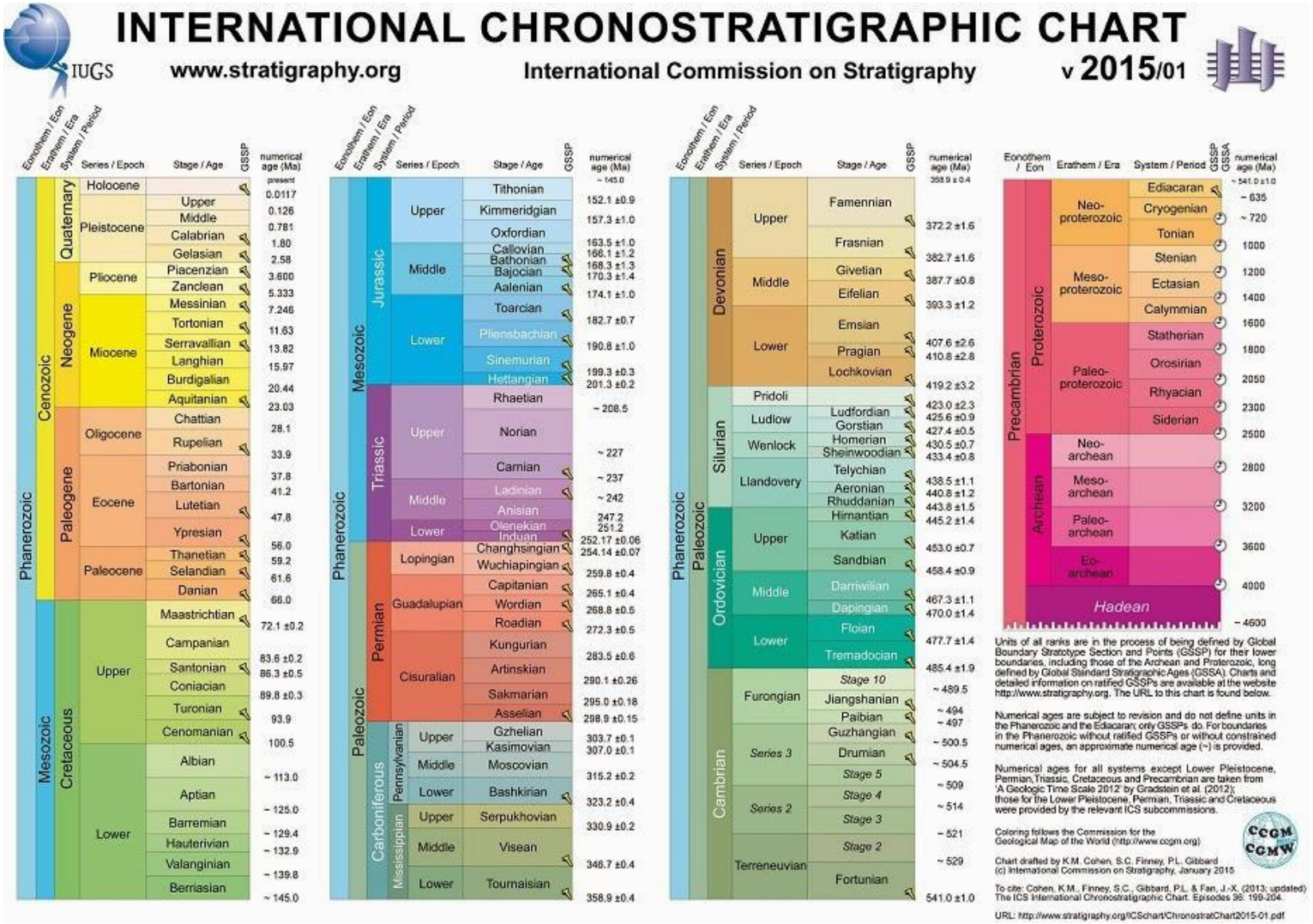

Figure 2: International Chronostratigraphic Chart 2015. Taken from http://www.geologyin.com/2015/04/download-international.html.